# SPERMATOGENESIS AND CHROMATIN CONDENSATION IN THE MALE GERM CELLS OF THE GIANT AFRICAN SNAIL, ACHATINA FULICA BOWDICH

VIRIYA PANKAO



A THESIS SUBMITTED IN PARTIAL FULFILMENT
OF THE REQUIREMENTS FOR
THE DEGREE OF MASTER OF SCIENCE (ANATOMY)
FACULTY OF GRADUATE STUDIES
MAHIDOL UNIVERSITY
2000



ISBN 974-665-038-6

Thesis
entitled

# SPERMATOGENESIS AND CHROMATIN CONDENSATION IN THE MALE GERM CELLS OF THE GIANT LAND SNAIL, ACHATINA FULICA BOWDICH

Viriya Pankao
.....
Miss Viriya Pankao
Candidate

Chaitip Wanichanon
.....
Assoc. Prof. Chaitip Wanichanon,
Ph.D.
Major-Advisor

.....
Prof. Prasert Sobhon,
Ph.D.
Co-advisor

M. Kruatrachue
.....
Prof. Maleeya Kruatrachue,
Ph.D.
Co-advisor

Prapee Sretarugsa
.....
Assoc. Prof. Prapee Sretarugsa,
Ph.D.
Co-advisor

.....
Prof. Liangchai Limlomwongse,
Ph.D.
Dean
Faculty of Graduate Studies

.....
Assoc.Prof. Vijittra Lerdkamolkarn
Ph.D.
Chairman
Master of Science Program
in Anatomy, Faculty of Science

Thesis
entitled

# SPERMATOGENESIS AND CHROMATIN CONDENSATION IN THE MALE GERM CELLS OF THE GIANT AFRICAN SNAIL, ACHATINA FULICA BOWDICH

was submitted to the Faculty of Graduate Studies, Mahidol University for the degree of Master of Science (Anatomy)

on

November 2, 2000

Viriya Pankao
.....
Miss Viriya Pankao
Candidate

Chaitip Wanichanon
.....
Assoc. Prof. Chaitip Wanichanon,
Ph.D.
Chairman

Prapee Sretarugsa
.....
Assoc.Prof. Prapee Sretarugsa,
Ph.D.
Member

Prasert Sobhon
.....
Prof. Prasert Sobhon,
Ph.D.
Member

M. Kruatrachue
.....
Prof. Maleeya Kruatrachue,
Ph.D.
Member

Liangchai Limlomwongse
.....
Prof. Liangchai Limlomwongse,
Ph.D.
Dean
Faculty of Graduate Studies
Mahidol University

Amaret Bhumiratana
.....
Prof. Amaret Bhumiratana,
Ph.D.
Dean
Faculty of Science
Mahidol University

# ACKNOWLEDGEMENT

I wish to acknowledge the support of many persons without whom this research and my thesis would not have been acconplished. First, of course, I would like to express my deepest gratitude and sincere appreciation to Assoc. Prof. Dr.Chaitip Wanichanon, my major advisor, and Prof. Dr. Prasert Sobhon, my co-advisor, for their kindness, valuable advice, guidance, and encouragement throughout this work. I am so impressed with their generous donation of time whenever I asked them to explain or discuss problems concerning my study and thesis.

Also, I am deeply grateful to Prof. Dr. Maleeya Kruatrachue who gave me the opportunity to study under her direction. I truly appreciate her encouragement and help during years of my study. I am especially indebted to Assoc. Prof. Dr. Prapee Sretarugsa for her valuable guidance, attention, criticism, support and suggestion. I am also thankful to Miss Somjai Apisawetakan and Mr. Vichai Linthong for their unending supports throughout this entire project. Special thanks are extended to Miss Kulathida Chaithirayanon and Miss Sasiporn Panasophonkul for their general helps.

I also would like to thank Miss Pornrut Rabintossaporn, Mr. Ardool Meepool, Mr. Worawit Suphamungmee, members of the Electron Microscopy Laboratory and the entire staff of the Anatomy Department who provided not only efficient and competent support.

I would also like to acknowledge the financial support for this research and my stipend from the Thailand Research Fund (Senior Research Scholar Fellowship to Prof. Dr. Prasert Sobhon).

Last, but not least, I wish to thank my parents and everybody in my family for their support and encouragement. Very special thanks and deepest appreciation are given to M.R. Sam-aungvarn Lamsam and her family who support my education from the very beginning. I apologize in advance for those I may have inadvertently omitted in these acknowledgements.



**Viriya Pankao**

4036396SCAN/M : MAJOR : ANATOMY; M.Sc. (ANATOMY)
KEYWORDS : ACHATINA FULICA/ GONADAL HISTOLOGY / SPERMATOGENESIS

VIRIYA PANKAO: SPERMATOGENESIS AND CHROMATIN CONDENSATION IN THE MALE GERM CELLS OF THE GIANT AFRICAN SNAIL, ACHATINA FULICA BOWDICH. THESIS ADVISORS: CHAITIP WANICHANON, Ph.D., PRASERT SOBHON, Ph.D., PRAPEE SRETARUGSA, Ph.D., MALEEYA KRUATRACHUE, Ph.D. 127 p. ISBN 974-665-038-6

The aim of this thesis was to study the ovotestis histology, ultrastructure and pattern of chromatin organization in male germ cells during spermatogenic processes in *A. fulica* by light and transmission electron microscopy. The ovotestis was composed of numerous small tubules which were seperated from the surrounding connective tissue by the basement membrane. Each tubule contained various stages of developing male and female germ cells, Sertoli cells, and follicular cells. Based on their size, shape and chromatin condensation pattern, the male germ cells could be classified into a spermatogonium (Sg), six stages of primary spermatocytes, *i.e.*, leptotene (LSc), zygotene (ZSc), pachytene (PSc), diplotene (DSc), diakinesis (DiSc) and metaphase (MSc) spermatocytes, secondary spermatocyte (SSC), ten stages of spermatids ($St_{1-10}$), and two stages of spermatozoon ($Sz_{1-2}$). Sg was a spherical-shaped cell; its nucleus contains mostly euchromatin and few small blocks of widely scattered heterochromatin. The heterochromatin blocks became larger and more numerous in LSc and ZSc, which was due to the winding of 30-nm fibers around a single-dense line that was the axis of chromatin condensation. The euchromatin contained individual 30-nm as well as 10-nm chromatin fibers. ZSc also had synaptonemal complex, the tripatite structure. The heterochromatin blocks were enlarged to form a few pieces of chromosomes in DSc and DiSc. The two halves of chromosomes in DiSc were segregated, then moved to be aligned along the equatorial region in MSc. SSc was a round cell, derived from the division of MSc, whose nucleus contained large clumps of heterochromatin along the nuclear envelope and in the central area. $St_{1-4}$ had round-shaped nuclei which became progressively smaller and denser. During transition of SSc to $St_1$ the dense chromosomes were reorganized into evenly distributed 30 and 10 nm fibers. Thereafter, 30-nm chromatin fibers started to be condensed into heterochromatin blocks again in $St_2$ and $St_3$. In $St_4$ the 30-nm fibers became homogeneously condensed throughout the nucleus. $St_5$ nucleus was gradually compressed on cephalo-caudal direction to become cup-shape and was indented further to assume an arrow or boomerang shape in $St_6$, while 30-nm fibers were decreased in size to about 20 nm, and were straightened to form 14-16 nm fibers in $St_7$. Then, the nucleus became a pear shape in $St_8$. In $St_9$ and $St_{10}$ the nucleus started to elongate to form a tapered anterior end, and the chromatin was completely condensed. The straight chromatin fibers were packed into bundles about 120 nm in width which coalesced into dense crystal lattice-liked structure in the spermatozoa. The spermatozoon had a falciform-shape head that contains completely condensed chromatin in the crystal lattice conformation with dense individual 10-nm lines separated by the intervals of 3-4 nm. It was covered anteriorly by a small acrosome. The neck region was composed of centriolar complex surrounded by a rhomboid shape crystalline substance. The mid-piece consisted of axonemal-fibrous complex surrounded by the helical mitochondrial sheath. The end-piece consisted of only axonemal complex surrounded by the plasma membrane.

4036396 SCAN / M : สาขาวิชา : กายวิภาคศาสตร์ ; วท.ม. (กายวิภาคศาสตร์)
วิริยา พันธ์ขาว : กระบวนการสร้างเซลล์สืบพันธุ์เพศผู้และลักษณะการขดตัวของโครมาตินในหอยทากยักษ์ ACHATINA FULICA BOWDICH (SPERMATOGENESIS AND CHROMATIN CONDENSATION IN THE MALE GERM CELLS OF THE GIANT AFRICAN SNAIL, ACHATINA FULICA BOWDICH) คณะกรรมการควบคุมวิทยานิพนธ์ : ชัยทิพย์ วนิชานนท์, Ph.D., ประเสริฐ โสภน, Ph.D., ประพีร์ เศรษฐรักษ์, Ph.D., มาลียา เครือตาชู, Ph.D.
127 หน้า. ISBN 974-665-038-6

วัตถุประสงค์ของงานวิจัยนี้คือ การศึกษาลักษณะทางจุลกายวิภาคศาสตร์ของเนื้อเยื่อในอวัยวะสืบพันธุ์ และศึกษาลักษณะการจัดระดับการเรียงตัวของไยโครมาตินในเซลล์สืบพันธุ์เพศผู้ในกระบวนการสร้างเซลล์อสุจิของหอยทากยักษ์ *Achatina fulica* โดยการสังเกตด้วยกล้องจุลทรรศน์ธรรมดา และกล้องจุลทรรศน์อิเล็กตรอน พบว่าภายในอวัยวะสืบพันธุ์มีท่อขนาดเล็กจำนวนมาก ซึ่งถูกแยกจากบริเวณเนื้อเยื่อเกี่ยวพันที่ล้อมรอบโดย basement membrane แต่ละท่อ (tubules) บรรจุเซลล์สืบพันธุ์เพศผู้และเซลล์สืบพันธุ์เพศเมีย, Sertoli cell และ follicular cell ขั้นตอนของกระบวนการสร้างเซลล์สืบพันธุ์เพศผู้สามารถแยกตามขนาด, รูปร่างของเซลล์และตามลักษณะการจัดลำดับการขดตัวของไยโครมาตินได้ 20 ขั้น เซลล์ Sg เป็นเซลล์ที่มีลักษณะกลม ในนิวเคลียสประกอบด้วย euchromatin เป็นส่วนใหญ่ และมีการเกาะกลุ่มของก้อน heterochromatin ขนาดเล็กกระจายอยู่ทั่วทั้งนิวเคลียส ก้อน heterochromatin นี้จะมีขนาดใหญ่ขึ้น และมีจำนวนมากขึ้นในระยะ LSc และ ZSc ซึ่งเนื่องมาจากมีการพันตัวของไยโครมาตินขนาด 30 nm รอบแกนการขดตัวของโครมาติน (Axis of chromatin condensation) ซึ่งจะเพิ่มปริมาณมากขึ้นในระยะ ZSc ซึ่งพบ synaptonemal complex ที่ปรากฏเป็นแผ่น 3 แถบเรียงกันอีกด้วย ก้อน heterochromatin รอบแกนจะขดแน่นเป็นท่อนขนาดใหญ่ต่อเนื่องกันและกลายเป็นท่อนยาว ส่วนของโครโมโซมที่พบในขั้น DiSc จะขยายใหญ่ขึ้นและท่อนโครโมโซมนี้จะถูกแยกจากกันเพื่อเคลื่อนไปอยู่ที่แกนกลางในขั้น MSc. เซลล์ในระยะต่อมาคือ SSc เป็นเซลล์ที่มีรูปร่างกลม นิวเคลียสมีก้อน heterochromatin ขนาดใหญ่ วางตัวเกาะกลุ่มตามขอบของ nuclear envelope และในบริเวณส่วนกลางนิวเคลียส ตั้งแต่ระยะ $St_{1-4}$ เซลล์มีนิวเคลียสรูปร่างกลม ซึ่งพบว่ามีขนาดเล็กลงเรื่อยๆ จากช่วง SSc ไป $St_1$ พบว่าโครมาตินที่เคยพันกันแน่นจะมีการจัดเรียงตัวใหม่จนประกอบด้วย euchromatin เกือบทั้งหมด และเริ่มมีการเกาะกลุ่มกันเป็น ก้อน heterochromatin อีกครั้งในขั้น $St_2$ และ $St_3$ จนทำให้มีความหนาแน่นมากและกระจายอยู่เกือบสม่ำเสมอทั่วทั้งนิวเคลียส ในขั้น $St_4$ เส้นไยโครมาตินขนาด 30 nm อยู่กันแน่นทั่วทั้งนิวเคลียส ซึ่งนิวเคลียสมีขนาดเล็กลง ในขั้น $St_5$ นิวเคลียสจะเปลี่ยนรูปร่างจากทรงกลมเป็นรูปถ้วย และจะบุ๋มเข้าไปตรงกลางมากขึ้นจนกลายเป็นรูปลูกศรหรือบูมเมอแรงในขั้น $St_6$ ซึ่งในขั้นนี้โครมาตินขนาด 30 nm มีขนาดเล็กลงเป็น 20 nm และยืดตัวออกเป็นขนาด 14-16 nm ในขั้น $St_7$ ปีกทั้งสองของนิวเคลียสโค้งเข้าหากันจนกลายเป็นรูปเกือกม้า หรือรูปไต ในขั้น $St_9$ และ $St_{10}$ นิวเคลียสจะเริ่มยืดยาวเรียวขึ้นทางด้านหน้าและโครมาตินขดตัวกันแน่นเต็มที่ เส้นโครมาตินที่ยืดออกเป็นเส้นตรงจะอยู่รวมกันเป็นมัดขนาด ~120 nm ซึ่งจะประสานรวมกันเป็นแท่งโครมาติน มีลักษณะคล้ายผลึก (crystal lattice-liked structure) เส้นทึบแต่ละเส้นในก้อนผลึกมีขนาด 10 nm ซึ่งแยกจากกันโดยช่องขนาด 3-4 nm ส่วนหัวของนิวเคลียสของ $Sz_2$ ประกอบด้วย acrosome ขนาดเล็ก ส่วน neck ประกอบด้วย centriolar complex ล้อมรอบโดย crystalline substance รูปร่างคล้ายสี่เหลี่ยมคางหมู ส่วน mid-piece ประกอบด้วย axonemal-fibrous sheath complex ล้อมรอบโดยแผ่นของไมโตคอนเดรีย ซึ่งพันอยู่รอบ ส่วน end-piece มีเพียง axonemal complex ซึ่งถูกล้อมรอบโดย plasma membrane

# LIST OF CONTENTS

# LIST OF CONTENTS (CONT)

# LIST OF TABLE

# LIST OF FIGURES

# LIST OF FIGURES (CONT)

# LIST OF FIGURES (CONT)

# LIST OF ABBREVIATIONS

| | | |
|---|---|---|
| Ac | = | acrosomal granule |
| alg | = | albumen gland |
| at | = | anterior tentacle |
| ax | = | axis of chromatin condensation |
| Ax | = | axoneme |
| bm | = | basement membrane |
| ce | = | centriole |
| ch | = | chromosome |
| co | = | common genital pore |
| cy | = | cytoplasm |
| dg | = | digestive gland |
| DiSc | = | diakinesis primary spermatocyte |
| DSc | = | diplotene primary spermatocyte |
| fa | = | fat cell |
| fc | = | follicular cell |
| fp | = | foot process |
| G | = | glycogen |
| gc | = | Golgi complex |
| H&E | = | hematoxylin and eosin |
| hc | = | heterochromatin |
| hd | = | hermaphroditic duct |
| he | = | head |

# LIST OF ABBREVIATIONS (CONT)

| | | |
|---|---|---|
| $L_1$ | = | level 1 |
| $L_2$ | = | level 2 |
| $L_3$ | = | level 3 |
| $L_4$ | = | level 4 |
| $L_5$ | = | level 5 |
| $L_6$ | = | level 6 |
| $L_7$ | = | level 7 |
| $L_8$ | = | level 8 |
| ld | = | lipid droplet |
| LSc | = | leptotene primary spermatocyte |
| Ly | = | lysosome |
| MB | = | methylene blue |
| mb | = | multigranular bodies |
| mi | = | mitochondria |
| mp | = | middle-piece |
| MSc | = | metaphase primary spermatocyte |
| Mt | = | microtubule |
| Mu | = | myoid cell |
| NE | = | nuclear envelope |
| no | = | nucleolus |
| Nu | = | nucleus |
| Oc | = | oocyte |

# LIST OF ABBREVIATIONS (CONT)

| | | |
|---|---|---|
| ov | = | ovotestis |
| P | = | prostate |
| pe | = | penis gland |
| pg | = | proacrosomal granules |
| PM | = | plasma membrane |
| pt | = | posterior tentacle |
| PSc | = | pachytene primary spermatocyte |
| rer | = | rough endoplasmic reticulum |
| Sc | = | spermatocyte |
| SE | = | Sertoli cell |
| Sg | = | spermatogonium |
| sh | = | shell |
| Sm | = | tubules |
| SSc | = | secondary spermatocyte |
| St | = | spermatid |
| $St_1$ | = | stage I spermatid |
| $St_2$ | = | stage II spermatid |
| $St_3$ | = | stage III spermatid |
| $St_4$ | = | stage IV spermatid |
| $St_5$ | = | stage V spermatid |
| $St_6$ | = | stage VI spermatid |
| $St_7$ | = | stage VII spermatid |

# LIST OF ABBREVIATIONS (CONT)

| | | |
|---|---|---|
| $St_8$ | = | stage VIII spermatid |
| sp | = | spermatheca |
| Sy | = | synaptonemal complex |
| Sz | = | spematozoa |
| T | = | tail |
| ut | = | uterus |
| va | = | electron lucent area |
| vd | = | vas deferen |
| ZSc | = | zygotene primary spermatocyte |

# CHAPTER I

# INTRODUCTION

The perfect terrestrial adaptation is found mostly in vertebrates and arthropods. Mollusks, which have come to live on land, are still dependent on a moist environment and are inactivated by drought and low temperature. This ability of the mollusks is related to some structural changes and considerable physiological adjustments which enable them to slump into inactivity that is most pronounced in hibernation and aestivation of land pulmonates. Pulmonates are essentially land and freshwater mollusks; they belong to one of the three subclasses of Gastropoda, the Pulmonata. The Pulmonata is divided into 3 orders: The Basommatophora with one pair of contractile cephalic tentacles bearing eyes at the base. The second order, Stylommatophora reaches the peak of pulmonate evolution; they are common terrestrial snails and slugs which usually have two pairs of invaginable tentacles with eyes at the tip of posterior pair. This genus of land snails include *Helix, Helicella, Cochicella, Bulimulus*, etc. The third order, the Systellommatophora includes many species of mostly tropical slugs. They possess two pairs of contractile tentacles with the eyes at the tip of the posterior pair. These slugs have neither an external nor internal shell (1).



*Achatina fulica*, the giant African land snail, belongs to the Phylum Mollusca, Class Gastropoda, Subclass Pulmonata, Order Stylommatophora, Suborder

Achatinacea, Family Achatinidae (2, 3). Members of this order are fully adapted to terrestrial environment and breathe by lung.

*A. fulica* is originally imported from Africa to North America, many Indo-Pacific Islands and East Asia (2). Since then it has spreaded widely and could be found everywhere, including Thailand. It is also prevalent in other Southeast and East Asia countries, including China, Taiwan and Japan where it is considered to be a serious pest problem of gardens and domestic crops because they consume a vast amount and many varieties of vegetation (2, 4). Although there have been efforts to process them into escargot, they are not much accepted as *Helix aspera* and *Helix pomatia*, species of land snails found in Europe such in Spain and France (2). However, if there is a good control of reproductive activity to get more amounts of products with the elimination of parasite infection, they can be escargots that have more economic importance. This snail is easy to keep in captivity, and it can be maintained on a herbivorous diet, eating both fresh and decaying vegetation. So it provides useful material for research in reproductive system. Interestingly, *Achatina* is hermaphrodite. It has a protandrous gonad in which oocytes and spermatozoa are produced simultaneously in close proximity. In order to control and improve the production of this snail, hence the basic knowledge of the reproductive biology of gonad needed to be considered more increasingly.

Most of previous studies have described about the patern of their nervous system with relative small numbers of larger cells in the ganglions (5, 6, 7). But in the reproductive system, there have been a number of studies on spermatogenesis and oogenesis of various species of pulmonate snails (8, 9, 10, 11, 12). But concerning the details of similar information in *Achatina fulica* have been reported in a few

number (12). Therefore, the aim of this study was to investigate the morphology, histological characteristics, and cellular association firstly of male gamete cells in the gonad of *A. fulica* by light and electron microscopy.

# CHAPTER II

# OBJECTIVES

1. To investigate the histology, spermatogenetic processes and cellular association within the ovotestis of *Achatina fulica* by light microscopy
2. To investigate the ultrastructural characteristics of various stages of the male gamete cells during spermatogenesis and spermiogenesis of *Achatina fulica* by transmission electron microscopy.
3. To investigate the organization and pattern of chromatin condensation during spermatogenesis and spermiogenesis by transmission electron microscopy.

# CHAPTER III

# LITERATURE REVIEW

All pulmonates are monoecious. Although they show functional protandry, but the reproductive system can fullfill the functions of male as well as female gametes. Concerning general morphology, the shell of *A. fulica* is narrow conoid and is approximately 2-3 inches in length (13). The color is variable, but usually consists of alternating brown and cream or white bands. The body is browny grey in color. It comprises a head which has a terminal mouth, two pairs of invaginable tentacles and eyes at the top of hinder pairs, a visceral mass made up the gonad, digestive gland, stomach, and loops of intestine, and a large foot with creeping sole and the pedal gland that discharges and lubricates along its creeping pathway (1, 2, 3).

## Reproductive Biology

*A. fulica* has a complex reproductive system. The gonad is called the "ovotestis" which usually appears white, yellow, orange, red or black according to species (14). In *A. fulica,* it appears as yellow mass, and is located at the apex of coiled shell where it is firmly embedded in the digestive gland (13). The pulmonates' ovotestes have been studied by many investigators. Such as in primitive basommatophorans were studied by Dancan (1) who found the first appearance of ovotestis as a solid cord of germinal epithelium when the snail was 5-mm long (1). Spermatogonia begin to appear about two weeks before the oogonia, when animal is fully mature, eggs and

sperms are present together (13). Initially, Pawson and Chase (1984), have studied the reproductive biology of this snail, and reported that the sexual maturity was reached at 5 months of age, with a peak in egg production between 210-270 days of age (15). Later in 1989, Ngowsiri, *et al.*, have performed more detailed study and also found that the ovotestis first appeared in 3-month-old snails and progressively increased in number as the snails reached the age of 7-8 months. However, when they reach older age, this number was decreased. In these snails, the male phase also occurred before the female phase, and when female phase became most active, the male phase decreased in function (14, 16).

The gonad consists of small units called "acini". Runham and Hogg (1979) have reported on the development of gonad of *Deroceras reticulatum*, a pulmonate snail, that the number of acini was increasing to 70-180 during differentiated stage (17). In later stages, the acini were increased in size and became lobes. Adult *A. fulica*'s ovotestis is composed of 5-7 lobes with about 1000-3000 acini in each lobe (13, 14, 15). Each acinus is completely lined at the basement membrane with the oocytes located at the periphery and each of them is covered by 3-4 layers of folicular cells except at the base (11, 13). As described above, the acini or tubules are compartmentalized into the female and male compartments. The female germ cells develop abluminally; they are separated from the male gamete cells by a continuous layers of the Sertoli cells, which has the cytoplasmic processes penetrating throughout the germinal epithelium (17, 18, 19). Thus, the male compartment is adjacent to the acinar lumen (10, 20). The pulmonate snail has internal fertilization. In *Lymnea Stagnalis* (21), when the snail acts as a male during copulation, sperms are transported from the stores in seminal vesicle via the male duct, the prostate gland, vas deferen,

and penis into the vagina of the copulation partner. A small part of the transferred sperm is stored; the main part is digested in the bursa copulatrix (18, 22). And when the mature oocytes are ovulated, they are fertilized in the hermaphroditic duct near the carrefour, where this duct gives rise to male and female pathways.

## Spermatogenic Process in *Achatina fulica*

The male gamete cells always occur in all the acini of terrestrial snail. The production of the male germ cells of pulmonate snail has been reported that; the primitive germ cells proliferate from germinal cells forming a discontinuous layer in germinal wall of each tubule, they undergo spermatogenesis or oogenesis at the original site of their proliferation (22). A cluster of spermatogonia may be derived from one primitive germ cell which develops around a Sertoli cell (15, 21, 22). The division and differentiation of the cells in each cluster are strictly synchronized (21, 23). Spermatocytes are progressively increased in size and number, and evenly become attached to the Sertoli cells at prophase stage (11, 22). Various stages of spermatogenesis and Sertoli cells have been studied in the pulmonate snails; such as a freshwater snails, *Biomphalaria glabrata* (11) and *Bulinus truncatus* (10) and the marine snail, *Littorina sikana* (8), and some of the other gastropods. These studies have invariably shown that the Sertoli cells are involved in the nutrition of male germ cells and phagocytosis of residual cytoplasm of late spermatids during spermiation (8, 10, 11). The Sertoli cells are connected by septate desmosomes, and they contain carbonic anhydrase, an enzyme involved in ion-exchange process (9, 23, 24). In 1989, Elsaadany (10) has suggested that the Sertoli cell of *Bulinus truncatus*, a

freshwater snail, has the morphological features of steroid producing cells which are involved in hormone production. Such information is still lacking in *A. fulica.*

A further consequence of this morphology of the ovotestis is that the ultrastructure of the male germ cells during spermatogenesis and spermiogenesis shows nuclei which undergo the process of condensation that starts in early spermatids and culminates in spermatozoa. The ultrastructural changes of various stage cells during early spermatogenesis in gastropods are generally classified into spermatogonia, five or six stages of spermatocytes and secondary spermatocyte based on the nuclear changes and the characteristics of chromatin during cell divisions (9, 10, 12, 23, 25). In 1991, Sretarugsa, *et al.* (12), reported the ultrastructural changes during spermatogenesis of *A. fulica* and the morphology of mature spermatozoa. They classified the cells in spermiogenesis into 4 stages based on the shape, chromatin appearance, and organization of cytoplasmic organelles. Stage I spermatid contained an uniformly-dense nucleus. Stage II spermatid had similar features to the previous stage, but the mitochondria were accumulated to one side of the cell. Stage III spermatid had a cup-shaped nucleus containing evenly distributed chromatin. Stage IV spermatid was characterized by a cone-shaped nucleus with dense chromatin rods and narrow intervening spaces. The mature spermatozoa consisted of three main parts: the elongated head with highly condensed chromatin, the middle-piece consisting of straight flagellum and helical mitochondria sheath, and the tail showing the outpocket of glycogen granules in the proximal part (12).

Chromatin condensation during spermiogenesis has been studied in *Murex brandaris* (27) which show distinct events such as the formation of granules (18-20 nm in diameter) which are arranged into fibers (10-15 nm in diameter) that are

transformed further into lamellae (17 nm thickness). Partial lamellar fusion decreases the thickness of each lamella to 11 nm. From other studies, the pattern of nuclear condensation has been described as "fibrillar-lamellar" type in internally-fertilized sperm of most meso- and all neogastropods, opisthobranchs and pulmonates (28, 29, 30, 31, 32, 33). This pattern of chromatin condensation was described in three successive phases: granular, fibrillar and lamellar structures, then finally become tightly packed in myelin-like whorls (26, 30, 31, 34). In contrast, the externally-fertilized sperm in primitive gastropods (33, 35, 36, 37, 38), scaphopods (39) and bivalves (40, 41) appears to be "granular" type. Initial report of the modified spermatozoa of *Achatina fulica* indicated that the chromatin condensation pattern belongs to the first type (34). It is interesting to investigate how DNA in the spermatids are packaged through various orders of chromatin organization.

Other structural changes which appear to be characteristics of mature sperm are the acrosomal formation and tail differentiation. The complex acrosome in gastropod was found in *Arion rufus*, (31); *Nucella lapillus* (42) and *Anguispira alternata* (43); it consists of a cylindrical structure with a membrane-bound vesicle. In other Stylommatophorans such as *Agriolimax reticulatus* (44), a typical acrosome could not be seen , but a finely granular homogeneous material is seen surround the apex of the nucleus (45). In contrast, only a single acrosomal granule can be observed near the nucleus in the slug, *Arion ater* (46).

Concerning the tail formation, common modification of the spermatozoon is the formation of mitochondria mid-piece. In many species the mitochondria increase in number and are spreaded down the flagellar axoneme. The pulmonate gastropods perhaps show the greatest degree of mitochondria modeling (26, 28, 45). As

maturation proceeds, mitochondria of *Achatina zeba* fuse in a continuous sheath around the axoneme, forming a mitochondrial derivative (28). Enclosed within this derivative and spiralling along the axoneme, is a compartment containing glycogen as has been reported in many Stylommatophorans and some Basommatophorans (47, 48, 49). The mitochondrial derivative and glycogen complex may not extend for to the entire length of the tail. The section without the mitochrondrial derivative is known as the end piece (12, 29, 49).

Therefore, The aim of the present study was to investigate the ultrastructure of the cells in spermatogenesis process and spermatozoa, and to observe the pattern of chromatin fibers packing during spermiogenesis in *Achatina fulica*.

# CHAPTER IV

# MATERIALS AND METHODS

## Collection of *Achatina fulica* Specimens

Adult *A. fulica* were collected from the natural habitat, such as garden surrounding houses or office building that they reside in abundance. Small pieces of fixed gonads were prepared for light microscopic observations by the procedures of paraffin and semithin methods, and the sections were observed under an Olympus Vanox microscope.

## Procedure for Light Microscopy

The shells of the snails were removed and their ovotestes were cut and fixed in Bouin's fixative at 4°C overnight. They were washed in 70% ethyl alcohol to remove the Bouin's fixative. Then, they were dehydrated in a graded series of ethyl alcohol (70-100%) for 30 minutes each, cleared with dioxane, infiltrated and embedded in paraffin wax. Thereafter, the blocks of specimens were sectioned at 5-micron thickness, and finally stained with hematoxylin and eosin.

## Procedure for Transmission Electron Microscopy



The ovotestes were cut and sliced into very small pieces and fixed in a solution of 4% glutaraldehyde plus 2% paraformaldehyde in 0.1M sodium cacodylate buffer at $4^0$ C for overnight. Then the specimens were washed in 0.1M sodium

cacodylate buffer and postfixed in 1% osmium tetroxide in 0.1M sodium cacodylate buffer at $4^0$ C for one hour at $4^0$ C. Subsequently, the specimens were dehydrated in a graded series of ethyl alcohol (50-100%) for 30 minutes each, cleared in two changes of propylene oxide (PO), infiltrated in a mixture of propylene oxide and Aradite 502 resin at the ratio of 3:1 for two hours, 2:1 for one hour, and 1:2 for overnight. Then they were embedded in pure Aradite 502 resin, and finally polymerized at $30^0$ C, $45^0$ C and $60^0$ C for 24, 48, 48 hours, respectively. Blocks of specimens were sectioned with a Sorvall MT-2 ultramicrotome using glass knives at 1 micron and 300-500 $A^0$ thickness. The thin sections were picked up with copper grids, stained sequentially with uranyl acetate and lead citrate, and then examined under a Hitachi H-300 transmission electron microscope operating at 75 KV. In addition, the semithin sections were stained with 1% methylene blue and observed under an Olympus Vanox microscope.

## Procedure for Measurement of Chromatin Fibers

Various stages of male germ cells in *Achatina fulica* were classified. The organizational level and pattern of chromatin condensation in the male germ cells from five animals were observed and measured. The images of each chromatin fibers in at least five nuclei were viewed via Kodak electron microscopic negative films and measured under a Nikon profile projector, based on Catalase Crytals (Agar Aids) magnification calibration.

# Paraffin Section Method

Live adult land snails

↓

The gonad was removed and fixed in Bouin's solution

at $4^0$ C for overnight

↓

Dehydrated through increasing concentration of alcohol

(70-100%) for 30 min. each

↓

Cleared in Dioxane

↓

Infiltrated and embedded in paraffin

↓

Sectioned and stained with H&E

↓

Observed under light microscope

## Semithin and Thin Section Methods

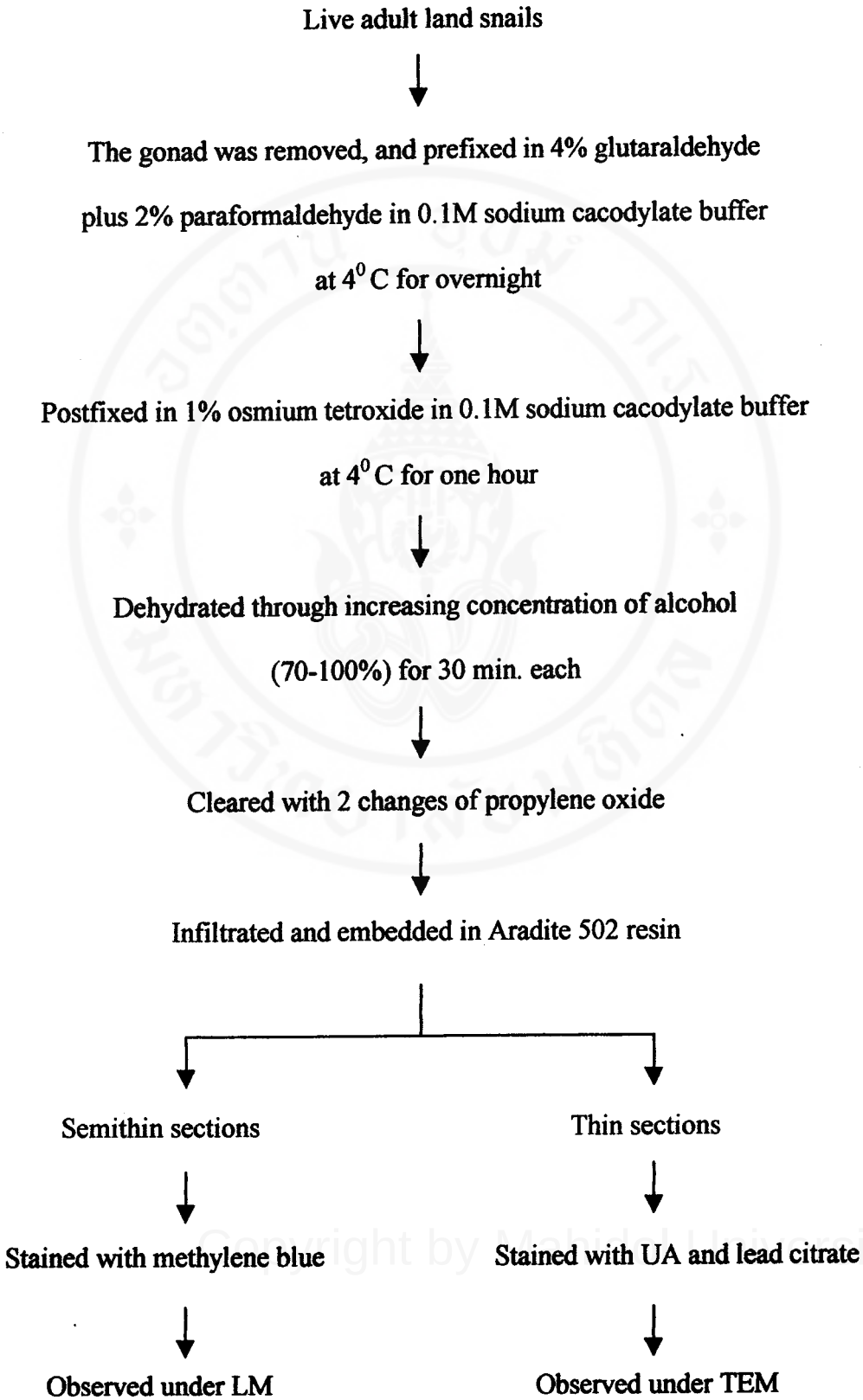

# CHAPTER V

# RESULTS

## General Morphology of the Reproductive System in *Achatina fulica*

*Achatina fulica*'s body is enclosed in a yellow-brown right-handed coiled shell. It is 7 to 8 cm long and 4 to 5 cm wide, and consists of a head, 2 pairs of a visceral mass and a large foot with a creeping sole. The head bears 2 pairs of retractable tentacles, the anterior ones being shorter than the posterior. The posterior tentacles bear the eyes at their distal tips. (Figs. 1A-C). A small opening to the common genital duct is found below and slightly behind the base of the right posterior tentacle. This common genital opening could be found clearly during the breeding season (Figs. 1B; 2A, B). When copulation occurs, the intromittant muscular penis of one snail will be everted and inserted into the duct of its partner (Figs. 2A, B). *A. fulica* has a complex reproductive system, and its ovotestis is located in the inner coiled face of the digestive gland enclosed within the apex of the shell. It appears yellow in color. The gonad and the base of albumen gland are connected by the hermaphroditic duct (Figs. 3A, B). Beyond this, male and female gametes follow separate pathways. The male part has secretory organs, *i.e.*, the prostate gland, which is connected to the vas deferens that passes through the body wall and opens into the penis. The female part comprises of the uterus, oviduct and vagina (Figs. 4A, B).

## Gonadal Histology

The ovotestis is embedded in and mixed with the digestive gland. Histologically, the ovotestis consists of numerous small tubules which are separated from each other by a loose network of connective tissue (Figs. 5A-C). Each tubule contains various stages of developing male and female germ cells (Figs. 5B, D), Sertoli cells, and follicular cells. The oogenic cells commonly lie close to the basement membrane and are surrounded by thin processes of follicular cells. Spermatogenetic cells, including spermatogonia, early and late stages of spermatocytes, aggregated in groups, make up the main mass of the germinal epithelium of each tubules (Figs. 5A-D), while the clusters of spermatozoa are found in the adluminal part. The heads of spermatozoa are usually embedded in the cytoplasm of large Sertoli cells which are situated on the basement membrane (Figs. 5C; 8E).

## Classification of Spermatogenic Cells

The spermatogenic cells appearing in the ovotestis could be classified into 19 stages according to the cell sizes, their structural features and chromatin condensation pattern as observed under the light and transmission electron microscopes.

**Spermatogonium (Sg)** is a spherical or oval-shaped cell 7 to 8 μm in size. Its nucleus is round or ovoid with a diameter about 5 to 6 μm. Under LM and TEM, the nucleus contains mostly euchromatin and small blocks of heterochromatin scattering throughout. It also possesses one or two very prominent nucleoli. The cytoplasm exhibits moderate to intense basophilia depending on the amount of ribosomes (Figs. 6A,

B; 9B); it also contains few developing rough endoplasmic reticulum, only a few mitochondria and small Golgi complex (Figs.9E, F). Within the nucleus, the chromatin fibers consist of 2 levels, *i.e.*, 10 and 30 nm fibers; the former appears as thin zigzag lines while the latter appears mostly as dense dots in cross sections, and thus assumed to be highly coiled (Fig. 9C, D; Table 1).

**Primary spermatocytes (PrSc)** consist of 6 stages, *i.e.*, leptotene (LSc), zygotene (ZSc), pachytene (PSc), diplotene (DSc), diakinetic (DiSc) and metaphase (MSc). The most distinctive differences among various stages of PrSc are the relative amount of euchromatin versus heterochromatin and the patterns of chromatin condensation.

**Leptotene spermatocytes (LSc)** (Figs. 6C; 10A, C) This spherical-shaped cell is larger than Sg with a diameter about 13-15 μm, and it has a large round nucleus about 10 μm in diameter. There are small blocks of heterochromatin scattered evenly throughout the nucleus. The nucleolus is also present, but it is smaller than that of Sg. The cytoplasm is stained light blue with methylene blue; thus, this cell has less basophilic cytoplasm than Sg. Under TEM, the euchromatic area contains 2 levels of chromatin organization, *i.e.*, the 30-nm fundamental chromatin fibers which mostly appear as dense dots in cross sections, and 10-nm fibers which appear as zigzag lines (Figs.10D-F). Moreover, there is the first appearance of thick dense lines that form the axis of chromatin condensation which could be found projecting from the nuclear membrane as well as scattering in the central area of the nucleus. Judging from the tight threading of 30-nm chromatin fibers around it, this structure is believed to be the initiation site of

chromosome condensation (Fig. 10C-F). The cytoplasm also contains abundant ribosomes, rough endoplasmic reticulum, increasing number of mitochondria and larger Golgi complexes (Fig. 10A-C).

**Zygotene spermatocyte (ZSc)** (Fig. 6D; 11A, B) This cell has approximately the same size as LSc. Under LM, it is distinguished from LSc by the heterochromatin which becomes increasingly thread- or cord-liked. The nucleolus is still fairly prominent as that of LSc (Fig. 6D). The cytoplasmic basophilia is decreased. At TEM level, the nucleus contains increasingly dense heterochromatin blocks, each surrounding the longer axis of chromatin condensation, and the synaptonemal complexes which could not be found in LSc (Fig. 11C-F). The synaptonemal complex is distinguished from the axis of condensation by the tripatite structure that has a conspicuous central element separated from the two lateral elements by clear spaces which are traversed by straight filamentous elements. Chromatin fibers (30nm) from adjacent chromosomes are attached to the side of each lateral element of the synaptonemal complex (Fig. 11E). The cytoplasm has similar feature as that of LSc (Figs. 11A, B).

**Pachytene spermatocyte (PSc)** This cell still shows a round shape with smaller size than that of LSc (about 12-13 μm in the cell and 8-9 μm nuclear diameters). The nucleus of PSc is round and still contains fairly prominent nucleolus (Figs. 6E; 12A, B). Under LM, the nucleus contains heterochromatin that becomes condensed into long thick threads or cords that are entwined into loops radiating from the nucleolus (Fig. 6E). Under TEM, this chromatin appears as dense interconnecting clumps of heterochromatin cords that consist of closely packed 30-nm fibers (Figs. 12D, E; Table 1). The cytoplasm

also contains rough endoplasmic reticulum, large amount of well-developed mitochondria, and large Golgi complexes (Figs. 12A, C, F).

**Diplotene spermatocyte (DSc)** (Fig 6F, 13A-D) This cell is about 10-12 μm in size. As revealed by LM, its nucleus (about 8 μm in diameter) shows thicker threads of heterochromatin that are increasingly condensed and become more closely packed. Hence, the nucleus appears denser and darker than that of PSc, and the nucleolus disappears. Under TEM, the 30-nm fundamental chromatin fibers are packed more tightly and these packing occurs both within the nucleus and near the nuclear membrane. The features of cytoplasmic organelles still appear similar to those of earlier stages (Fig. 13A).

**Diakenetic and Metaphase spermatocytes (DSc and MSc)** At LM level, these stages of cells show large pieces of highly condensed chromatin that begin to be separated from each other in diakenetic stage (Figs. 6G, H), and move to be aligned at the equatorial region in metaphase stage when the nuclear membrane completely disappears (Figs. 6G, H). At TEM level, these stages exhibit the large chromatin blocks that are parts of the chromosomes, which are formed by the tight aggregation of individual 30 nm chromatin fibers (Fig. 14A). The organelles consisting mainly of RER and mitochondria appear in the cytoplasmic area surrounding the chromosomes which are no longer surrounded by the nuclear membrane (Figs. 13E, F; 14A, B; Table 1).

**Secondary spermatocyte (SSc)** assumes a more oval shape and becomes larger in size with diameter about 14-16 μm, while the nuclear diameter is about 7 μm(Fig. 6C). SSc is the result of the first meiotic division, and the cell is encountered infrequently.

Under LM, the nucleus shows 7 to 9 large clumps of heterochromatin along the nuclear envelope, and 1 to 2 clumps in the central area (Fig. 6C). Under TEM, the large clumps are made up of tightly packed 30-nm chromatin fibers, while 10-nm fibers are distributed in the nucleoplasm around the heterochromatin blocks (Figs. 14D, E; Table 1). The cytoplasm has similar features as those in the previous stages (Figs. 14C, F).

**Spermiogenic Cells and Spermatozoa**

There are ten stages of spermatids ($St_{1-10}$) depending on the size, nuclear shape and chromatin condensation pattern.

**Spermatid stage 1 ($St_1$)** This cell is about 15 μm in size and has round-shaped nucleus (about 6-7 μm in diameter). Under LM, the nucleus of this cell is smaller than that of spermatocyte, and the cell is located close to the lumen. It is stained light blue with only few small blocks of heterochromatin scattered throughout. The cytoplasm appears pale blue after staining with methylene blue, and also contains numerous mitochondria (Fig. 7A). Under TEM, the chromatin consists almost entirely of euchromatin which exists at 2 levels, *i.e.*, 10 nm and 30 nm (Fig. 15C; Table 1). There are only few small blocks of heterochromatin scattered in the central area of the nucleus. In addition to abundant mitochondria and some ribosomes, the cytoplasm also contains very large Golgi complex with multiple section, each consisting of 3-4 stacks of cisternae, interconnected with the neighbouring sections (Figs.15B, D-F). This "multisectorial" Golgi complexes show evidence of active secretory activities in the forms of two types of membrane-bound granules at trans-face. These two types of granules consist of the smaller and very dense proacrosomal granule and the

multigranular body which contains numerous dense vesicles within one membraneous sac (Figs. 15D, E, F).

**Spermatid stage 2 ($St_2$)** This round-shaped cell is about 20x12 μm in size and contains spherical nucleus which is about 5-6 μm in diameter. At LM level, it shows more densely stained nucleus due to increasing amount of heterochromatin (Fig. 7B). At TEM level, the nucleus, which is localized between Golgi complex and the group of mitochondria, is characterized by the thickening of the cephalic part of the nuclear membrane close to the Golgi complex (Figs. 16A-C). This is believed to be the site for adherence of acrosomal vesicle, and is the future apex of condensed sperm within the nucleus. There are patches of heterochromatin spreading throughout, and in the euchromatic area. The chromatin still exists in two sizes, *i.e.*, 10 nm and 30 nm (Figs. 16B, C; Table 1). The Golgi complex remains closely associated with the outer surface of the tentative acrosomal site of the nuclear membrane. This multisectorial Golgi complex still actively synthesize both types of granules, *i.e.*, the dense proacrosomal granules (Figs. 16D, F), and the "multigranular body", which may be formed by the the accumulation of dense core vesicles within a single large membrane sack (Figs. 16D. E).

**Spermatid stage 3 ($St_3$)** This cell has about the same size as $St_2$, but it contains smaller but still spherical nucleus. Under LM, increasing number of evenly-scattered heterchromatin blocks and patches are observed in the nucleus as dark blue stained bodies (Fig. 7C). Under TEM, the tightly aggregated 30-nm chromatin fibers make up the heterochromatin blocks and patches. Furthermore, the caudal nuclear membrane is also visibly thickened; and a large patch of heterochromatin made of the tight aggregation

of 30-nm fibers were observed to be tightly attached to this caudal the nuclear envelope (Figs. 17A-D; Table 1). Concurrently, there the large Golgi complexes migrate to the caudal part of the cell's cytoplasm and it comes to be localized near the clusters of mitochondria in the same region (Figs. 17A, E, F).

**Spermatid stage 4 ($St_4$)** This cell becomes oval in shape (about 20x11 μm) and the nucleus begins to be flattened on the caudal side facing the large group of mitochondria, where the nuclear envelope is markedly thickened with condensing chromatin mass, while the remaining chromatin appears lighter and has uniform density throughout the nucleus (Fig. 7D). Under TEM, the nucleus still contains 10-nm and 30-nm chromatin fibers (Figs. 18B-D; Table 1). At the cephalic and caudal parts of the nuclear membrane, the 30 nm fibers are aggregated in increasing amount causing these areas of the nuclear envelope to appear thicker and denser (Figs. 18A-D). The cytoplasm shows progressive migration to the caudal part of the cell and becomes more elongated, and the Golgi complexes are migrating further to the caudal end of the cytoplasm and is separated from the nucleus by a large group of mitochondria (Figs. 18E, F, G).

**Spermatid stage 5 ($St_5$)** This cell shows the nucleus which is highly flattened, with the caudal side more indented. Thus, the nucleus is transformed into oblong shape with the size about 2×7 μm. At LM level, the nucleus gradually migrates to the cephalic pole of the cell which assumes a comet shape (Fig. 7E). When observed under TEM, the chromatin, which comprises mostly of 30-nm fundamental fibers (Figs. 19 A, B; table 1), is evenly distributed, but becomes denser because of the decrease in size of the nucleus. The thickened caudal nuclear envelope shows the implantation fossa at the indented

region in which the centriole is lodged and becomes tightly linked with the caudal nuclear membrane. This is the beginning of the the tail formation, while the rest of the tail which consists of the axoneme extends from the distal centriole. The clusters of mitochondria are observed surrounding the axoneme (Fig. 19A, B).

**Spermatid stage 6 ($St_6$)** This cell has similar features as $St_5$ except the nucleus is gradually compressed in the cephalo-caudal direction to become a curved disc. Under LM, the nuclear is stained intensely blue due to the evenly condensed chromatin (Fig. 8E). Under TEM, the random-coiled 30-nm chromatin fibers gradually straightened into smaller filaments about 20 nm in diameter that corresponds to level 3 (Figs. 19C, D; Table 1). These chromatin fibers are dispersed throughout the nucleoplasm and are more tightly packed hence the nucleus appears denser. The developing acrosome can be found at the cephalic pole of the nucleus (Figs. 19E, F), while of the tail has extended further from the centriole (Fig. 19C).

**Spermatid stage 7 ($St_7$)** The nucleus is bent further to assume an arrow- or boomerang-like shape (about 3×7 μm) (Figs. 7F, 8A). At LM level, the chromatin is highly condensed and appears more intense in comparison to the preceding stages. The cytoplasm is lightly stained, while the dense granulated structures which assume to be mitochondria become concentrated in the caudal cytoplasm around the forming tail (Fig. 7A). At TEM level, the conformation of 20-nm chromatin fibers (level 3) in $St_6$ changes from partially coiling to assume the straight-parallel conformation (level 4), with each chromatin fiber about 14 to 16 μm in thickness; and these fibers seem to extend in

parallel from the caudal to the cephalic parts of the nuclear envelope (Figs. 20A, B, C; Table 1).

**Spermatid stage 8 ($St_8$)** The nucleus of this stage has a pear shape due to the "pulling in" of the wings of the arrow-shaped nucleus of $St_7$ (Figs. 20D, E, F) similarly to the folding of an umbrella. Under LM, the nucleus is stained dark blue, and in the concavity of the caudal side of the nucleus the centriole becomes the proximal part of the tail which exhibits marked elongation (Fig. 8B). Under TEM, the nucleus shows completely straight chromatin fibers (level 4) which extend in the parallel conformation from the caudal to the cephalic parts of nuclear membrane (Figs. 20E, F; Table 1). The connecting piece of the tail is completely formed and appears as the crystal-liked structure around the centriolar-axonemal complex, while the remaining portions of the tail are still growing and developing.

**Spermatid stage 9 ($St_9$)** This cell has a paddle-like shape. Its nucleus starts to elongate with increasingly tapered anterior end to become cone-like shape. Under LM the nucleus is stained to the same intensity as in the preceding stage, while the cytoplasm is stained light blue (Fig. 8B). The tail is filled with numerous mitochondria which are concentrated around the axoneme; and the Golgi complexes are translocated to the most caudal end of the cell which still has a considerable mass of cytoplasm. As revealed by TEM, the straight-paralleled chromatin fibers (level 4) are closely packed to become large parallel bundles each measured about 110 to 117 nm in width Figs. 22B-F; Table 1). Each bundle consists of 7 to 10 fibers tightly packed together, and separated from other bundles by light narrow channels (Figs.22B, C). However, there are still a few

isolated level 4 straight fibers. This stage shows the almost complete formation of the tail which is recognizable by many structures that ensheath the axoneme (Fig. 21).

In the present study, the tail complex of stage 9 spermatid could be divided into 6 levels according to the cross sectional characteristics (Fig. 21). The first level is the region of the base of the nucleus which is indented by the centriolar core (Figs. 22D, E). The second level consists of the crystal-liked structure surrounding the centriolar-axoneme core (Figs. 22D, F). The third level is composed of 4-5 layers of mitochondrail derivatives that are surrounding the axoneme-fibrous sheath complex (Figs. 23A, B). The fourth level is equivalent to the mid-piece of mammalian sperm and consists of the segment of the tail surrounded by 4 layers of mitochondria derivative (Figs. 23C, E). The fifth level shows the reduction of mitochondria derivative to one layer around the axoneme-fibrous sheath complex (Figs. 23D, E). The sixth level passes through the caudal most end of the tail where the Golgi complex is reduced in size but still remains in the multisectorial fashion (Figs. 23F, G; 24A). During the formation of the complex tail of stage 9 spermatid, there may be a newly formed mitochondria where membrane are derived from the Golgi complex. These newly formed mitochondria exhibiting mitochondrial sheaths wrap around the axoneme fibrous sheath complex of the tail (Figs. 24A-F).

**Spermatid stage 10 ($St_{10}$)** This cell has a long slender shape with the size about 6x2 μm. Its nucleus is elongated to form a spindle-shaped head which is still embedded in the cytoplasm of the Sertoli cell cytoplasm. The excess cytoplasm (residual body) of the cell is released from the head and remains only at the caudal part of the cell (Fig. 8C).

Under TEM, the chromatin consists of thick bundles, each measured about 110 to 120 nm in width (Figs. 25D-F; Table 1). And each bundle is composed of closely packed 7-10 level 4 straight fibers.

The acrosome is now completely formed at the most anterior tip extending beyond the nucleus (Figs. 25A-C). It looks like a dense cup fitting over a dense cylindrical rod which represents the anterior tip of the sperm head. The cell membrane covers the entire acrosomal complex (Figs. 25A-C). Thus the tail is completely formed (Fig. 8D).

**Spermatozoa (Sz)** There are 2 stages of spermatozoa: $Sz_1$ is the immature spermatozoon that begins to show highly elongated nucleus with dense chromatin, a very small acrosome which is not visible in semithin sections, and a very long helical tail without surrounding cytoplasm (Fig. 8E). Under TEM the nucleus shows dense chromatin that exists in crystalline-like lattice, in which the individual fiber appears as straight line about 10 nm in width, separated from its neighbor by the intervals 3-4 nm in width. However, in $Sz_2$, there are still some oval lightly-stained spaces left in the nucleus (Figs. 26A-D).

The mature spermatozoa ($Sz_2$) are aggregated in a large group embedded in the cytoplasm of the Sertoli cells (Figs. 8E; 27A). The nucleus is fully elongated and slightly tapered at the anterior end with the size about 6x1 μm. Under LM, the spermatozoon shows fully elongated and falciform-shaped nucleus (about 1x7 μm in size) with completely dense chromatin, and it has a very long tail which lacks the surrounding cytoplasm. At TEM level, although the nucleus is homogeneously dense, the crystal-

lattice-liked conformation could still be observed. Each space between the crystal lattice is at constant length about 3-4 nm (Figs. 27B, D; 28B-E).

The tail of mature spermatozoon represents one of the most complex structure among the animal sperm's tail. Along its entire length, the tail consists of two columns of cytoplasm and axoneme-fibrous sheath complex twisted around each other in helical formation along the long axis (Figs. 25A; 26A). Therefore, the tail could be divided into eight levels based on the structures that surround the axoneme and the cross sectional profiles.

The first level ($L_1$) is the neck region which is the top portion of centriolar core. This level shows the centriolar core of the flagellum surrounded by homogeneous structure which filled up the inner portion of implantation fossa at the base of nucleus (Figs. 27E, F).

The second level ($L_2$) is located below $L_1$ and consists of the crystal-like structures around the axoneme-fibrous sheath complex, with the latter consisting of nine longitudinal dense rods (Fig. 26C-E; 27E, F).

The third level ($L_3$) contains the most caudal part of the nucleus and concentric lamellae of mitochondria derivatives of mitochondria surrounding axial complex complex filament (Figs. 28C-F; 28E; 29A-C). There is the beginning of cytoplasmic column nearby (Fig. 28E; 29A).

The forth level ($L_4$) is the mid-piece of the tail (Figs. 18D, E; 29D, E), which shows 4-6 layers of concentric lamellae of mitochondria derivative around the axial

complex and the cytoplasmic column surrounded by mitochondria derivatives around containing glycogen on one side of the axial complex (Figs. 29D, E).

The fifth level ($L_5$) has only one layer of mitochondrial derivatives. Within the cytoplasmic column, there are numerous glycogen granules (Figs. 30A-D). The cytoplasmic column is filled with glycogen granules (Figs. 30A-D).

The sixth level ($L_6$) has similar features as $L_5$ , but there is no mitochondria layers. The fibrous sheath around the axoneme is also absent but the axonemal complex and the cytoplasmic column is surrounded by 2-3 layers of fence-liked cylindrical sheath (Figs.30D, E).

The seventh level ($L_7$) is similar to $L_6$, but it is characterized by the disappearance of the cytoplasmic column (Fig. 30 G).

The eighth level ($L_8$) is the last portion of the tail which consists of the axoneme covered only by the plasma membrane (Fig. 30H).

## Sertoli Cell and Follicular Cell

Sertoli cell is the largest cell in the ovotestis, and it could be easily distinguished by the large round nucleus with regularly arranged heterochromatin patches (Figs. 8A; E, 31A-C). The cytoplasm contains numerous lipid droplets and few large dense granules (Fig. 8E). When observed under TEM, these dense heterochromatin patches are scattered evenly throughout, and there is a deep indentation at one side of the nucleus (Figs. 31A, C). The cytoplasm is branched into long processes: the basal processes maintain continuous contact with the follicular cells and the basal lamina, and the apical processes

extend to the lumen of the ovotestis' tubules, and some are in contact with spermatocytes and spermatids. Numerous organelles that appear include lysosomes, abundant rough endoplasmic reticulum, large amount of mitochondria, and a relatively small Golgi complex (Figs.31C-F).

The follicular cell is located on the basal lamina adjacent to the Sertoli cells (Figs. 32E, F; 33A, B). It has an ovoid nucleus with thin strip of heterochromatin lining the inner surface of the nuclear envelope, and small blocks scattered in the center of nucleoplasm. The cytoplasm shows moderate amount of mitochondria and many small granules consisting of a dense core surrounding by light halo ring. It also has long processes of cytoplasm, that together with the processes of the Sertoli cell, line on the basal lamina of the tubules (Figs. 32A; E, F; 33A-C). Thus, the cellular sheet lining the basal lamina is composed of the cytoplasmic processes of Sertoli cells interdigitated with each other, and with those of the follicular cells (Figs. 32A; 33C-F). Invariably, the long processes of the Sertoli cell's cytoplasm usually cover the long cytoplasmic processes of follicular cells. Hence, this cellular sheet separates spermatogenic cells from the basal lamina. The final maturation of spermatids also takes place in the cytoplasm of Sertoli cells. Occasionally, desmosome can be seen between spermatocytes, spermatids and Sertoli cells (Fig. 32C).

**Figure 1.** Surface anatomy of *Achatina fulica*

A) Photomicrograph of an adult *A. fulica* in the late rainy season showing shell (sh), foot process (fp), and 2 cephalic tentacles, *i.e.*, anterior (at) and posterior (pt).

B) Photomicrograph of an adult *A. fulica* in the early rainy season showing shell (sh), foot process (fp), 2 cephalic tentacles, *i.e.*, anterior (at) and posterior (pt), and prominent penis at the common genital pore (co).

C) An adult snail is feeding on a fruit in the early rainy season.

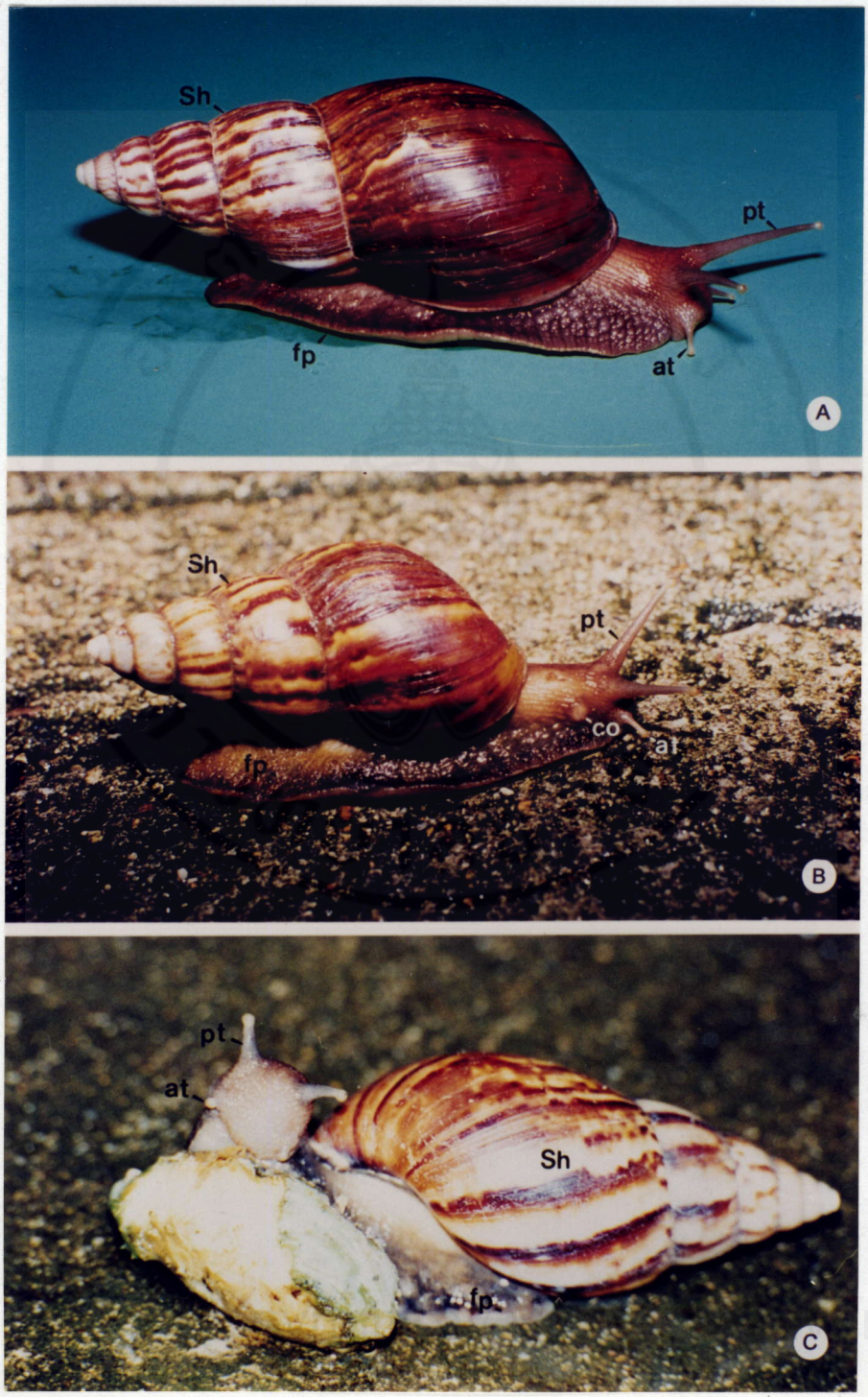
Sh
pt
fp
at
A
Sh
pt
co
at
fp
B
pt
at
Sh
fp
C

**Figure 2.** Copulation of *A. fulica*

A, B) Photomicrographs of two adults *A. fulica* in the early rain season showing their muscular penis (pe) which are everted and inserted into the vagina of their partners.

**Figure 3.** Gross anatomy of *A. fulica*

A) Photomicrograph of a giant land snail after removal of the coiled shell. The ovotestis (ov) appears yellow in color, and is embedded and mixed with the coiled digestive gland (dg) at the caudal part. It is connected with the albumen gland (alg) via the hermaphroditic duct (hd). The cephalic part in A. also shows the retracted head (he) and the foot process (fp).

B) Macrophotograph of the same specimen showing the ovotestis (ov) embedded in the coiled digestive gland (dg), hermaphroditic duct (hd), and albumen gland (alg).

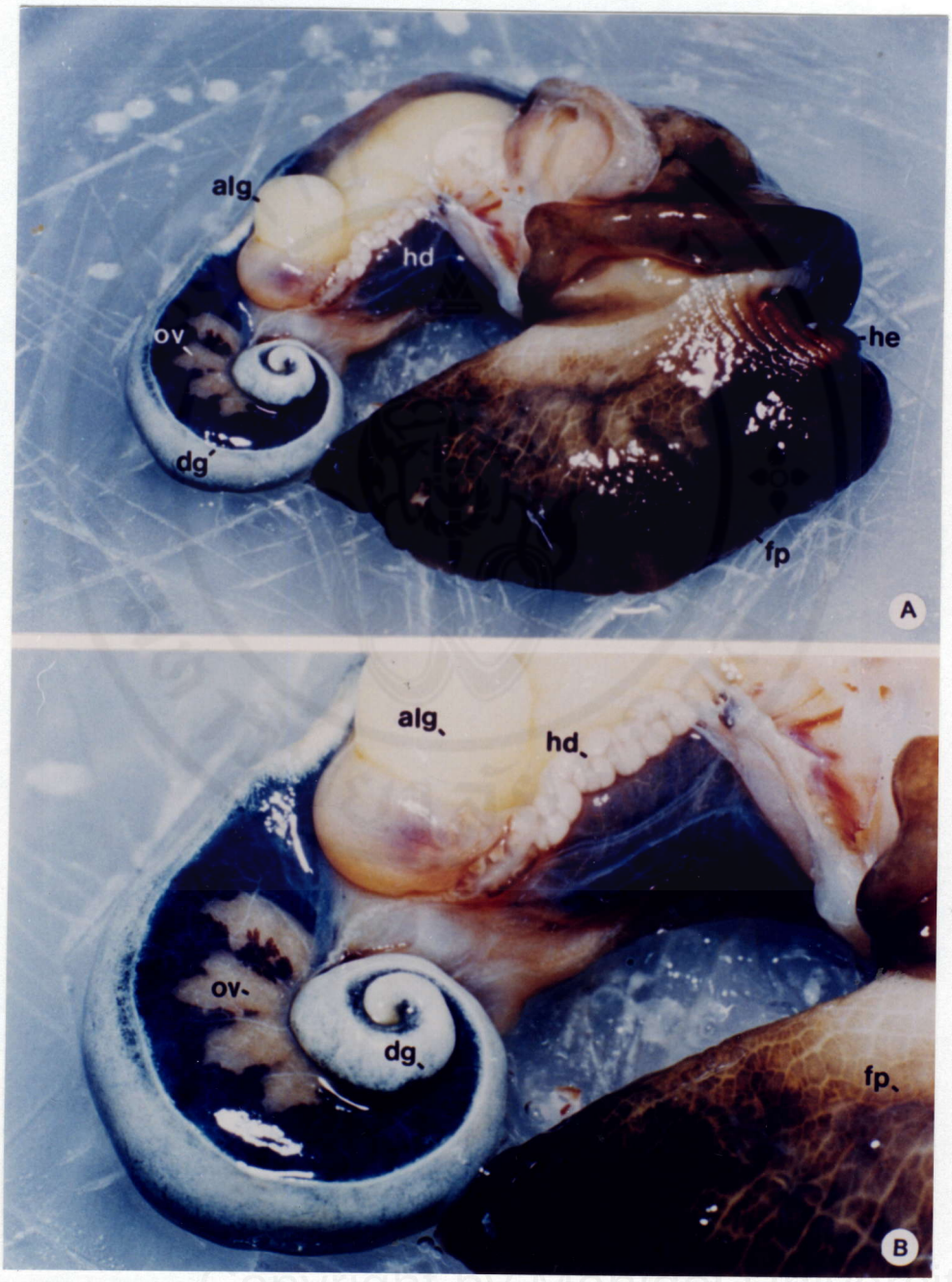

**Figure 4.** The reproductive system of *A. fulica*

A) Photomicrograph of *A. fulica* after removal of the shell and mantle showing the visceral organs. (alg-albumen gland; dg-digestive gland; hd-hermaphroditic duct; P-prostate gland; vd-vas deferens; ov-ovotestis)

B) Further dissection of the body showing that the reproductive system is divided into male and female pathways. The male pathway consists of the prostate gland (P), vas deferens (vd), and penis (pe) located in the common genital opening. The female pathway mainly consists of the uterus (ut), oviduct, and vagina that is connected to the same genital opening. (dg-digestive; sp-spermatheca)

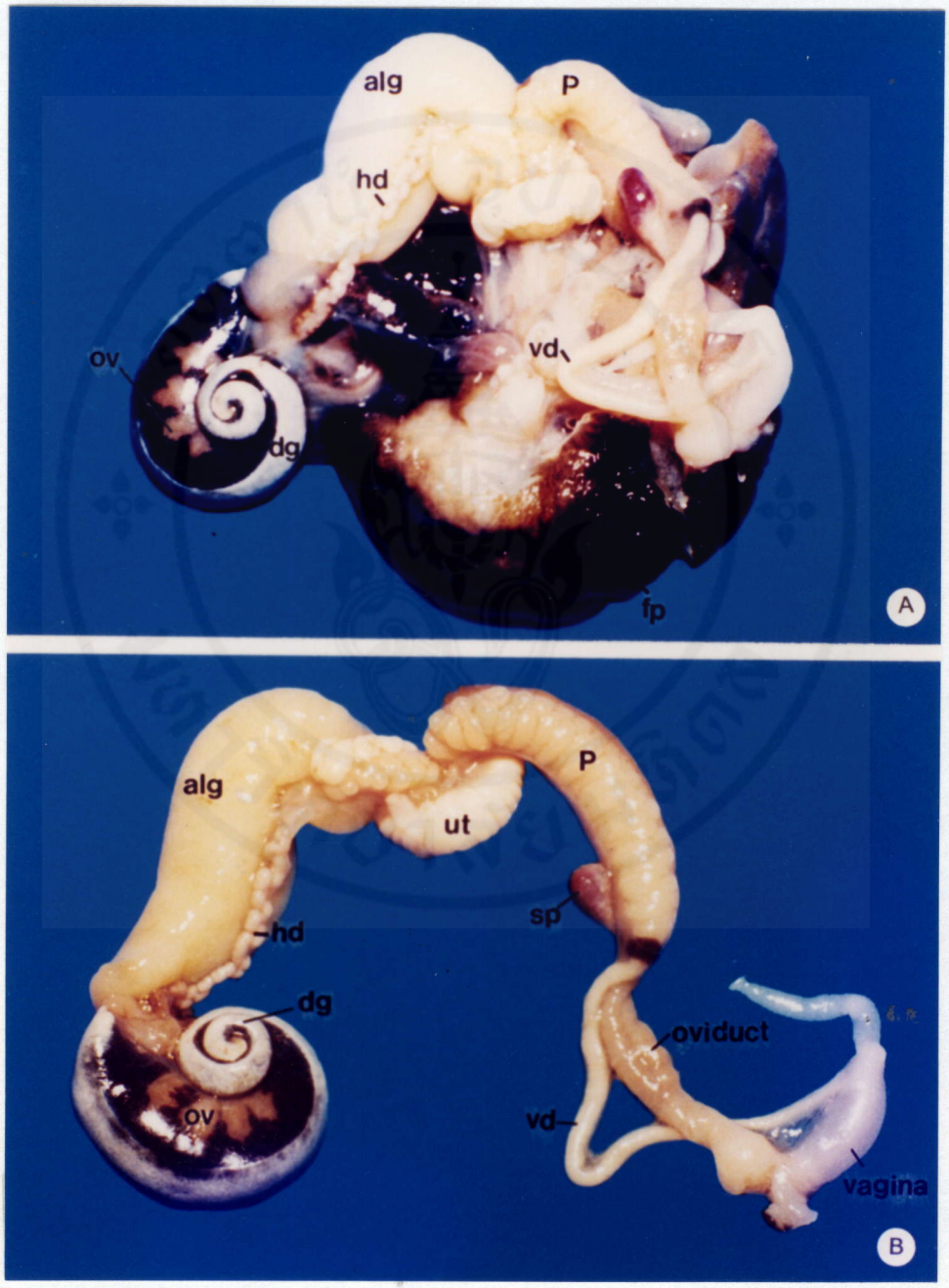

**Figure 5.** Photomicrographs of *A. fulica* stained with hematoxylin and eosin (H&E), and with methylene blue (MB)

A, B, C) Paraffin sections of the ovotestis of *A. fulica* showing tubules (Sm) containing both developing male germ cells (Sc, St, Sz) and female germ cells (Oc). The center of each tubule is filled with the tails of spermatozoa. Tubules are separated by loose connective tissue containing fat cells (fa), and parts of the digestive glands (dg) are located within the same vicinity.

D) Semithin section of a tubule of an ovotestis showing germinal epithelium consisting of developing male germ cells (Sc, St) and packets of spermatozoa (Sz), and a female germ cell (Oc).

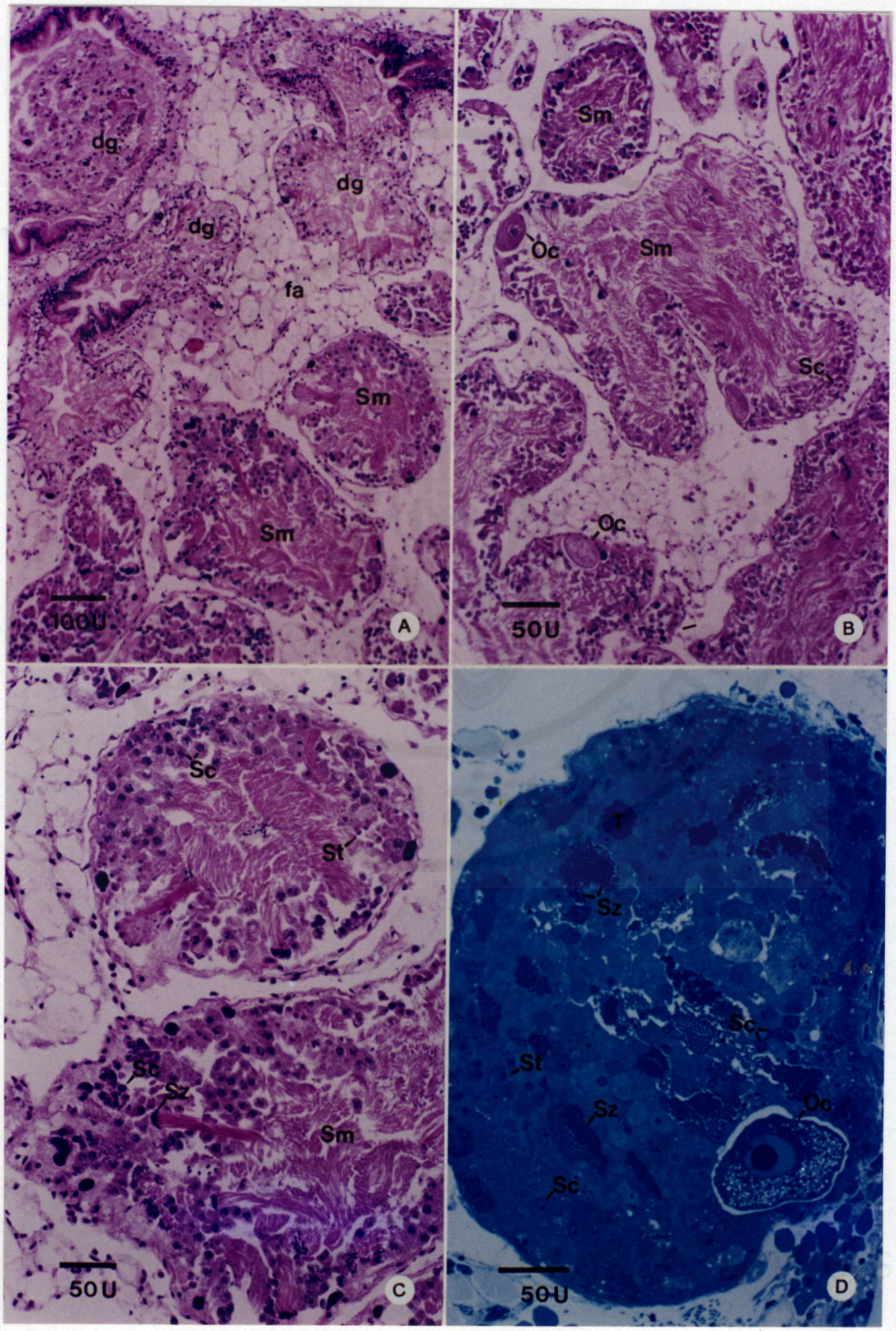
dg
dg
dg
fa
Sm
Sm
100U
A
Sm
Oc
Sm
Sc
Oc
50U
B
Sc
St
Sc
Sz
Sm
50U
C
T
Sz
Sc
St
Sz
Oc
Sc
50U
D

**Figure 6.** Semithin sections of *A. fulica*'s tubules stained with MB showing various stages of cells in spermatogenesis:

A, B) Spermatogonia are the smallest cells ranging from those that have clear nuclei with prominent nucleoli and thin rims of pale blue or slightly basophilic cytoplasm (Sg-in A) to those that are larger with nuclei having lace-like heterochromatin, prominent nucleoli and increased amount of basophilic cytoplasm (Sg-in B).

C) Leptotene primary spermatozytes (LSc), each showing dense dots of heterochromatin scattering throughout the nucleus which still contains small nucleolus. The cytoplasm has light basophilia and contains a large member of mitochondria (arrow). Secondary spermatocytes (SSc) exhibit clumping of heterochromatin into large blocks along the nuclear envelope and in the center of the nuclei.

D) Zygotene primary spermatozytes (ZSc), each exhibiting thicker blocks of heterochromatin which become cord-liked. The nucleolus is sizable (arrow).

E) Pachytene primary spermatozytes (PSc), each showing intertwining thick chromatin cords and very prominent nucleolus (arrow). (T-tail, Sz-spermatozoa)

F) Diplotene primary spermatocytes (DSc), each exhibiting small nucleus with closely packed thick cords of chromatin.

G, H) Diakinetic primary spermatocytes (DiSc), each showing large and fewer pieces of chromosomes that are moving to be aligned in a row at the equatorial region in metaphase spermatocyte (MSc-in H and F).

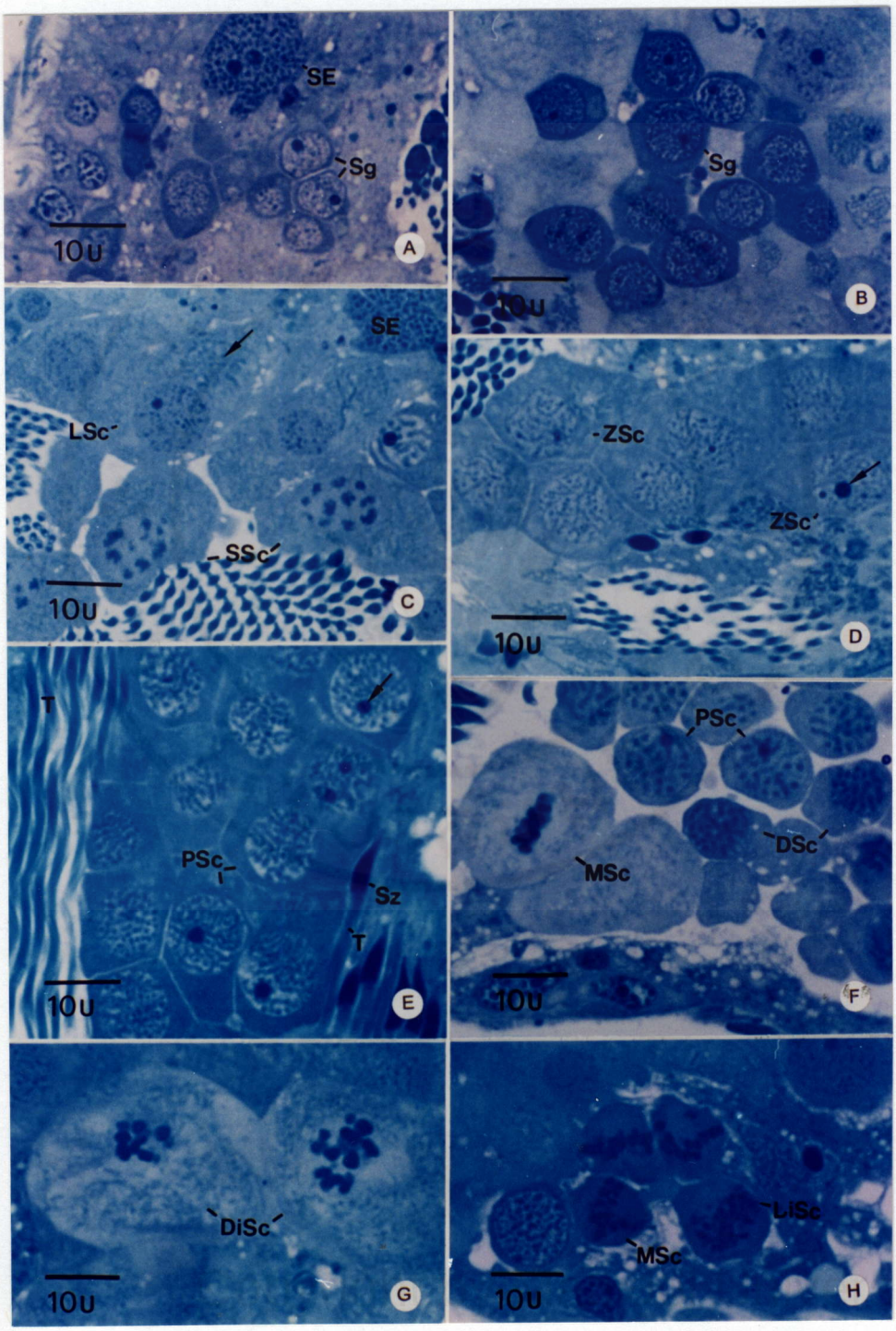
SE
Sg
10u
A
Sg
10u
B
SE
LSc
SSc
10u
C
ZSc
ZSc
10u
D
T
PSc
Sz
T
10u
E
PSc
DSc
MSc
10u
F
DiSc
10u
G
LiSc
MSc
10u
H

**Figure 7.** Semithin sections of *A. fulica*'s tubules stained with MB during early spermatids:

A) The nucleus of stage 1 spermatid (1) is much smaller than in PSc and SSc but is still round and contains fine granules of heterochromatin. The cytoplasm is lightly basophilic and contains numerous mitochondria (arrow).

B) In stage 2 spermatid (2), the nucleus is decreased in size and appears denser, while becoming more eccentrically-located. The main mass of cytoplasm moves to one side and contains numerous mitochondria (mi) as well as a very large Golgi complex (gc).

C) In stage 3 spermatid (3), the nucleus is decreased further in size but nucleoplasm becomes denser and contains larger blocks of heterochromatin. The cytoplasm contains large Golgi complex (gc) and numerous mitochondria.

D) In Stage 4 spermatid (4), the nucleus becomes uniformly dense with one side marked by thickened chromatin mass along the nuclear envelope (arrow). The cytoplasm assumes an oval shape and contains numerous mitochondria (mi) in tight cluster.

E, F) In stage 5 spermatid (5), the nucleus assumes flat disc and is translocated to one side of the cell, and the trailing cytoplasm contains numerous mitochondria (mi). In stage 6 spermatid (6), the nucleus is more oblong and assumes a curved disk-shape, while in stage 7 spermatid (7) the nucleus becomes opaque due to the fully condensed chromatin, and it assumes an arrow or boomerang-shape. (Oc-oocyte)

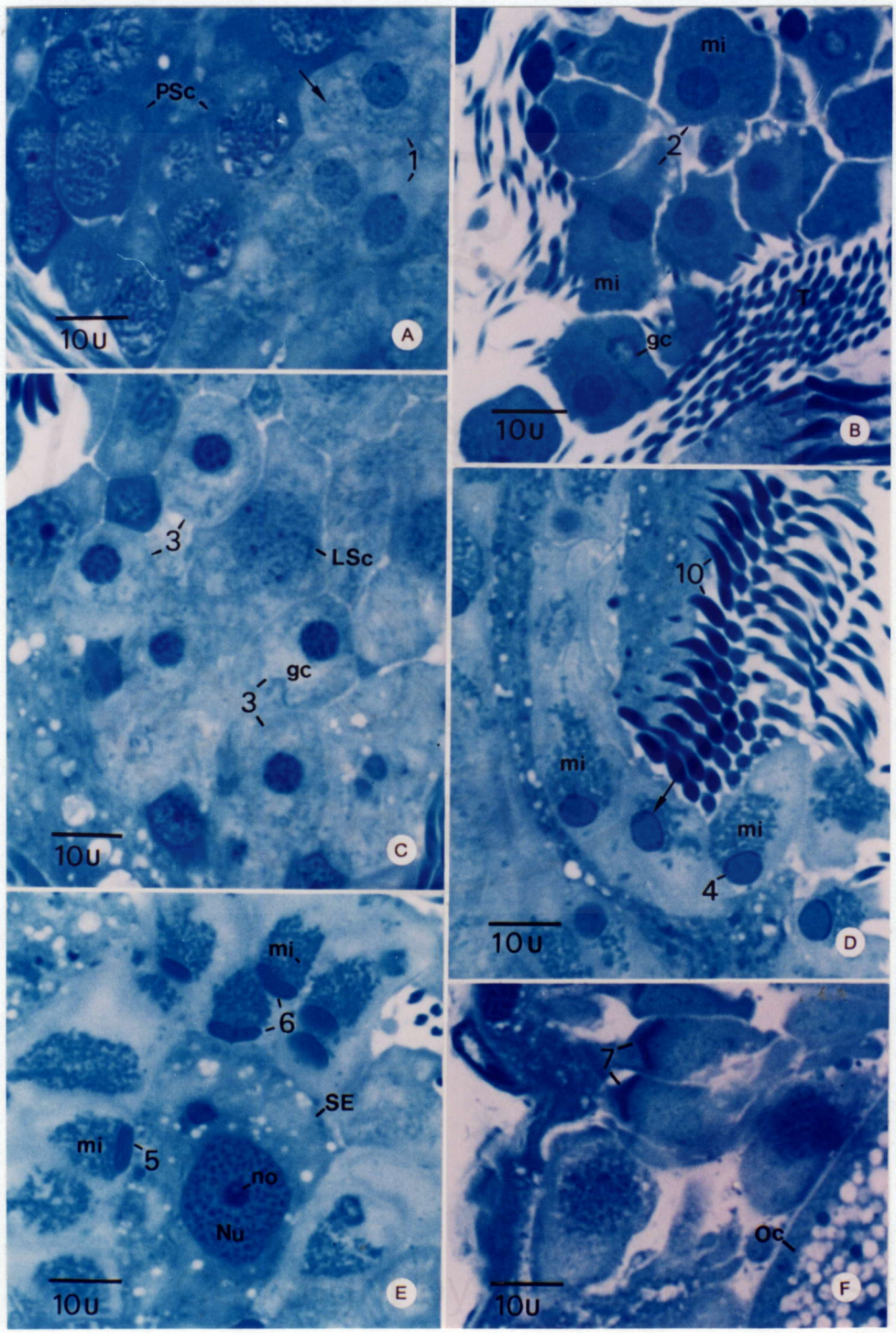
PSc
1
10u
A
mi
2
mi
T
gc
10u
B
3
LSc
gc
3
10u
C
10
mi
mi
4
10u
D
mi
6
SE
mi
5
no
Nu
10u
E
7
Oc
10u
F

**Figure 8.** Semithin sections of *A. fulica*'s tubules stained with MB showing late spermatids:

A) Stage 7 spermatid (7) showing boomerang-shaped nucleus with completely condensed chromatin and numerous mitochondria (mi) in the trailing cytoplasm.

B) Stage 8 spermatid (8) showing cone-shaped nucleus with completely condensed and opaque chromatin, and the long tail sprouting out from the nuclear fossa (arrow). Mitochondria (mi) become concentrated around the tail (T) and Golgi complexes (gc) move to the caudal end of the trailing cytoplasm.

C, D) Stage 9 spermatid (9-in C) showing a dense oval-shaped nucleus with the opaque chromatin. The tail (T) is fully lengthened and surrounded by numerous mitochondria. Golgi complex is much decreased in size. In stage 10 spermatids (10-in C and D), the anterior end of the completely opaque nucleus becomes pointed and slightly curved.

E) Fully mature spermatozoa (Sz) showing elongated and falciform-shaped nuclei which are completely opaque. The tails (T) become cylindrical and devoided of the cytoplasmic mass. Groups of spermatozoa have their heads embedded within the apical cytoplasm of a Sertoli cell (SE), which is the largest cell whose nucleus contains uniform patches of heterochromatin, and the cytoplasm contains numerous lipid droplets (ld) and a few dense granules (arrow). (Nu-nucleus)

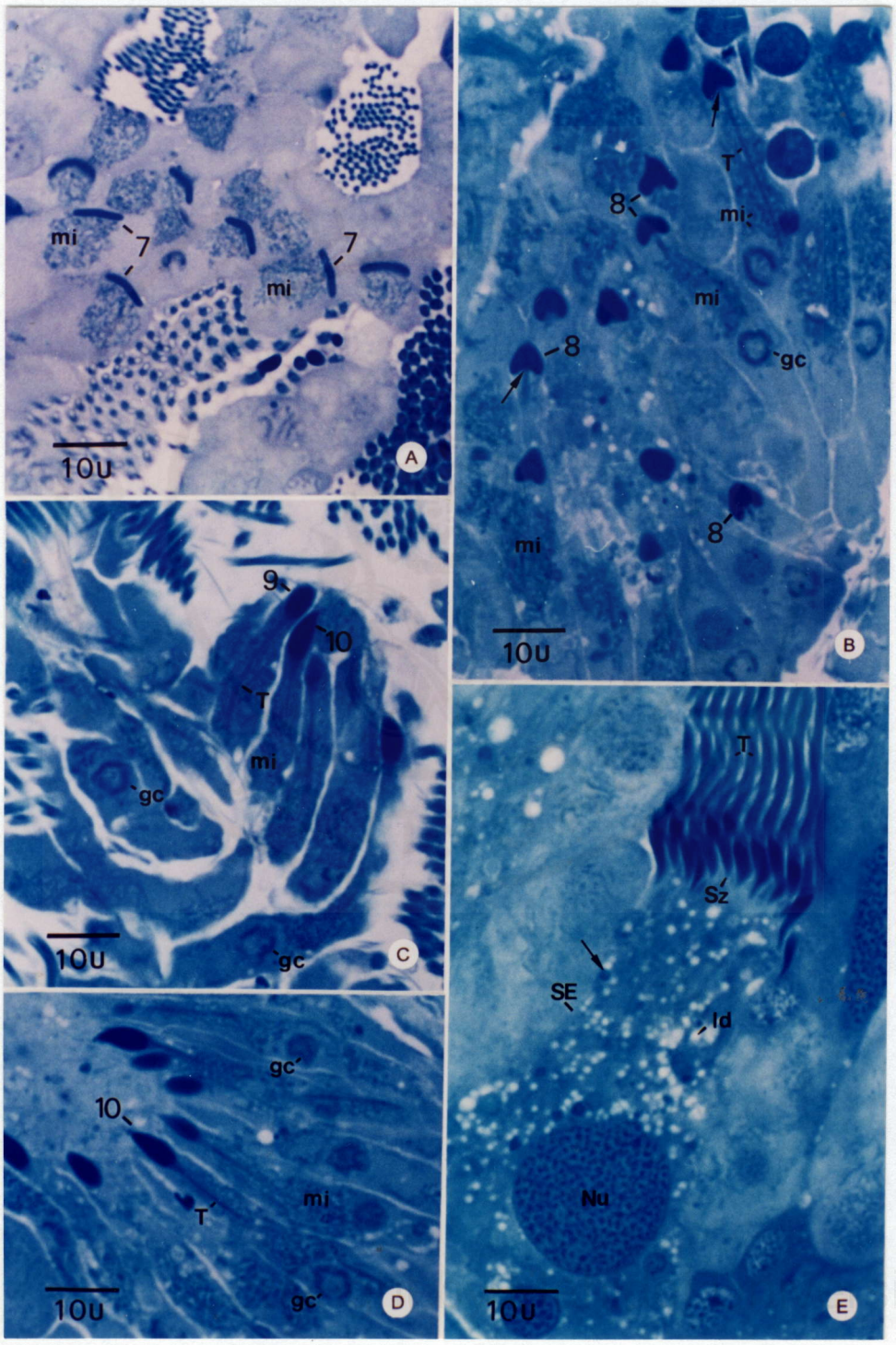
mi
7
7
mi
10u
A
T
8
mi
mi
8
gc
8
mi
10u
B
9
10
T
mi
gc
10u
gc
C
T
Sz
SE
Id
Nu
10u
E
gc
10
mi
T
10u
gc
D

**Figure 9.** Classification of cells in *A. fulica*'s tubules under TEM

A) TEM micrograph of the basal part of the tubules showing that the Sertoli cell (SE) has the largest nuclei containing scattered heterochromatin (hc) and a prominent nucleolus (no) and it is located on the basement membrane (bm). In the nearby area, there are the follicular cells (fc) with oval nucleus and cytoplasm rich in mitochondria (mi).

B) An adjacent area showing spermatogonia (Sg) whose round-shaped nuclei contained mostly euchromatins.

C, D) Higher magnifications showing prominent nucleolus surrounded by thin zigzag 10 nm (1) and 20 nm (2) whose cross sections appear as dense dots of heterchromatin.

E, F) A nearby area in the cytoplasm showing developing rough endoplasmic reticulum (rer), small amount of mitochondria (mi), and small Golgi complex (gc).

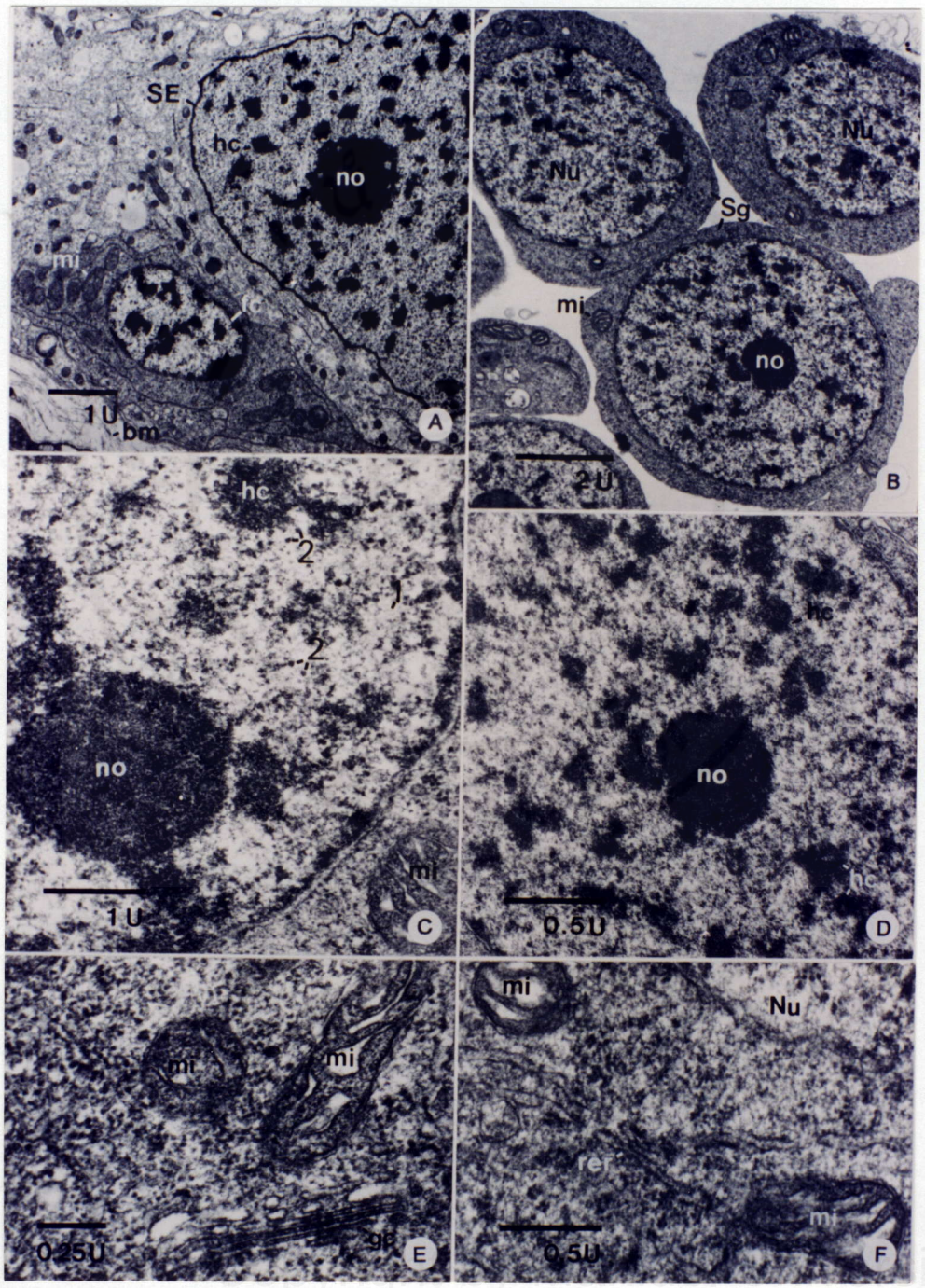
SE
hc
no
mi
rc
1 U
bm
A
Nu
Nu
Sg
mi
no
2 U
B
hc
2
1
2
no
mi
1 U
C
hc
no
0.5U
D
mi
mi
mi
0.25U
gc
E
mi
Nu
rer
mi
0.5U
F

**Figure 10.** Electron micrographs of leptotene primary spermatocyte

A, B) The early leptotene primary spermatocyte (LSc) showing the round nucleus (Nu) and the cytoplasm containing increasing number of mitochondria (mi) and larger Golgi complex (gc).

C-F) Another of leptotene stage showing a large nucleus with prominent nucleolus (no), and the first appearance of dense lines that form axis of chromatin condensation (ax). In E. and F., the chromatin fibers exist 2 levels: the thin zigzag 10-nm fibers (1) and 30-nm fibers whose cross sections appear as dense dots (2). Small blocks of heterochromatin are formed by the tightly packed 30-nm fibers. In F. the axis of chromatin condensation is surrounded by a tight aggregation of 30-nm fibers (2).

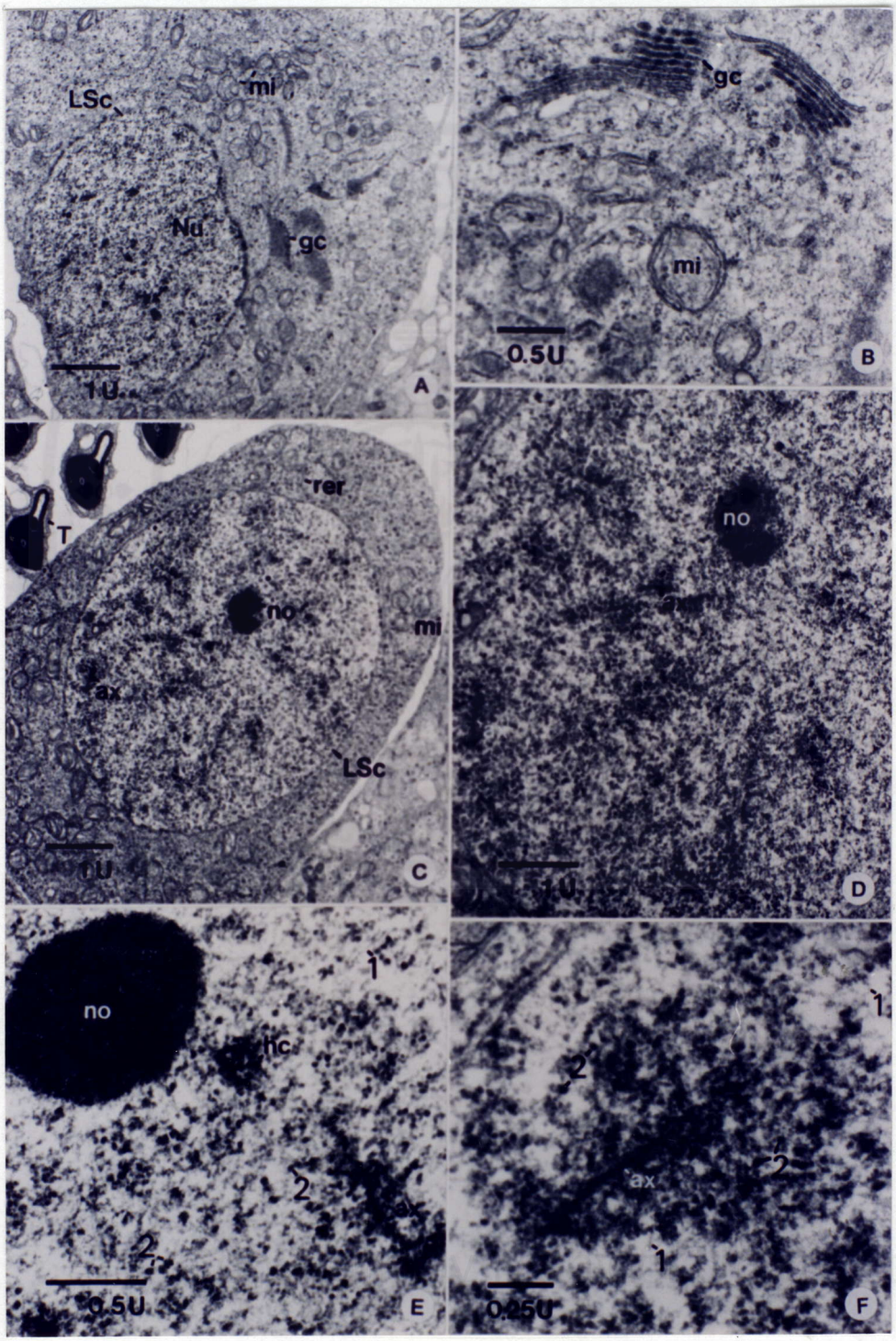
LSc
mi
Nu
gc
1U
A
gc
mi
0.5U
B
rer
T
no
mi
ax
LSc
1U
C
no
1
2
2
0.5U
E
no
1
2
2
ax
1
0.25U
F

**Figure 11.** Electron micrographs of zygotene primary spermatocytes

A, B) Zygotene primary spermatocytes (ZSc) showing the nucleus with increasing density of heterochromatin, and longer axis of chromatin condensation and synaptonemal complex (sy) that could not be found in the previous stages.

C, D) High magnifications showing the axis of chromatin condensation (ax) and the chromatin that still appear in 2 sizes: 10 nm (1) and 20 nm (2) fibers.

E, F) High magnifications the appearance of tripatite structure of synaptonemal complex showing a conspicuous central element separated from and paralleled to the two lateral elements. In F. shows that the nucleolus (no) is still fairly prominent as in LSc.

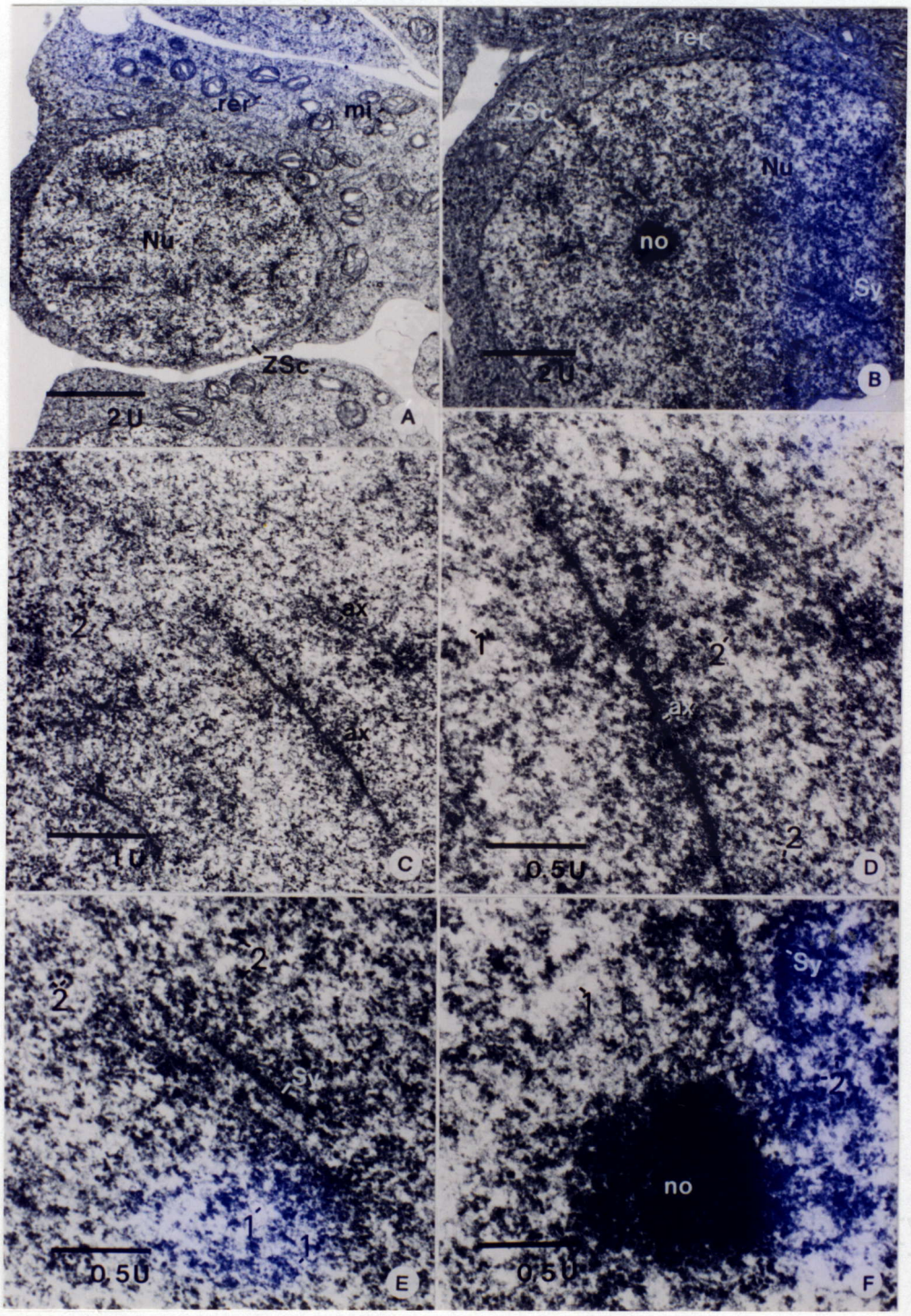
rer
mi
Nu
ZSc
2u
A
rer
ZSc
Nu
no
Sy
2u
B
2
ax
ax
1u
C
1
2
ax
0.5u
2
D
2
2
Sy
1
1
0.5u
E
Sy
1
2
no
0.5u
F

**Figure 12**. Electron micrographs of pachytene primary spermatocytes

A-C) Pachytene primary spermatocytes, each showing smaller sizes of the nuclei (Nu) with still fairly prominent nucleoli, and the heterochromatin (hc) becomes condensed into long thick threads.

D, F) At high magnifiication, these chromatins show a dense interconnected clumps of heterochromatin (hc). The 10 nm fibers (1) and 30 nm (2) fibers are also shown in D and the cytoplasmic organelles in F. show the larger size of Golgi complex (gc), mitochondria (mi) and RER (rer).

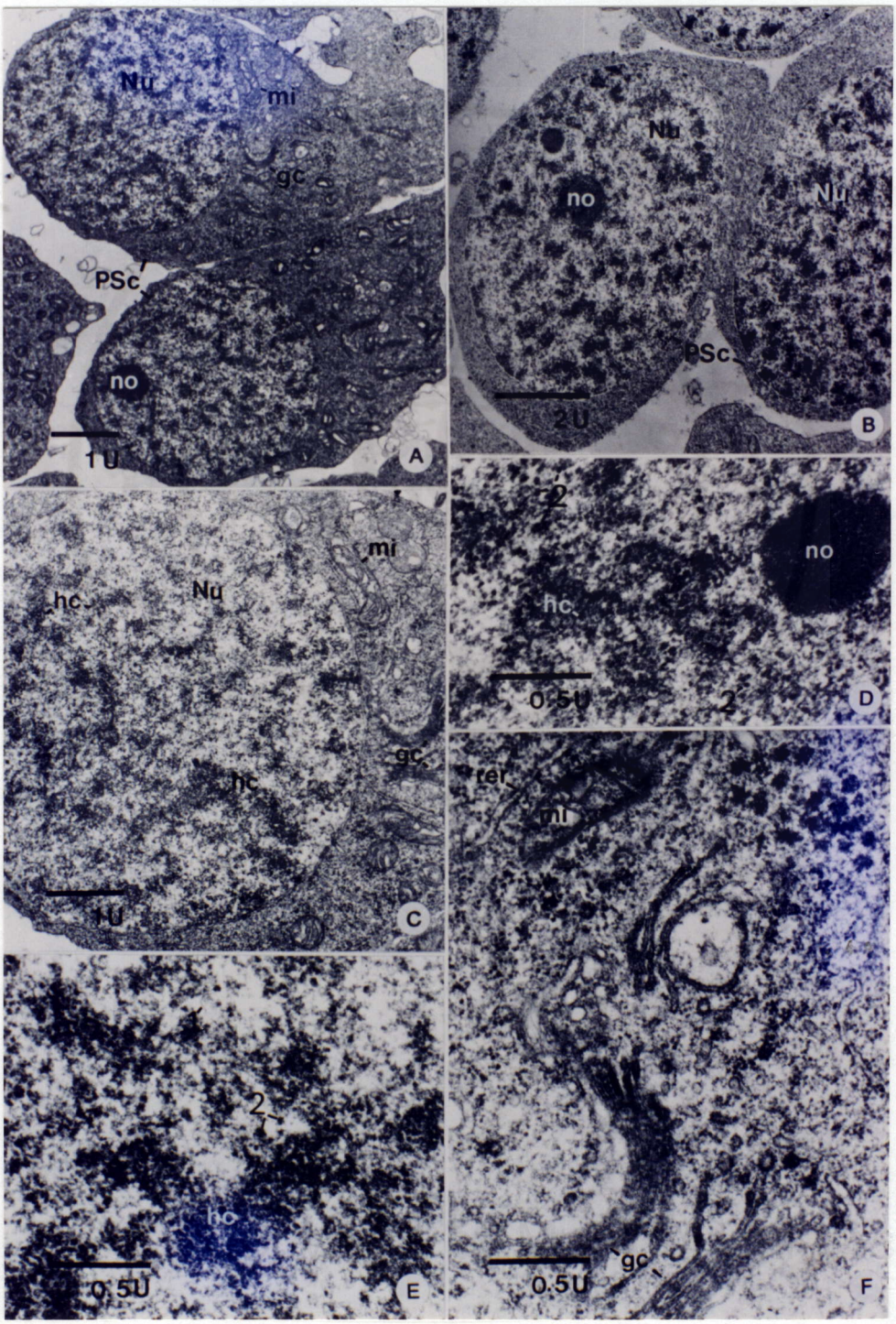
Nu
mi
gc
PSc
no
1 U
A
Nu
no
Nu
PSc
2 U
B
mi
hc
Nu
gc
hc
1 U
C
2
no
hc
0.5 U
2
D
2
hc
0.5 U
E
rer
mi
gc
0.5 U
F

**Figure 13.** Electron micrographs of diplotene and diakinesis primary spermatocyte

A, B) Diplotene primary spermatocyte (DSc) showing the smaller sized nucleus with more tightly packed heterchromatin. The cytoplasm also shows the increasing size of Golgi complex (gc) and the clusters of mitochondria (mi) which are scattered around the cell.

C, D) The nucleus of this cell has more heterochromatin than euchromatin; and chromatin fibers also exist 2 sizes, i.e., 10 nm and 30 nm fibers (1, 2 respectively). Figure C. shows that packing of chromatin occurs at the nuclear envelope (NE). Figure D. shows that the packing also occurs in the central area.

E, F) Diakinesis primary spermatocyte (DiSc) showing large blocks of heterochromatin that are parts of the completely formed chromosome (ch). The cytoplasm consists of RER and mitochondria (mi) which are seen around the nucleus.

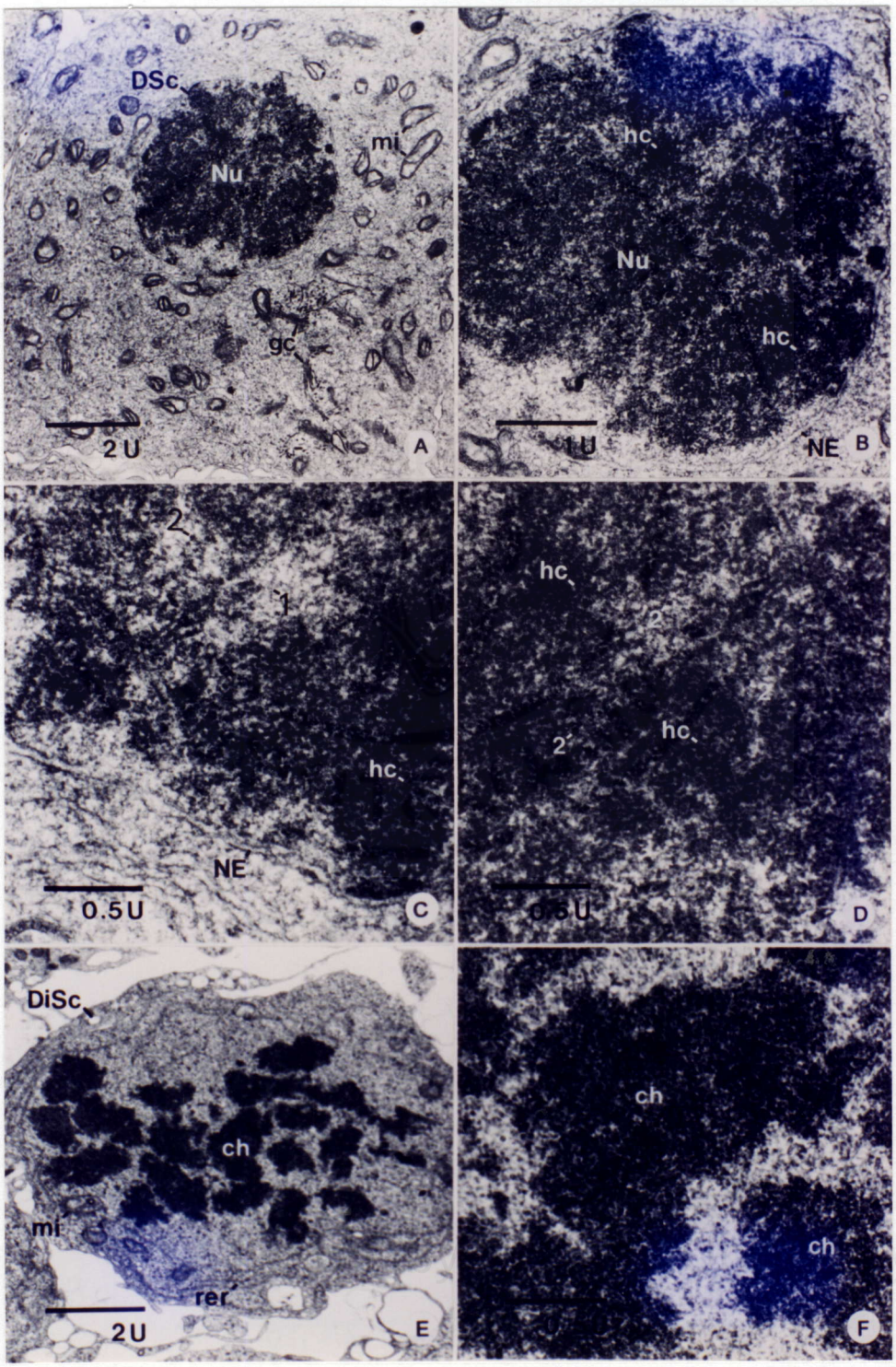
DSc
Nu
mi
gc
2 U
A
hc
Nu
hc
1 U
NE
B
2
1
hc
NE
0.5 U
C
hc
2
2
hc
0.5 U
D
DiSc
ch
mi
rer
2 U
E
ch
ch
F

**Figure 14.** Electron micrographs of metaphase primary spermatocyte and secondary spermatocyte

A, B) Metaphase primary spermatocyte (MSc) containing large blocks of heterochromatin which are pieces of chromosomes (ch). In B., the chromatin blocks are formed by a tight aggregation of 30-nm fibers. There are large amounts of mitochondria (mi) in the cytoplasm.

C-F) Secondary spermatocyte (SSc) whose nucleus contains large clumps of thick chromatin (hc) scattered throughout and attached to the nuclear envelope (NE). The chromatin each still maintains the sizes of 30-nm (2) and 10-nm chromatin fibers. The cytoplasm contains similar features as in the preceding stage. High magnification of these cells are also shown in E. and F.

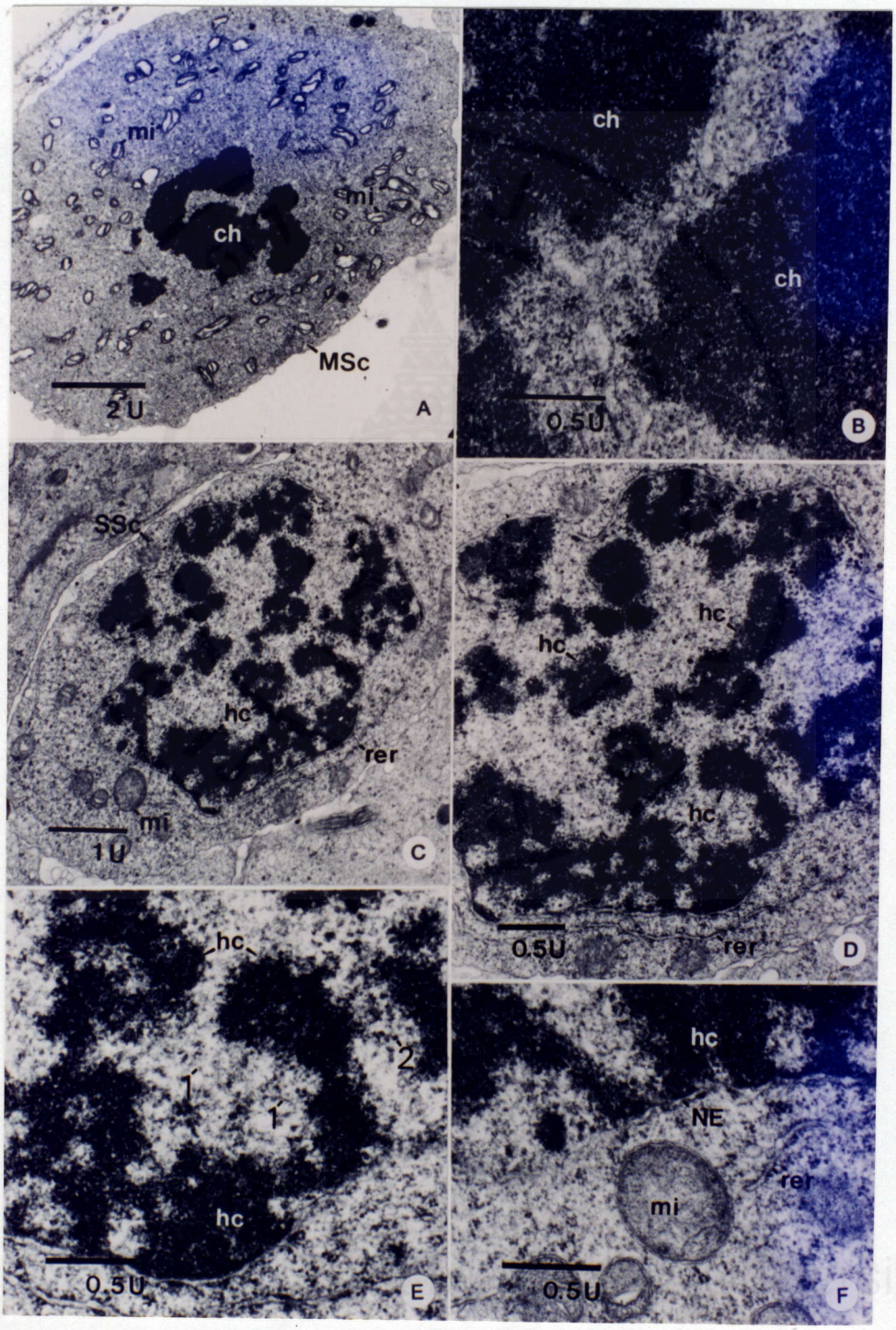
mi
mi
ch
MSc
2U
A
ch
ch
0.5U
B
SSc
hc
rer
mi
1U
C
hc
hc
hc
0.5U
rer
D
hc
1
1
2
hc
0.5U
E
hc
NE
rer
mi
0.5U
F

**Figure 15.** Electron micrographs of stage 1 spermatid

A, B) Stage 1 spermatid ($St_1$) whose nucleus shows mostly distributed euchromatin, and small heterochromatin blocks are drizzly scattered. The cytoplasm shows numerous mitochondria and very large Golgi complexes, which are arranged in "multisectorial" structure located on one side of the cell. Large amounts of mitochondria are also seen.

C) At high magnification, there are still 2 levels of chromatin are still observed: 10-nm fibers of level 1 (1) and 30-nm fibers of level 2 (2).

D, E, F) High magnification micrographs of multisectorial Golgi complexes showing clearly active synthetic activities in forming 2 types of granules, *i.e.*, proacrosomal granules (pg) and multigranular bodies (mb). In D and E. the mitochondria show many long cristae.

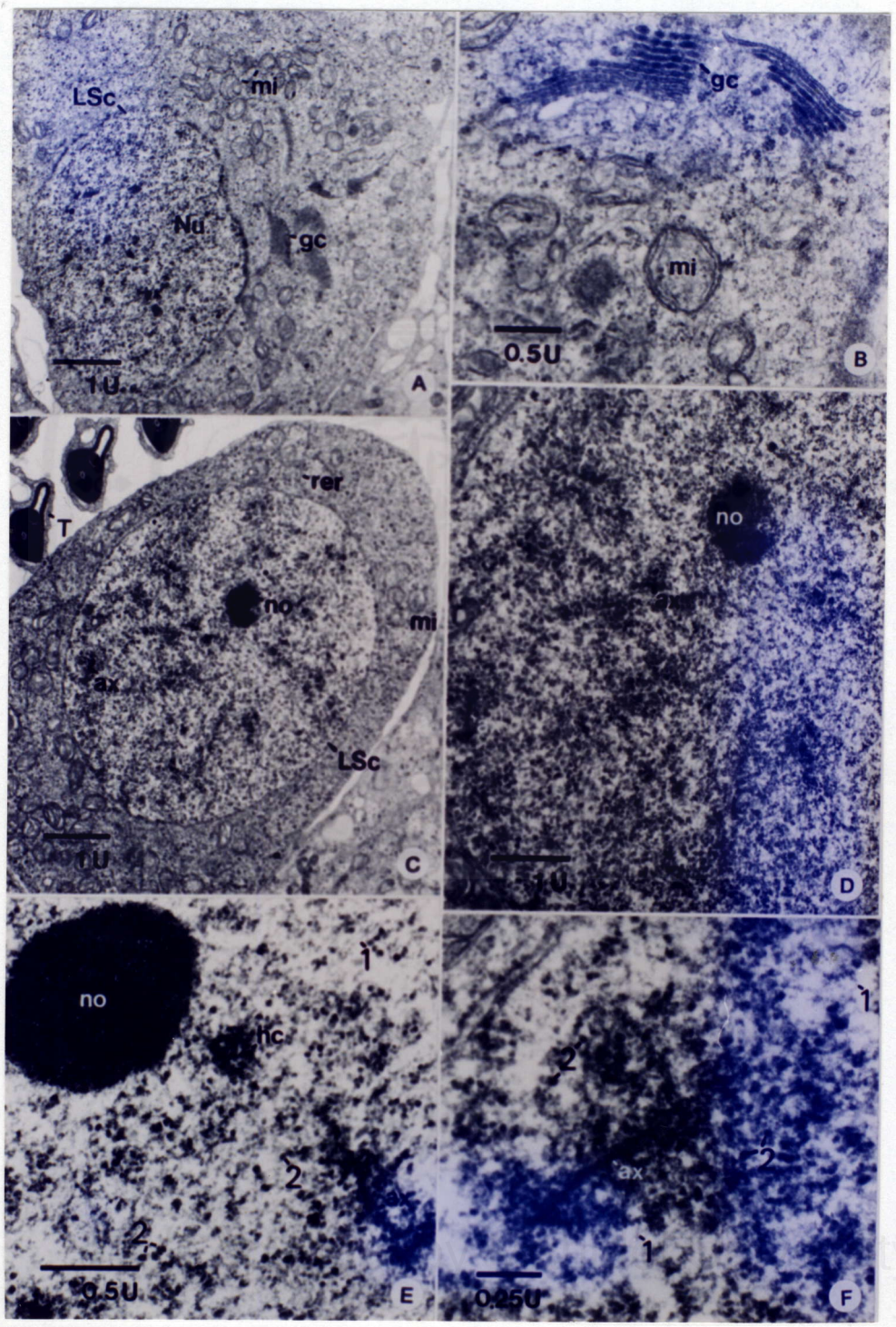
LSc
mi
Nu
gc
1U
A
gc
mi
0.5U
B
rer
T
no
mi
ax
LSc
1U
C
no
2
1U
D
no
1
hc
2
2
0.5U
E
1
2
ax
2
1
0.25U
F

**Figure 16.** Electron micrographs of stage 2 spermatids

A, B, C) Stage 2 spermatid ($St_2$) whose nuclei are located between Golgi complex (gc) and the clusters of mitochondria (mi). The nucleus shows thin layers of electron dense material on a part of nuclear envelope (arrow) which suppose to be the future acrosomal surface. The chromatin still exists in 2 two sizes, *i.e.*, 10-nm (1) and 30-nm (2) coiled fibers as shown in B. and C. At the cephalic part of the nucleus, there is a acrosomal granule (Ac) which is still developing.

D, E, F) Higher magnifications of the giant "multisectorial Golgi complexes" (gc) that still show active secretory-synthetic activities: proacrosomal granules (pg) and multigranular body (mb).

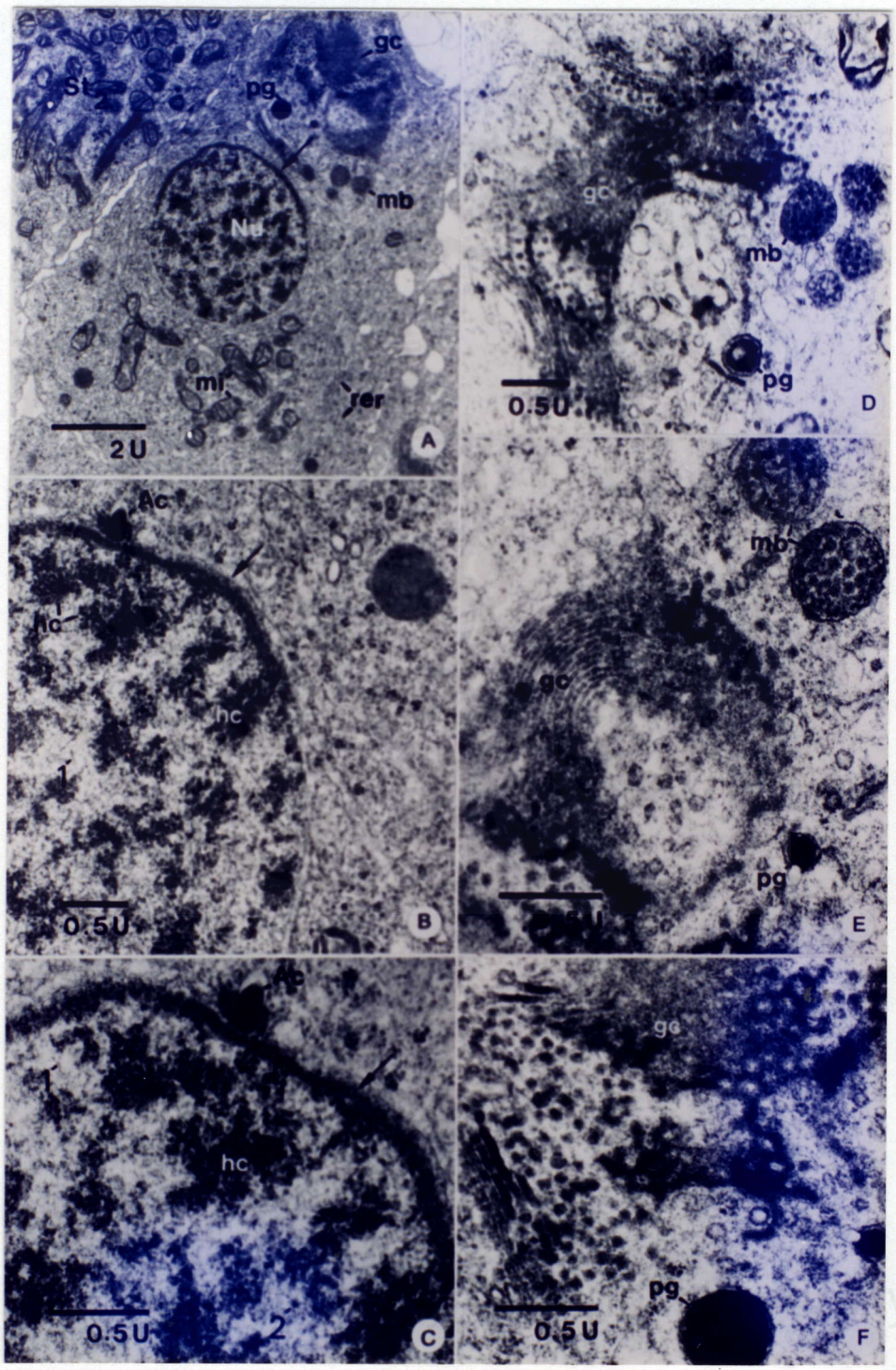
gc
St
pg
mb
Nu
mi
rer
2 U
A
gc
mb
pg
0.5U
D
Ac
hc
hc
1
0.5U
B
mb
gc
pg
E
Ac
1
hc
0.5U
2
C
gc
pg
0.5U
F

**Figure 17.** Electron micrographs of a stage 3 spermatid

A-D) Stage 3 spermatid ($St_3$) whose nucleus (Nu) migrates eccentrically to one side that is assumed to be the cephalic part. Acrosomal surface (black arrow) also shows thicker layer of electron dense nuclear envelope at the cephalic part. The 30-nm fibers (2) are mostly found and begin to aggregate at the caudal part of nucleus (white arrow). The 10-nm chromatin fibers (1) still exist in the nucleoplasm. Details of the cephalic and the caudal part of the nucleus are shown in C and D, respectively.

E,F) High power micrographs showing the stacks of very large Golgi complexes (gc) and many numerous mitochondria (mi).

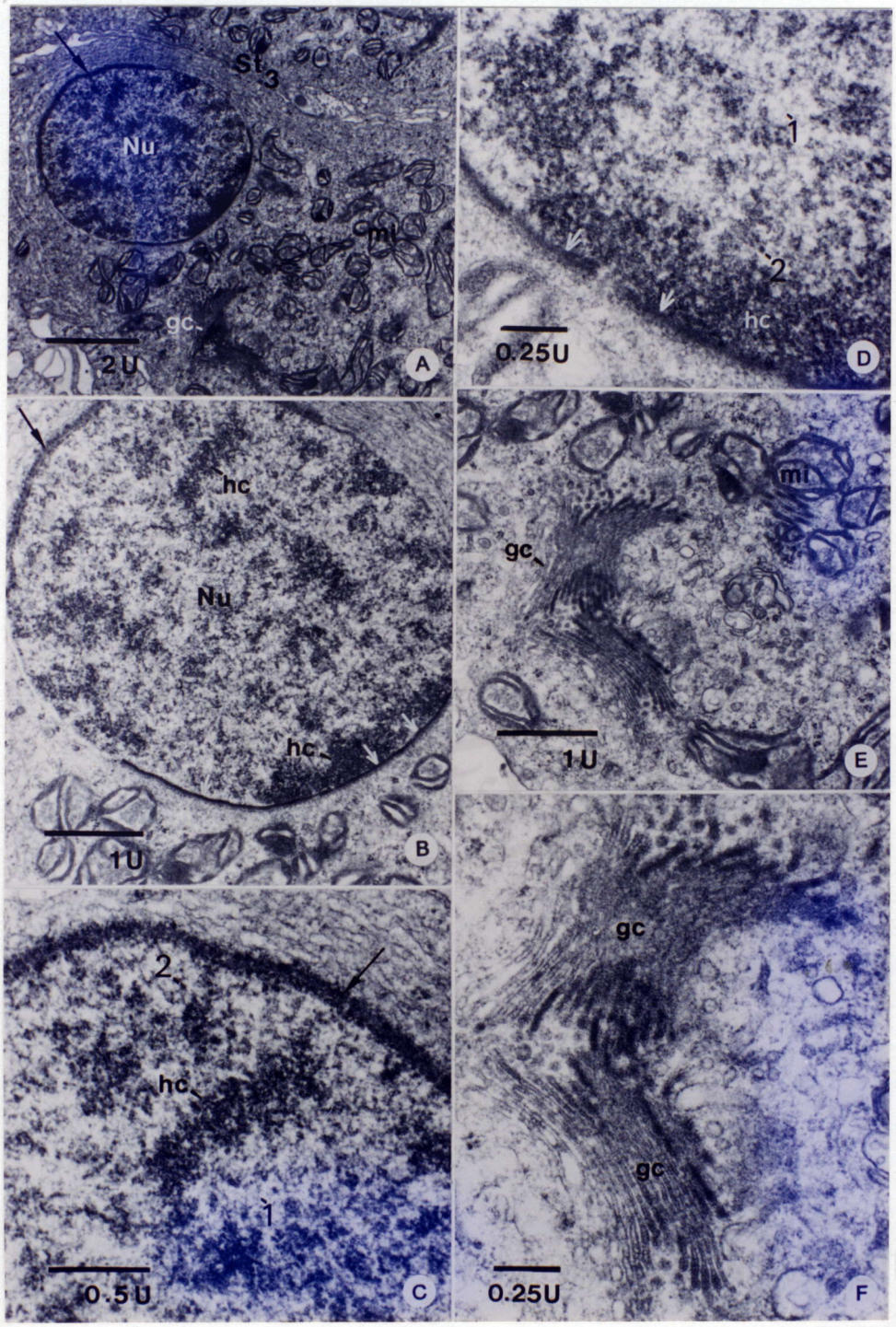

**Figure 18.** Electron micrographs of stage 4 spermatids

A-D) A stage 4 spermatid showing the nucleus (Nu) which become flatten from the caudal side facing a large groups of mitochondria (mi). The cephalic part of the nucleus shows the predicted acrosomal surface (black arrow), while the caudal part shows a marked line for differentiation of the tail (white arrow).

C, D) High magnifications showing the thickening with chromatin mass on the cephalic (black arrow in C.) and the caudal parts (white arrow in D) of nnuclear membrane. The chromatin consists of mostly 30-nm fibers (2) and a small amount of 10-nm fibers (1).

E) Low-magnification micrograph of a stage 4 spermatid showing a large amount of mitochondria (mi) located between the nucleus and the very large Golgi complexes.

F, G) High magnifications of the giant multisectorial Golgi complexes (gc) which are still active and show the proacrosomal granules (pg), and membrane-bound dense granules in the trans-face area. In E., there are also other granules called multigranular bodies (mb).

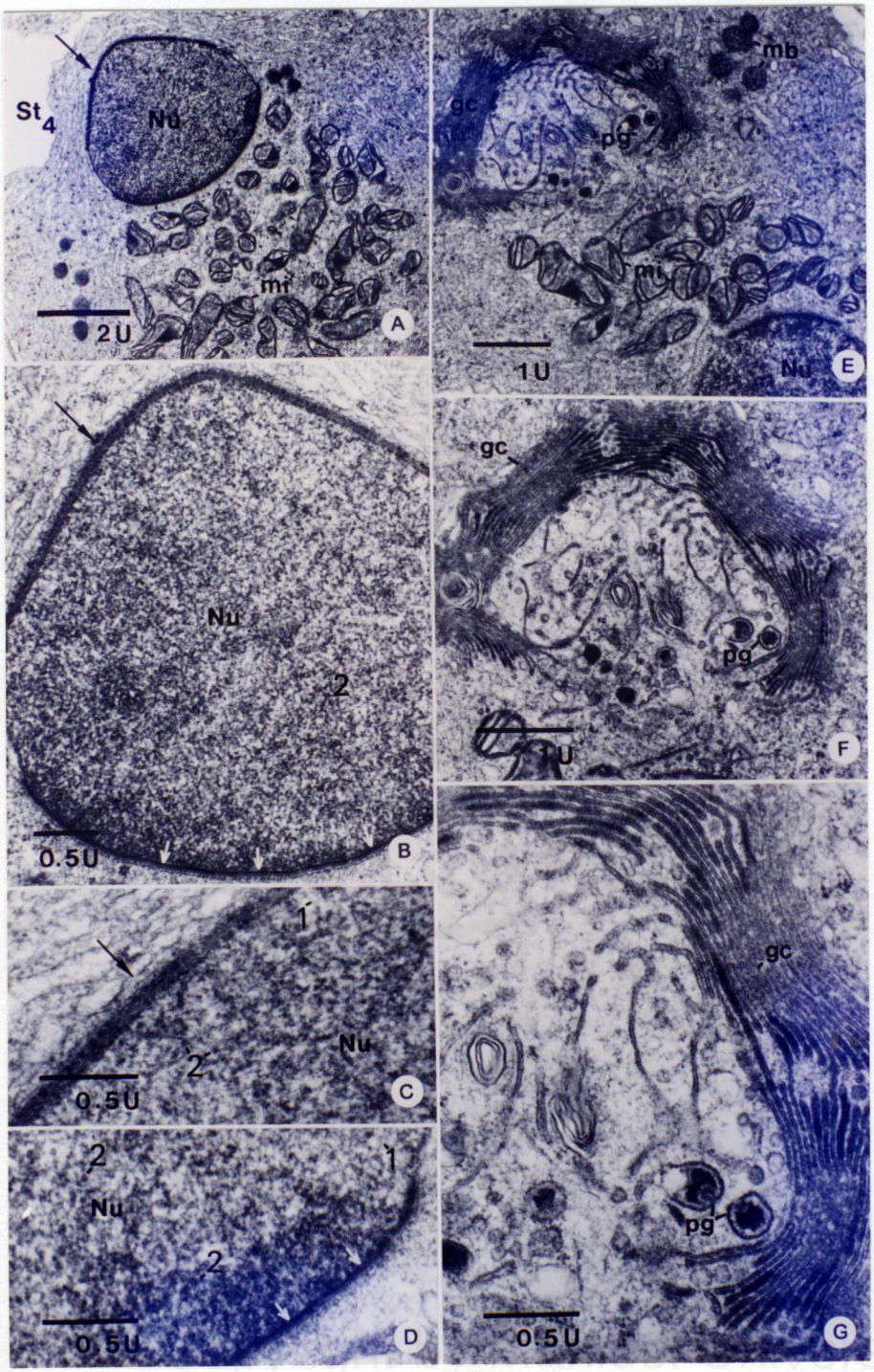
St4
Nu
mi
2U
A
mb
gc
pg
mi
1U
Nu
E
gc
pg
1U
F
Nu
2
0.5U
B
1
Nu
2
0.5U
C
2
1
Nu
2
0.5U
D
gc
pg
0.5U
G

**Figure 19.** Electron micrographs of stage 5 and stage 6 spermatids

A, B) A stage 5 spermatid ($St_5$) showing the nucleus (Nu) which is highly flattened, and is transformed into oblonged shape. At the base of the nucleus, there is fossa that contains the centriole (ce) which is elongated to form the tail. A large number of mitochondria (mi) are seen to surrounding the axoneme of the tail. The chromatin exists only one size, 30-nm fibers (2) that make the nucleus uniformly dense.

C, D) A stage 6 spermatid ($St_6$) whose nucleus (Nu) is gradually compressed in cephalo-caudal direction to become a curved disc and is more condensed. The cytoplasm also shows the cross section of the axoneme which is surrounded by a large number of mitochondria. In D., the chromatin fibers within the nucleus are gradually elongated into filaments about 20-nm fibers (3) equal to level 3 in table 1.

E, F) Another stage 6 spermatid showing the developing acrosome with cylindrical rod and is surrounded by two unknown materials located at the top of the triangular-shaped nucleus (Nu).

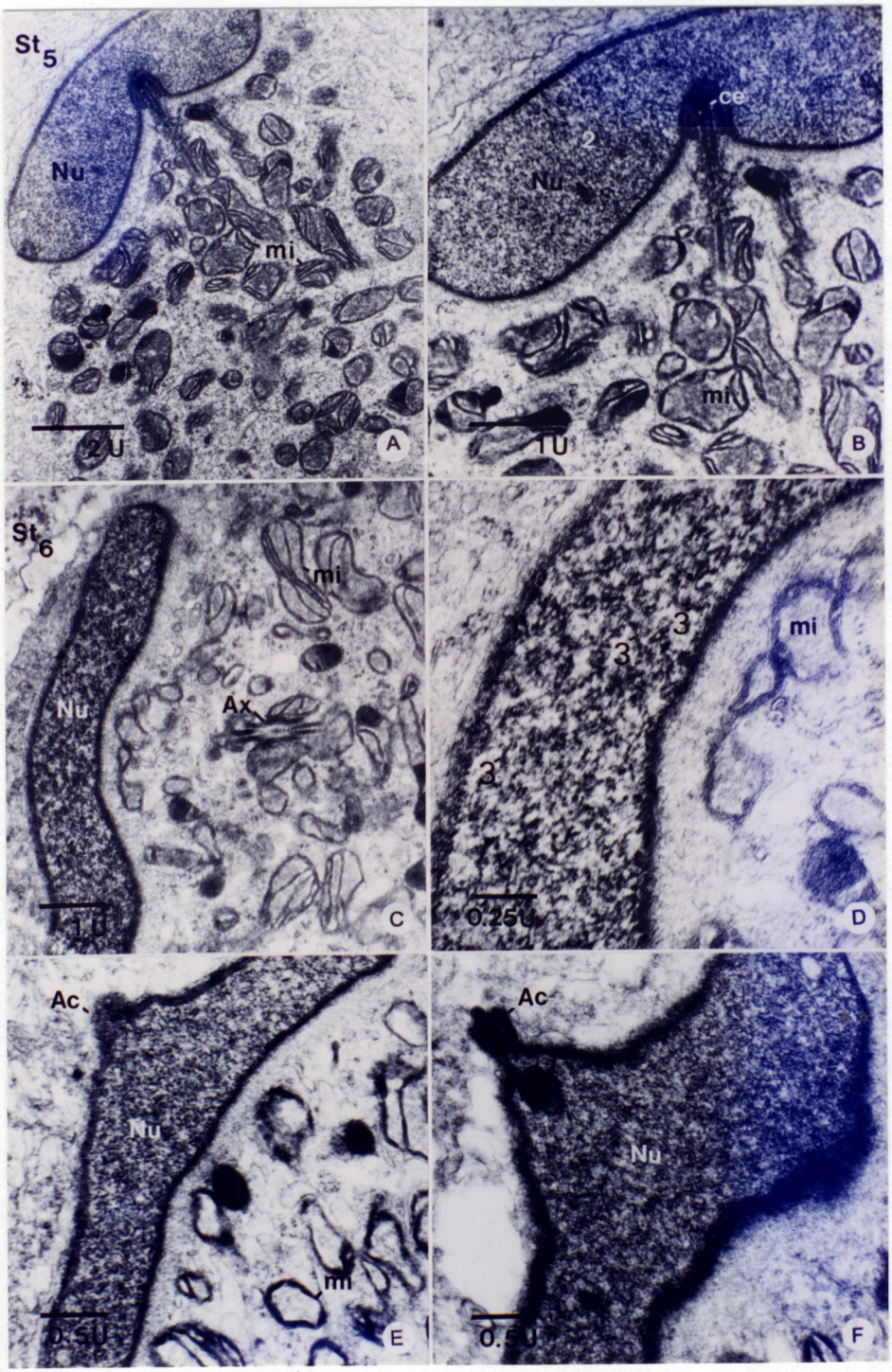
St5
Nu
mi
1U
A
ce
2
Nu
mi
1U
B
St6
mi
Nu
Ax
1U
C
3
3
3
mi
0.25U
D
Ac
Nu
mi
0.5U
E
Ac
Nu
0.5U
F

**Figure 20.** Electron micrographs of stage 7 and stage 8 spermatids

A, B) A stage7 spermatid ($St_7$) showing nucleus (Nu) which has an arrow- or boomerang-like shape and is densely stained. The chromatin shows transformation to straight parallel fibers (4 in B.) which extend from the inner surface of nuclear envelope at the caudal part to the cephalic part of the nucleus. The mid-piece (mp) of the tail, which consists of 9+2 doublets of axoneme microtubules shown in cross section, is located between two wings of the nucleus at the caudal portion. It is surrounded by numerous mitochondria.

C) Longitudinal section of a stage7 spermatid, showing an arrow-like nucleus containing the chromatin which become straight-paralleled fibers (4). The centriole (ce) is tightly embedded in the implantation fossa and continuing with the axonemal flgellum.

D) A stage 8 spermatid ($St_8$) showing a pear-like nucleus (Nu) with the chromatin consisting of straight-paralleled fibers (4), and the centriole at the base. The cytoplasm contains moderate amount of mitochondria (mi).

E, F) At high magnification, the straight fibers of chromatin (4) are arranged in the parallel conformation and extend from the inner surface of nuclear envelope (white arrow) at the caudal part to the cephalic part. The completely formed centriole (ce), which consists of crystal-like structure around the axoneme, is embedded within the caudal nucleus.

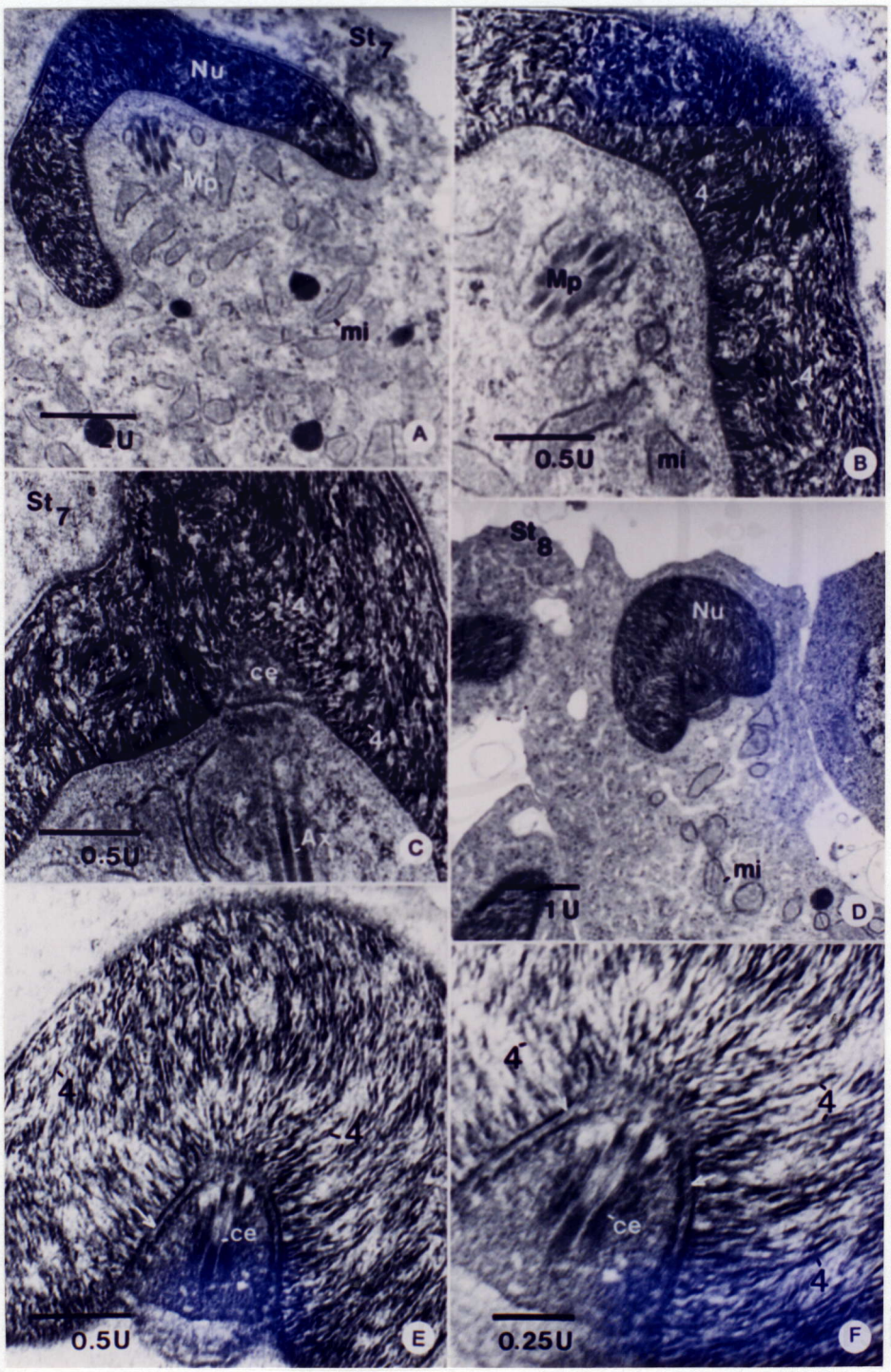
St7
Nu
Mp
mi
1U
A
4
Mp
0.5U
mi
B
St7
4
ce
4
0.5U
Ax
C
St8
Nu
mi
1U
D
4
4
4
ce
0.5U
E
4
4
ce
4
0.25U
F

**Figure 21.** A jigsaw electron micrograph of a stage 9 spermatid showing the head and different parts of developing tail with a large number of mitochondria (Mi) surrounding Golgi complexes (Gc). The tail is divided into 6 parts (1-6) for topographic study of the serial spaced cross sections.

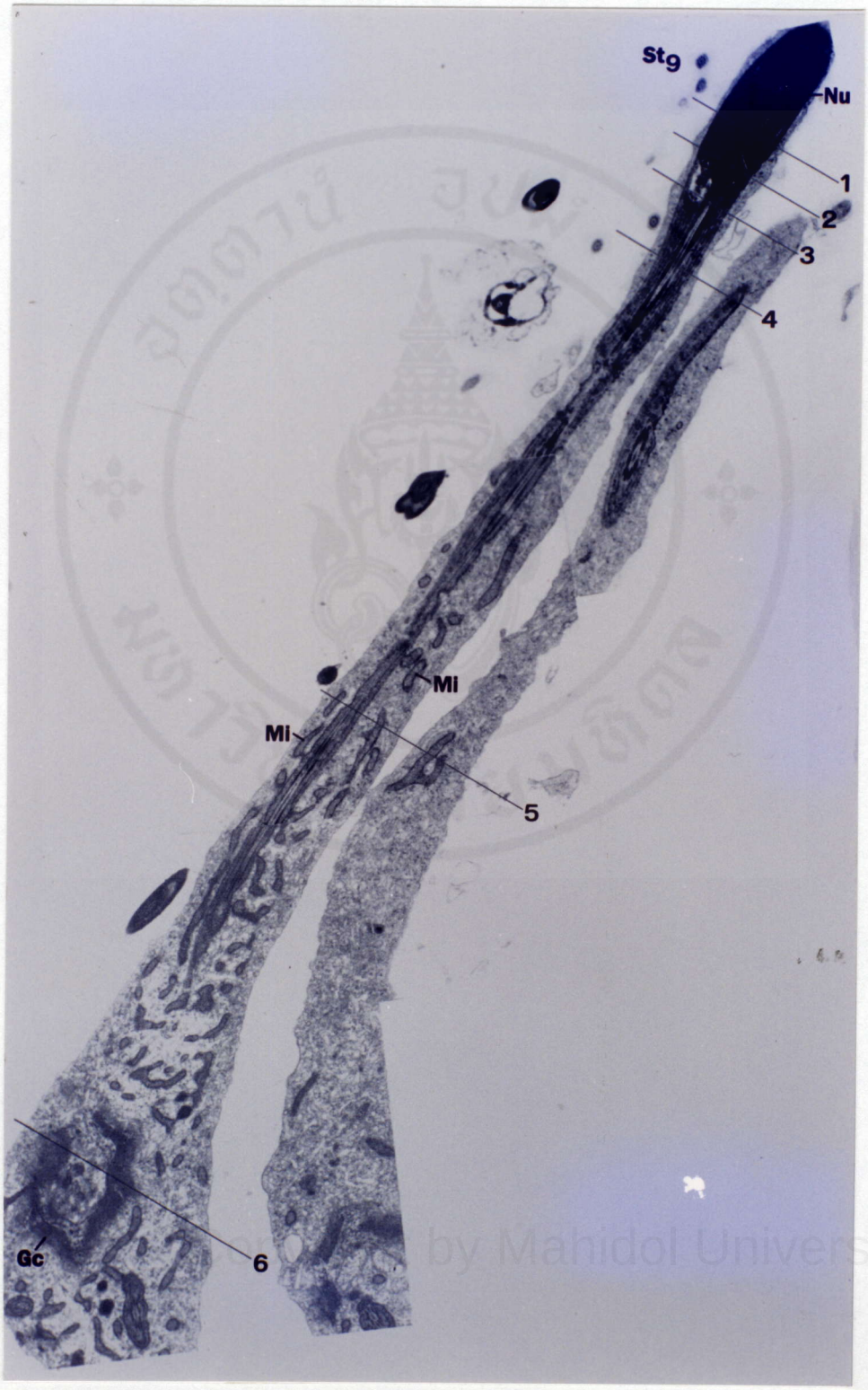

**Figure 22.** Electron micrographs of a stage9 spermatid

A) The anterior part of a stage 9 spermatid ($St_9$) whose nucleus shows highly condensed chromatin with increasingly tapered anterior end that has a cone-like shape. The caudal portion of the nucleus also shows a completely formed centriole which is continuing with the proximal part of the axoneme (Ax) surrounded by derivative structure of mitochondria (mi).

B, C) Higher magnification of longitudinal sections of the nucleus showing that the chromatin consists of 14-16 nm straight fibers (4) closely packed into the bundles (two-heads arrow). Each bundle is composed of 7-10 fibers tightly packed together. The arranged microtubules (Mt) are seen around the nucleus.

D, E, F) The head of stage 9 spermatids showing a centriole (ce) which is implanted into the fossa of the caudal nucleus. It is shown in longitudinal section in D., and cross section in E that is regarded as the first part. The second part, consisting of crystal-like structure (arrow) surrounding the axoneme, (Ax) is shown in oblique section in F.

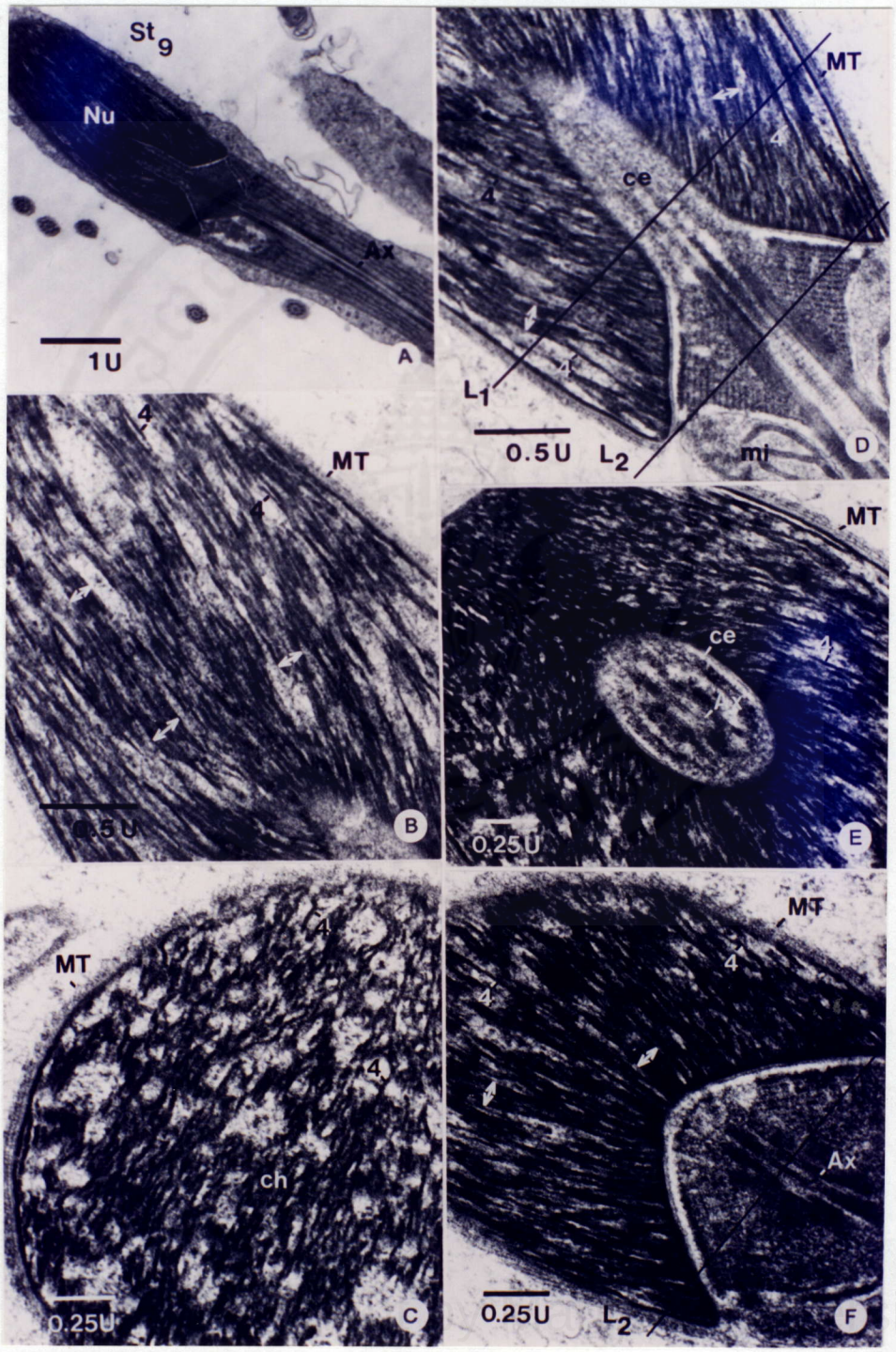
St 9
Nu
Ax
1U
A
MT
ce
4
L1
0.5U
L2
mi
D
MT
4
4
0.5U
B
MT
ce
4
0.25U
E
MT
4
4
ch
0.25U
C
MT
4
4
Ax
0.25U
L2
F

**Figure 23.** Topographic electron micrographs of a stage 9 spermatid

A, B) The neck level of a stage 9 spermatid, showing the longitudinal section of the third level of the developing tail that consists of the 9+2 doublets of axonemal microtubules surrounded by 4-5 layers of mitochondrial derivative (arrow) and the vacuole containing flocculent substances. The cross section of this level (Fig. B) shows a set of parallelly-arranged microtubules (Mt) that are seen around the mitochondrial derivatives.

C) The fourth level of the tail segment showing the axoneme (Ax) surrounded by about 4 layers of mitochondrial derivative (arrow).

D) The fifth level of the tail showing the (9+2) axonemal microtubules (Ax) which are surrounded by a group of mitochondria. The cross sections of the fourth and the fifth parts of the tail are shown in E.

F, G) The sixth level of the cell showing very large Golgi complexes that still remain at the caudal portion of the cell and many modified mitochondria (mi).

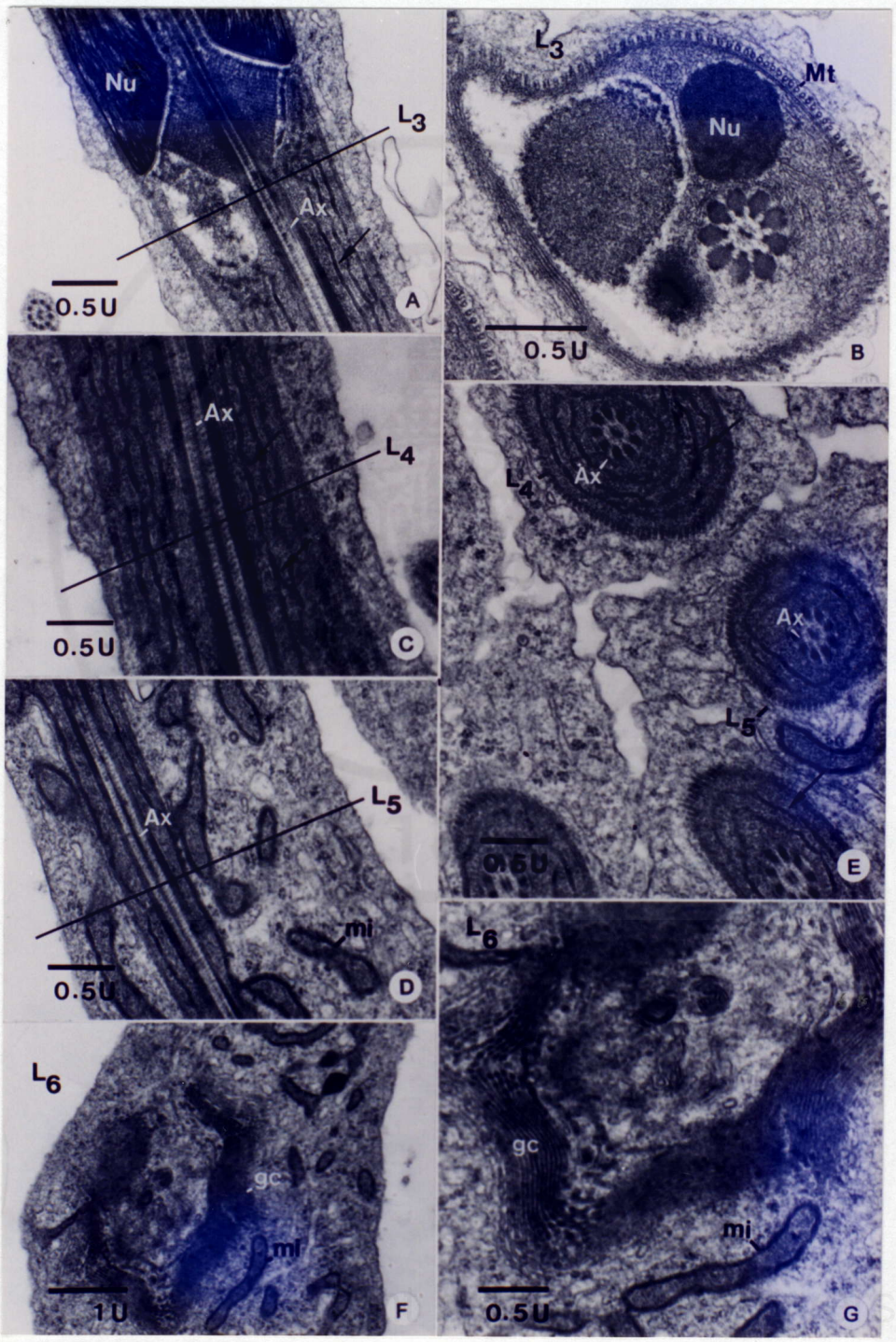
Nu
L3
Ax
0.5U
A
L3
Mt
Nu
0.5U
B
Ax
L4
0.5U
C
L4
Ax
Ax
L5
0.5U
E
Ax
L5
mi
0.5U
D
L6
gc
mi
1U
F
L6
gc
mi
0.5U
G

**Figure 24.** Transformation of mitochondria in the middle piece of stage9 spermatids

A) TEM Micrograph shows the cluster of mitochondria surrounding a cross section of axoneme (Ax); the active Golgi complexes are also seen in this vicinity.

B, C) Cross sections of the forming tails showing the axoneme surrounded by a few layers of mitochondrial derivative; and a row of microtubules is seen around this mitochondrial sheath. In C, very large Golgi complexes are also shown adjacent to the mitochondria.

D, E, F) The tail part showing mitochondrial derivatives (arrow) with their long inner membrane. The cristae become rearranged to form several layers of parallel concentric rings around the axoneme (Ax).

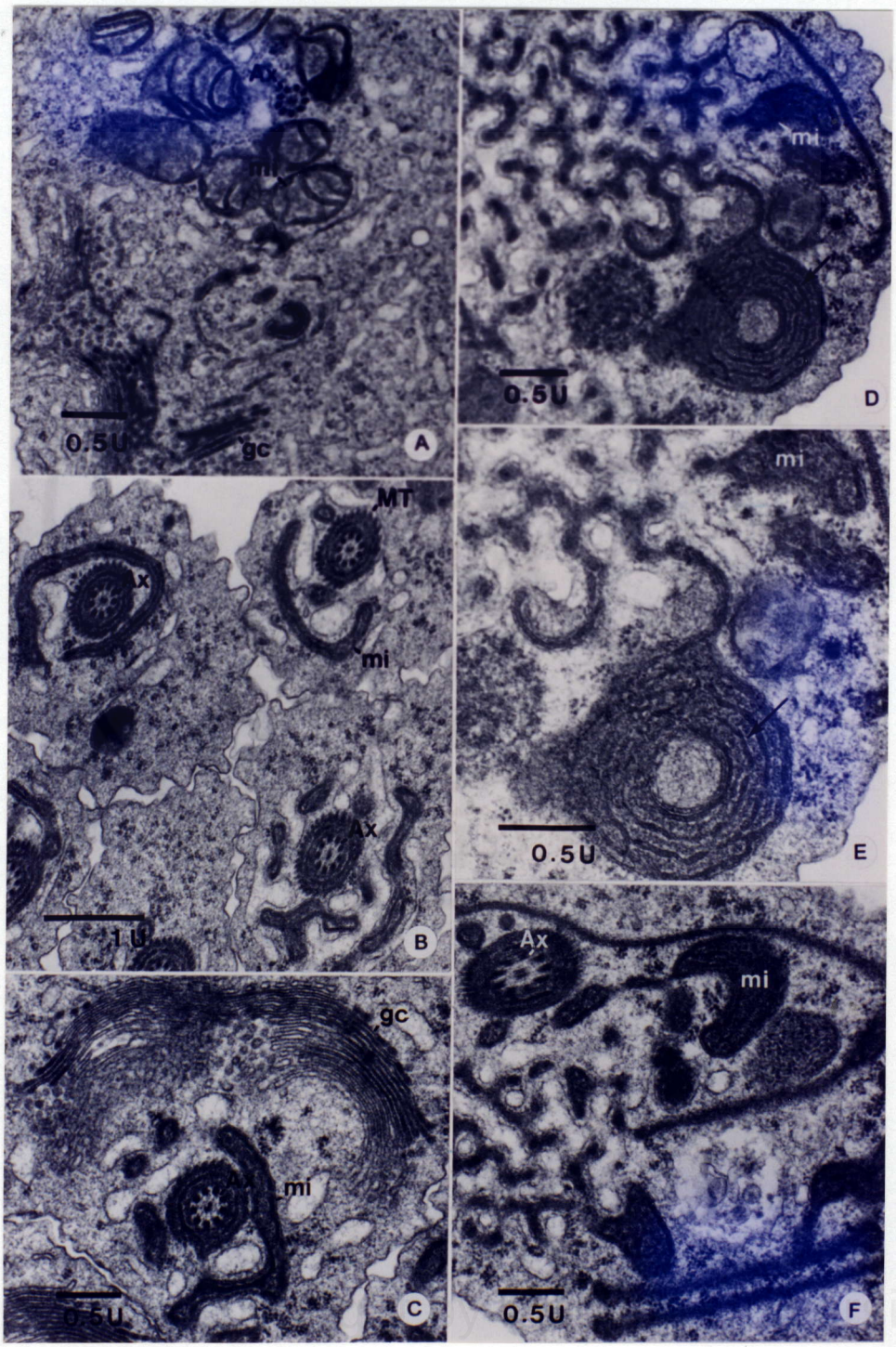
mi
0.5U
gc
A
mi
0.5U
D
MT
x
mi
Ax
1 U
B
mi
0.5U
E
gc
Ax
mi
0.5U
C
Ax
mi
0.5U
F

**Figure 25.** Electron microgeaphs of the head of stage 10 spermatid

A) A stage 10 spermatid ($St_{10}$) showing a slender nucleus (Nu) which occupies the head, and is composed of more condensed chromatin. Surrounding the most anterior tip of the nucleus is the acrosome (Ac) which is completely formed at this stage. (PM-plasma membrane)

B, C) Completely formed acrosome (Ac) consists of the cylindrical rod covered by a dense cup.

D, E) At high magnification, the chromatin shows dense bundles which represent closely packed 14-16 nm straight chromatin fibers. (Mt-microtubules)

F) A cross section through the nucleus and the centriolar core (ce) showing the increasingly condensed chromatin radiating from the centriole, and many irregular electronlucent (va) areas. The nucleus is entirely surrounded by a row of microtubules (Mt).

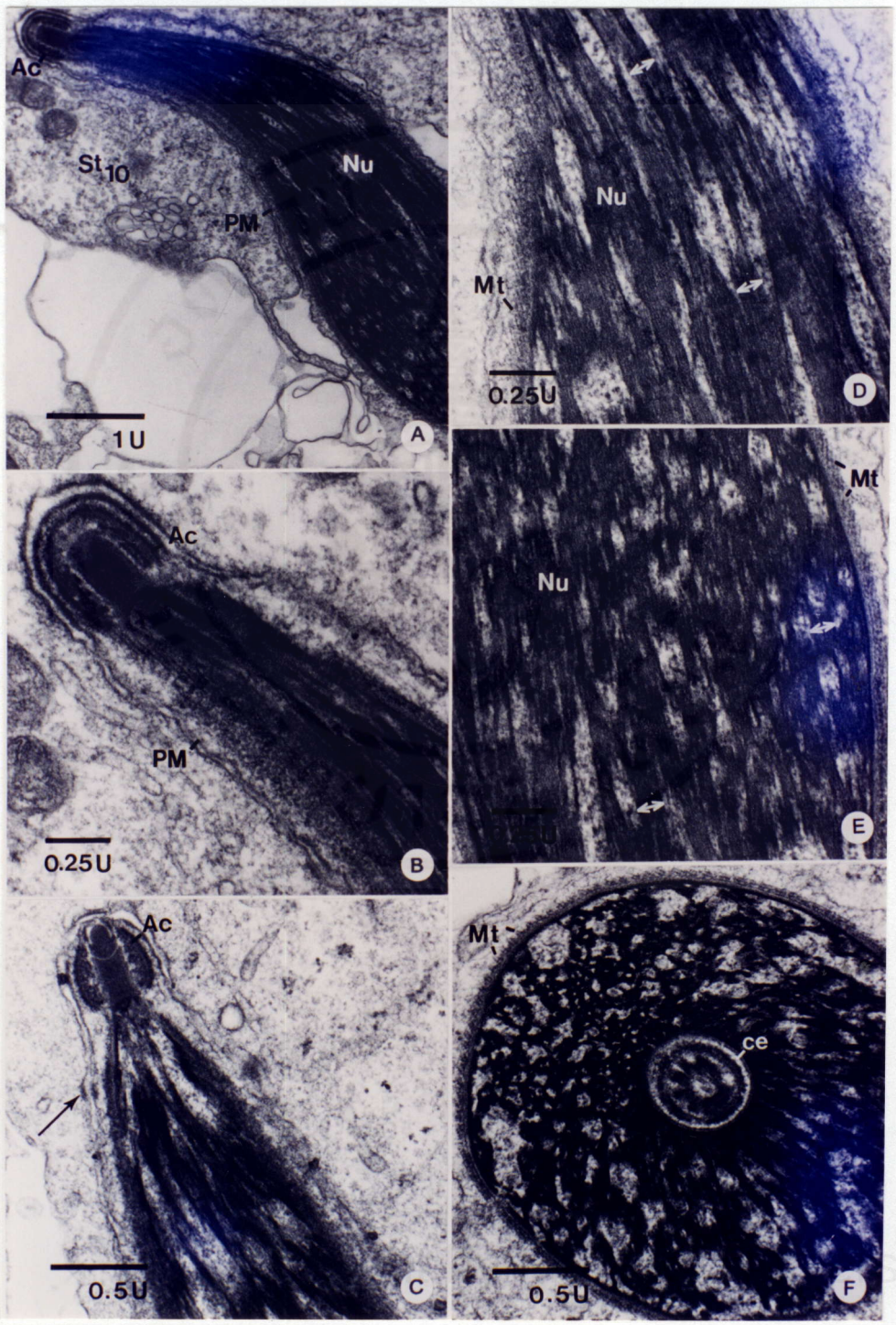
Ac
St 10
Nu
PM
1 U
A
Nu
Mt
0.25U
D
Ac
PM
0.25U
B
Mt
Nu
E
Ac
0.5U
C
Mt
ce
0.5U
F

**Figure 26.** Electron micrographs of the head of the immature spermatozoa

A) The immature spermatozoa ($Sz_1$) whose nucleus contains almost completely condensed chromatin (Nu). Only small electronlucent areas (va) are present. (ce-centriol; Mt-microtubules)

B-E) High magnification micrographs showing that each bundle (110-120 nm) of chromatin (ch) from the precedent stage becomes homogeneously condensed and leave only small electronlucent (va) areas. (cross section in-C. and oblique section in-E.)

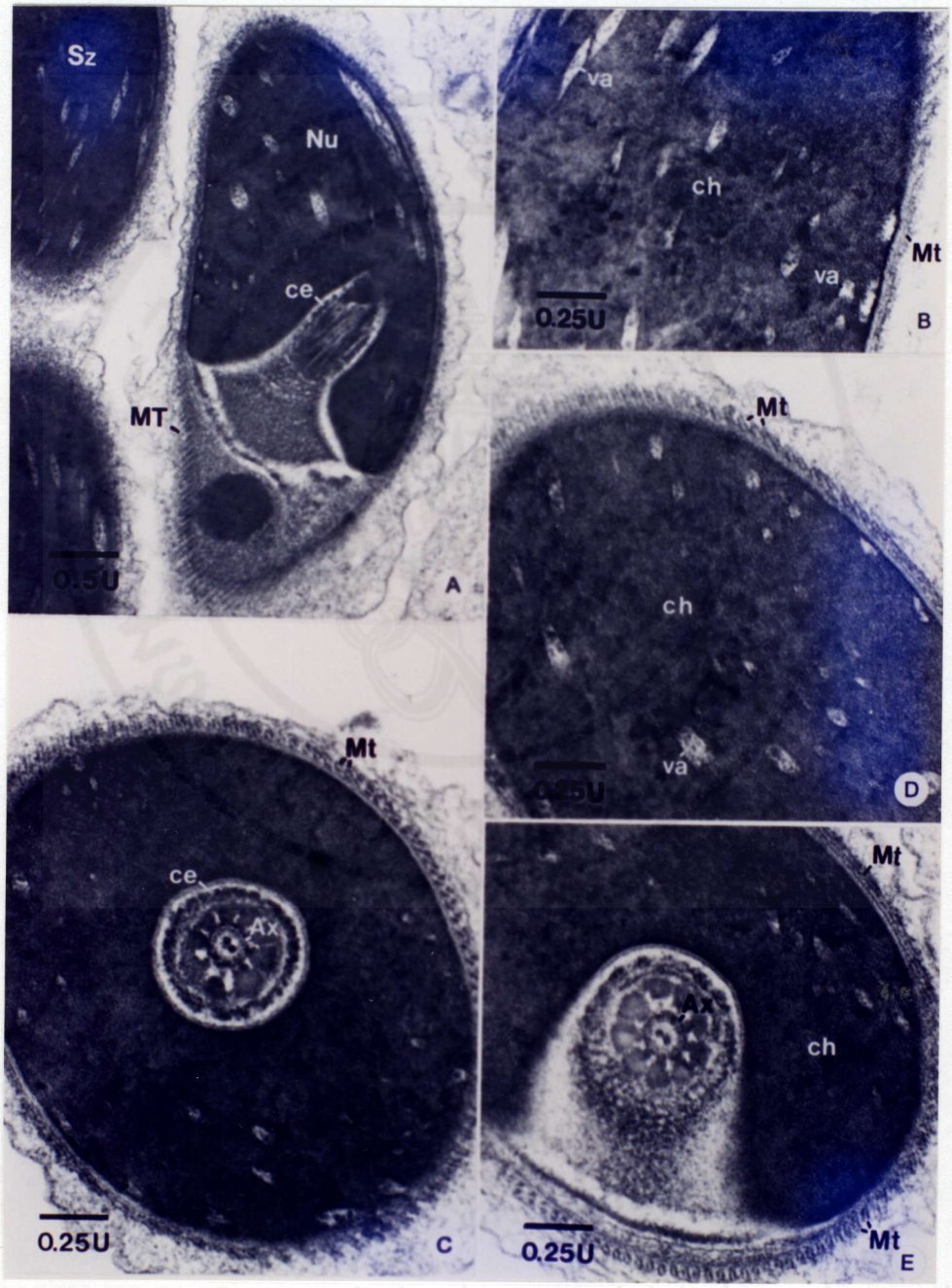

**Figure 27.** Electron micrographs of the mature spermatozoa

A-D) Anterior parts of mature spermatozoa ($Sz_2$) showing completely condensed and electron opaque chromatin in elongated nuclei (Nu).

F) Spaced serial cross sections of the proximal levels of the tails ($L_1$, $L_2$, $L_3$) showing axoneme surrounded by nearby structures.

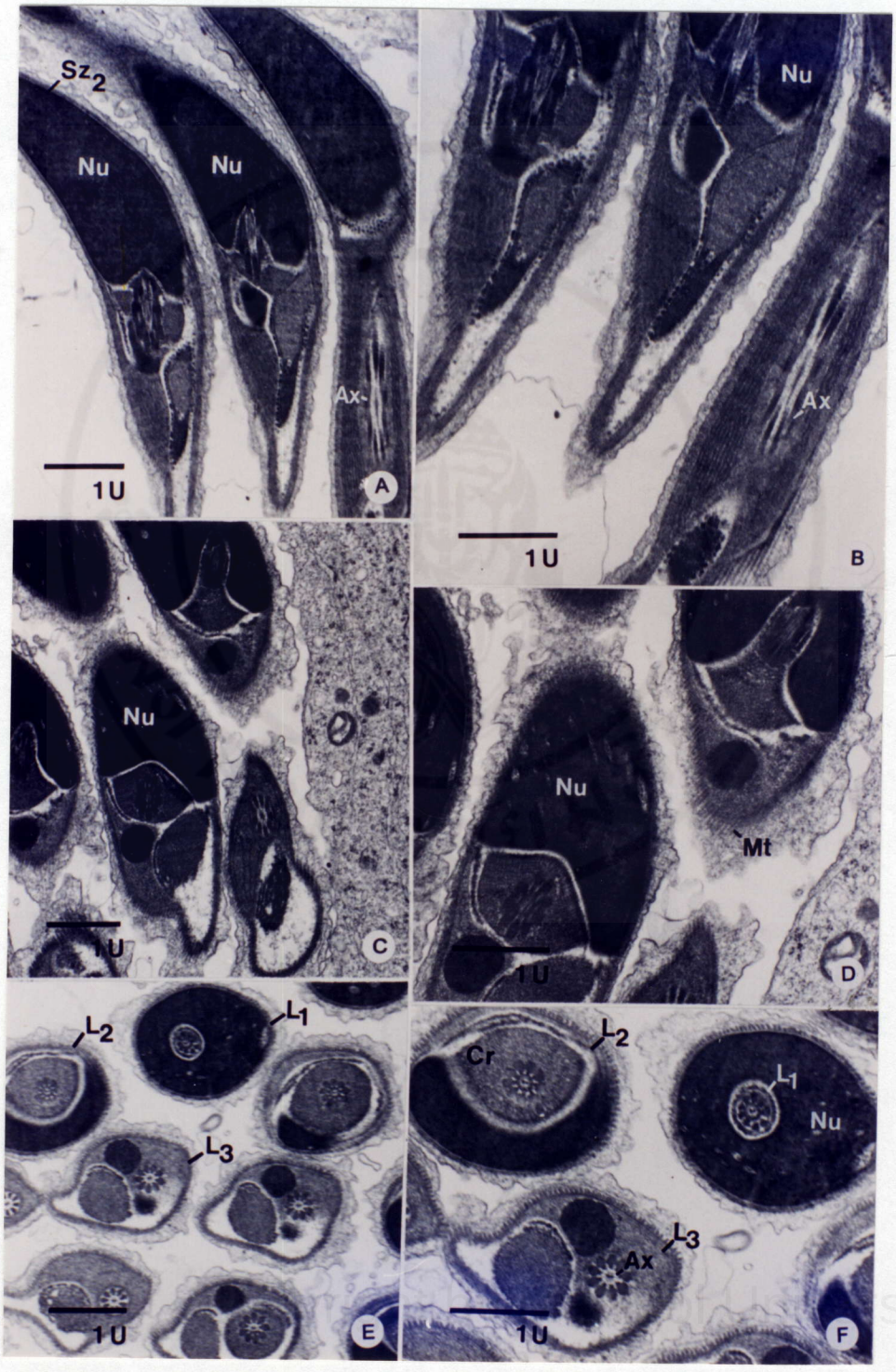
Sz2
Nu
Nu
Ax
1U
A
Nu
Ax
1U
B
Nu
1U
C
Nu
Mt
1U
D
L2
L1
L3
1U
E
Cr
L2
L1
Nu
L3
Ax
1U
F

**Figure 28.** Topographic electron micrographs of the head and connecting piece of mature spermatozoa

A) Cross sections of the completely formed spermatozoa's tail are shown. Sperm's tail is divided into 7 levels ($L_{1-7}$)

B, C, D) Longitudinal section of the spermatozoa ($Sz_2$) showing the centriolar core that consists of crystal-like structure (arrow) and the axoneme (Ax). At High magnification in C, a rhomboid crystalline-substance (arrows) is shown.

E) Cross sections of the tail segment ($L_2$, $L_3$). Level 2 ($L_2$), consists of the axonemal microtubules (9+2) surrounded by crystalline-like structure of the centriolar core. This level is at the lower part of spermatozoa's head. Level 3 ($L_3$) shows the similar features to $L_2$ except that the vacuole containing granular substances is seen juxtaposed to the axoneme.

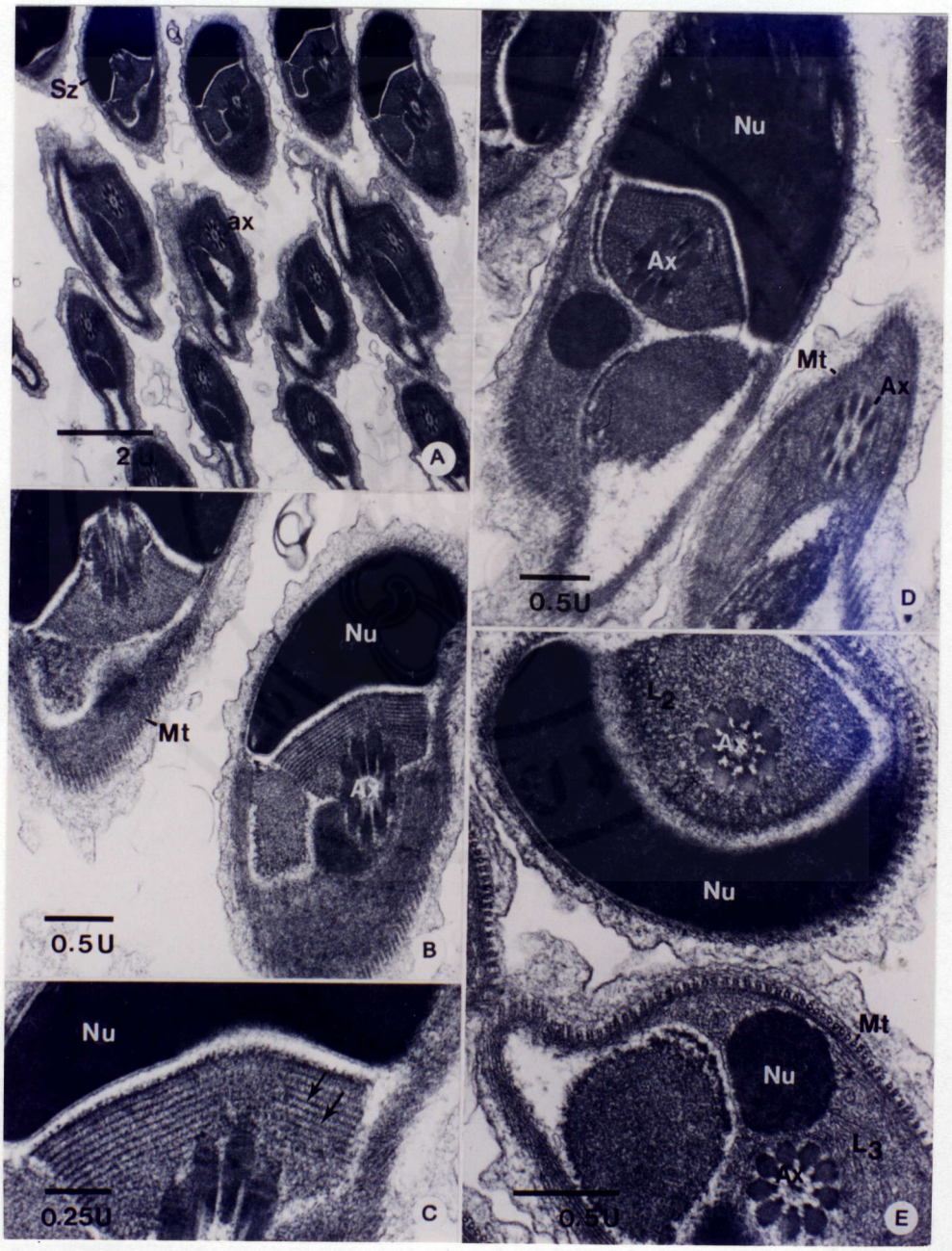

**Figure 29.** Topographic electron micrographs of connecting piece and mid-piece of mature spermatozoa

A, B, C) High magnifications of cross sections of the tail in level 3 ($L_3$) showing the axonemal (9+2) microtubules surrounded by a longitudinal column of dense fibrous sheath. It is juxtaposed to the mitochondrial derivatives and the vacuole containing granular substances. This level in A. is at the lowest part of spermatozoa's head (Nu). (Mt-microtubules)

D, E) Cross sections of level 4 ($L_4$), showing the mitochondrial derivatives (arrows) that form concentric 4-5 layers around the axonemal microtubules. (mi-mitochondria; PM-plasma membrane)

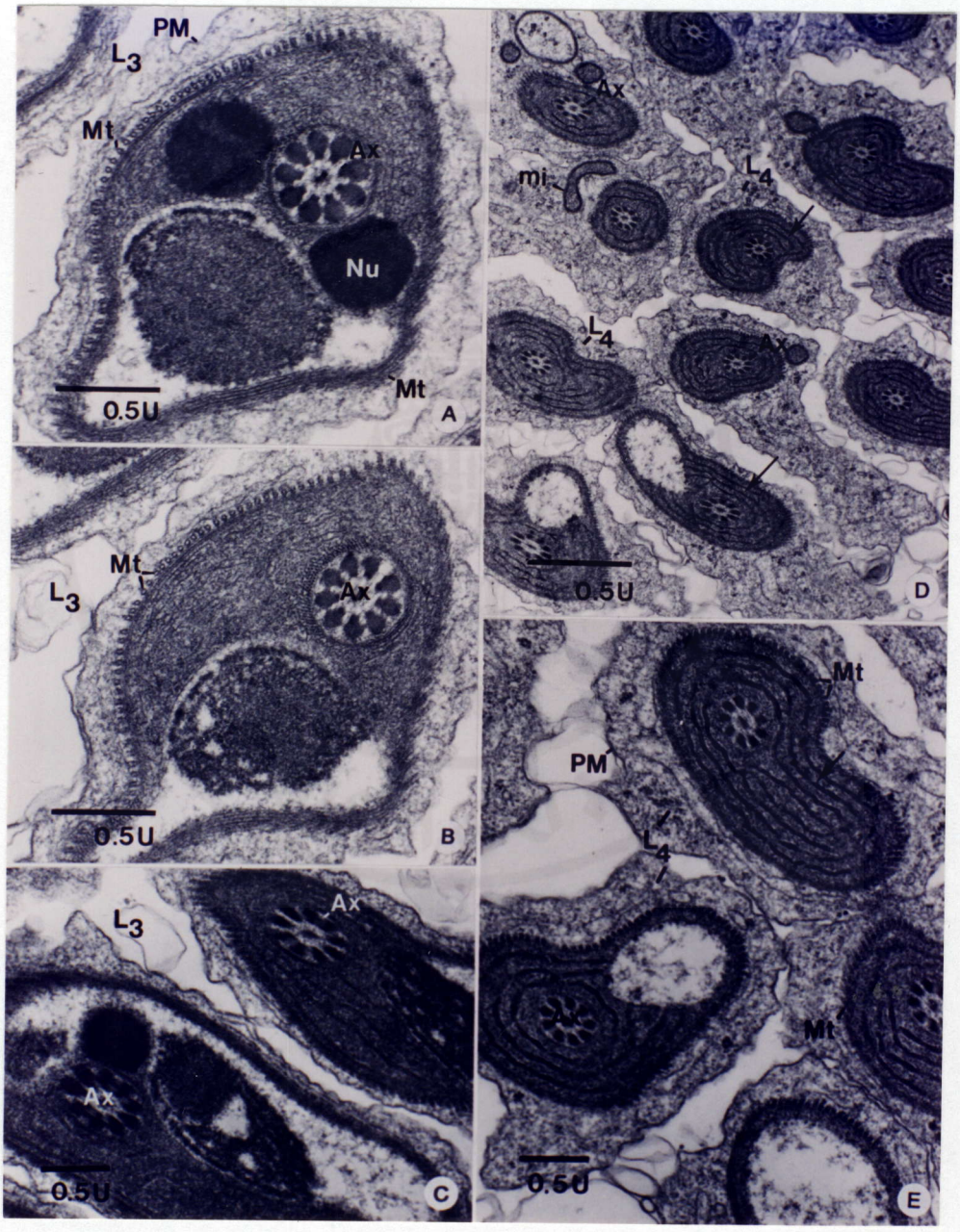

**Figure 30.** Topographic electron micrographs of the mid-piece and end piece of the mature spermatozoa

A, B) Level 5 of the tail showing decreasing concentric rows of mitochondria derivative that form helix containing glycogen-like material (G). (Long section in A. and cross sections in B. and C.)

D, E, F) Level 6 of the tail ($L_6$), showing the features that are similar to those of level 5 ($L_5$), but they are entirely slim down until the next level.

G) The level 7 ($L_7$) consists of the axonemal complex surrounded by 2 or 3 layers of cylindrical sheaths. The helical formations containing glycogen-like material completely disappeared.

H) The distal end of the tails ($L_8$), each showing only an axonemal core (Ax) surrounded by the plasma membrane (PM).

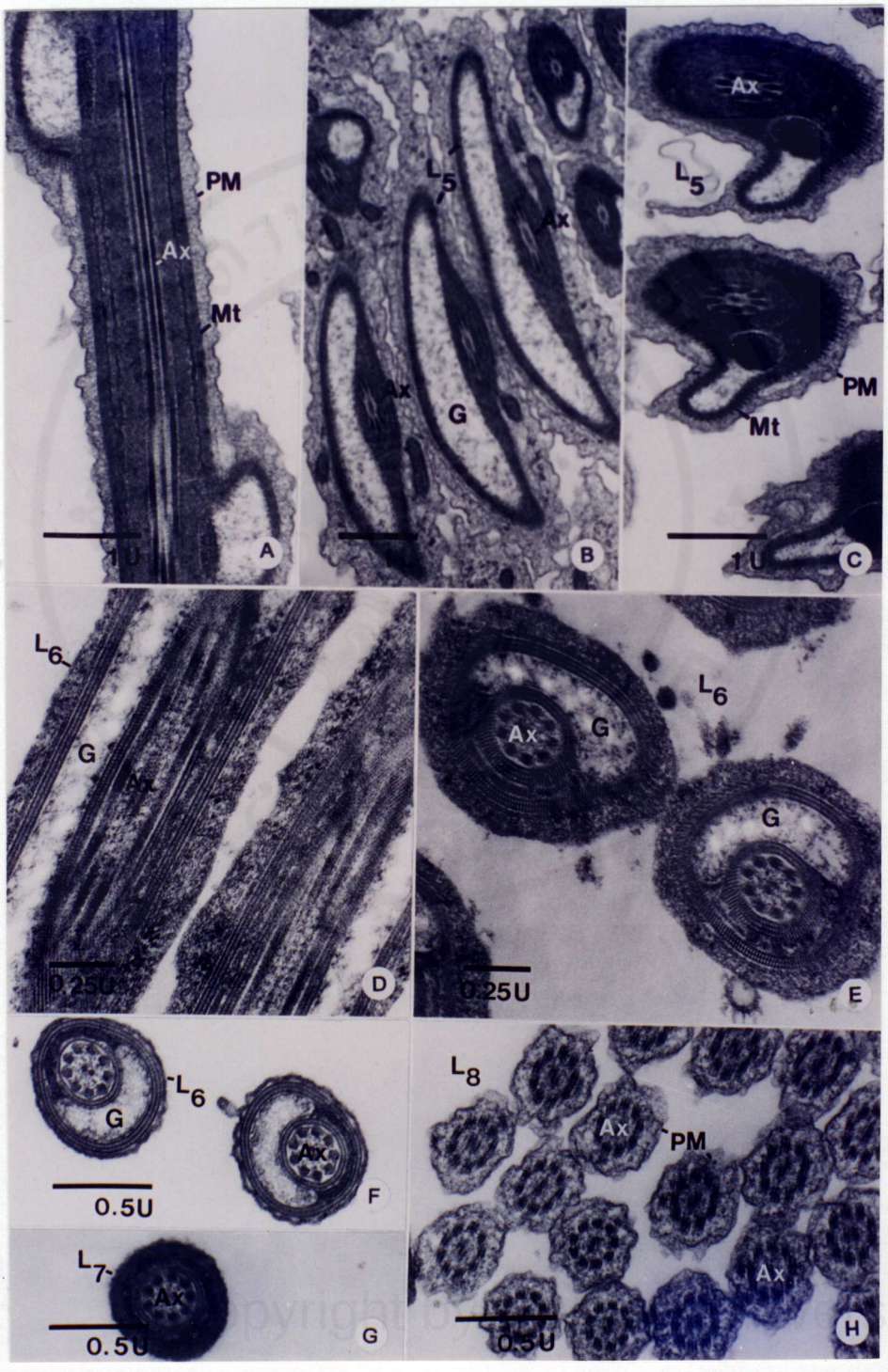
PM
Ax
Mt
1U
A
L5
Ax
Ax
G
B
Ax
L5
PM
Mt
1U
C
L6
G
Ax
0.25U
D
L6
Ax
G
G
0.25U
E
G
L6
Ax
0.5U
F
L8
Ax
PM
Ax
L7
Ax
0.5U
G
0.5U
H

**Figure 31.** Electron micrographs of Sertoli cells in tubules of the ovotestis

A, B) The Sertoli cell has a nucleus characteristically exhibiting a deep indentation and containing small heterochromatin blocks scattered throughout. It has long processes of cytoplasm orientated in contact with the basement membrane (bm). Numerous rough endoplasmic reticulum (rer) and some mitochondria are shown in B.

C-F) At high magnification, its cytoplasmic contents are composed of small Golgi complex (gc), moderate amount of mitochondria (mi), and large amount of RER (rer) located in close association with the nucleus. In addition, lysosomes (Ly) are seen as membrane-bound organelles containing diverse particulate material which is extremely electron dense.

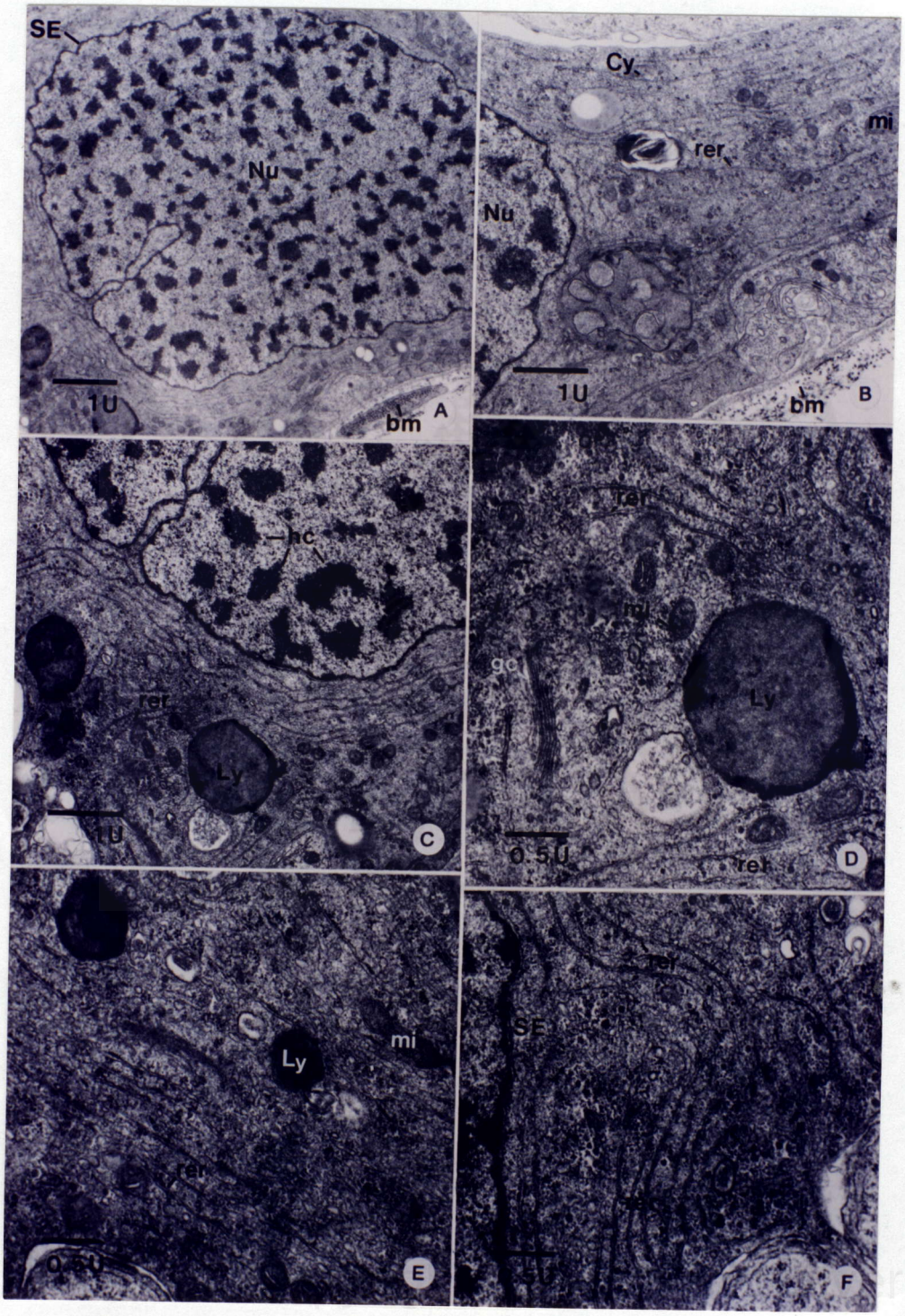
SE
Nu
1U
bm
A
Cy
rer
mi
Nu
1U
bm
B
hc
rer
Ly
1U
C
rer
mi
gc
Ly
0.5U
rer
D
Ly
mi
rer
0.5U
E
rer
SE
F

**Figure 32.** Electron micrographs of the basal compartment of tubules of the ovotestis

A) Electron micrograph shows the relationship of the Sertoli cell (SE) and follicular cell (fc) located above the basement membrane to the cells of spermatogenic units (Sc). They formed "haemolym-testis barrier" which functions to prevent the exposure of the gametes to passages of noxious substances.

B, C, D) The Sertoli cell is postulated to provide structural and metabolic support for the developing spermatogenic cells (Sc). It is bounded to the gamete cells by the septate desmosome. Fig. D. show that the Sertoli cell still envelops the heads (Nu) of many stage10 spermatids ($St_{10}$).

E, F) Electron micrographs showing the follicular cell which rests on the basement membrane (bm), and is covered by the cytoplasm of the Sertoli cell (SE). The follicular cell (fc) has an oval nucleus containing thin strips of heterochromatin (hc) along the inner surface of nuclear envelope, and some small irregular blocks scattered centrally.

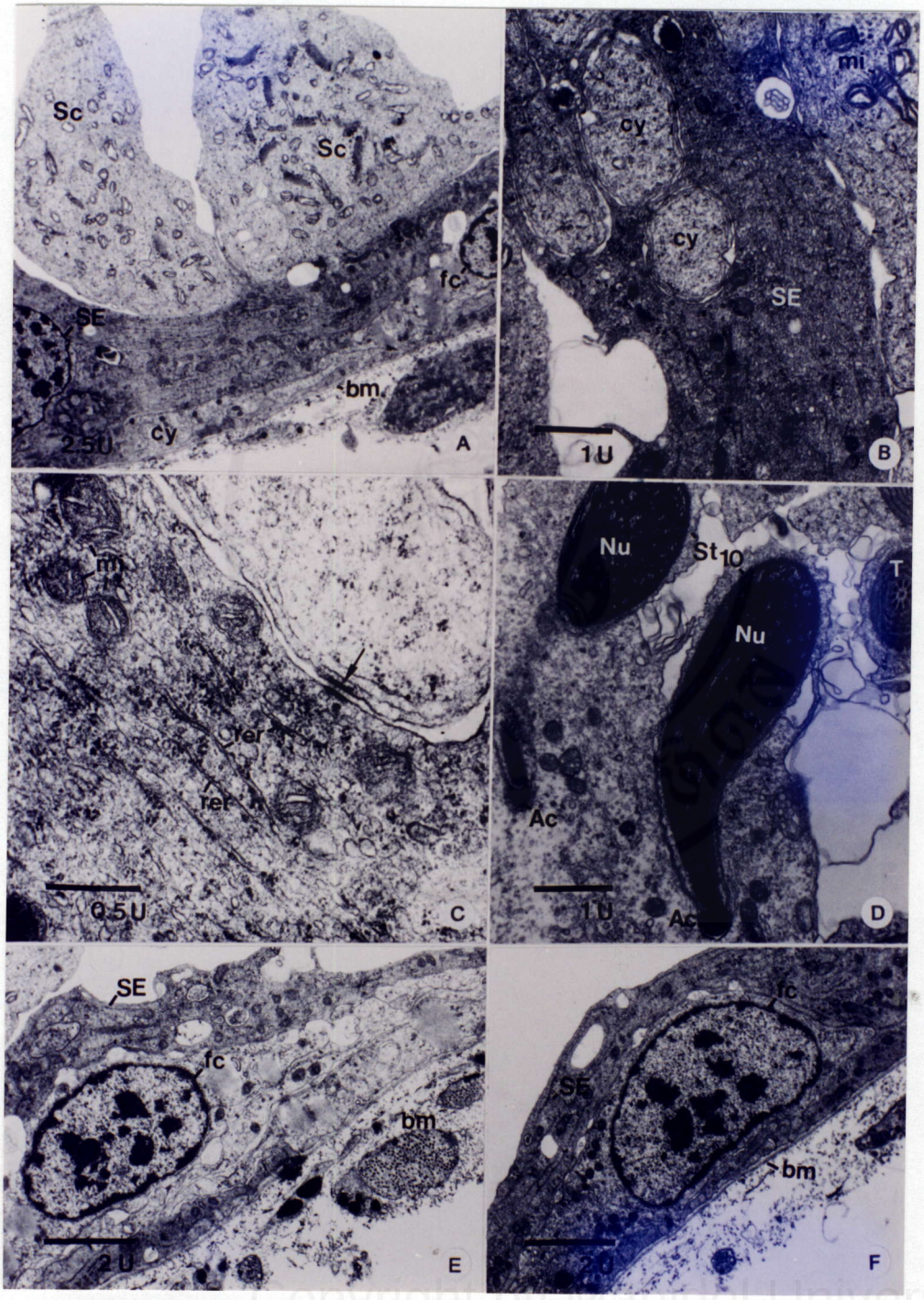

**Figure 33.** Electron micrographs of follicular cells in tubules of ovotetis

A) High magnification showing that follicular cell (fc) is located between the long process of Sertoli cell (SE) and the basement membrane (bm). Its nucleus (Nu) contains thin strip of heterochromatin (hc) along the inner surface of nuclear envelope, and some small-scattered heterochromatin.

B, C, D) The follicular cell (fc) show cytoplasm branching between the cytoplasmic processes of Sertoli cell (SE) and the basement membrane (bm). Note that the cytoplasm of the other Sertoli cell (cy) can be observed penetrating under the cytoplasm of the follicular cell. The junction between follicular cells is shown in D.

E, F) Low magnification shows the association of the structures that form "haemolym-testis barrier" in the ovotestis. This structure is composed of the cytoplasm of Sertoli cell (SE), cytoplasm of follicular cell (fc) and basement membrane (bm). (Mu-myoid cell)

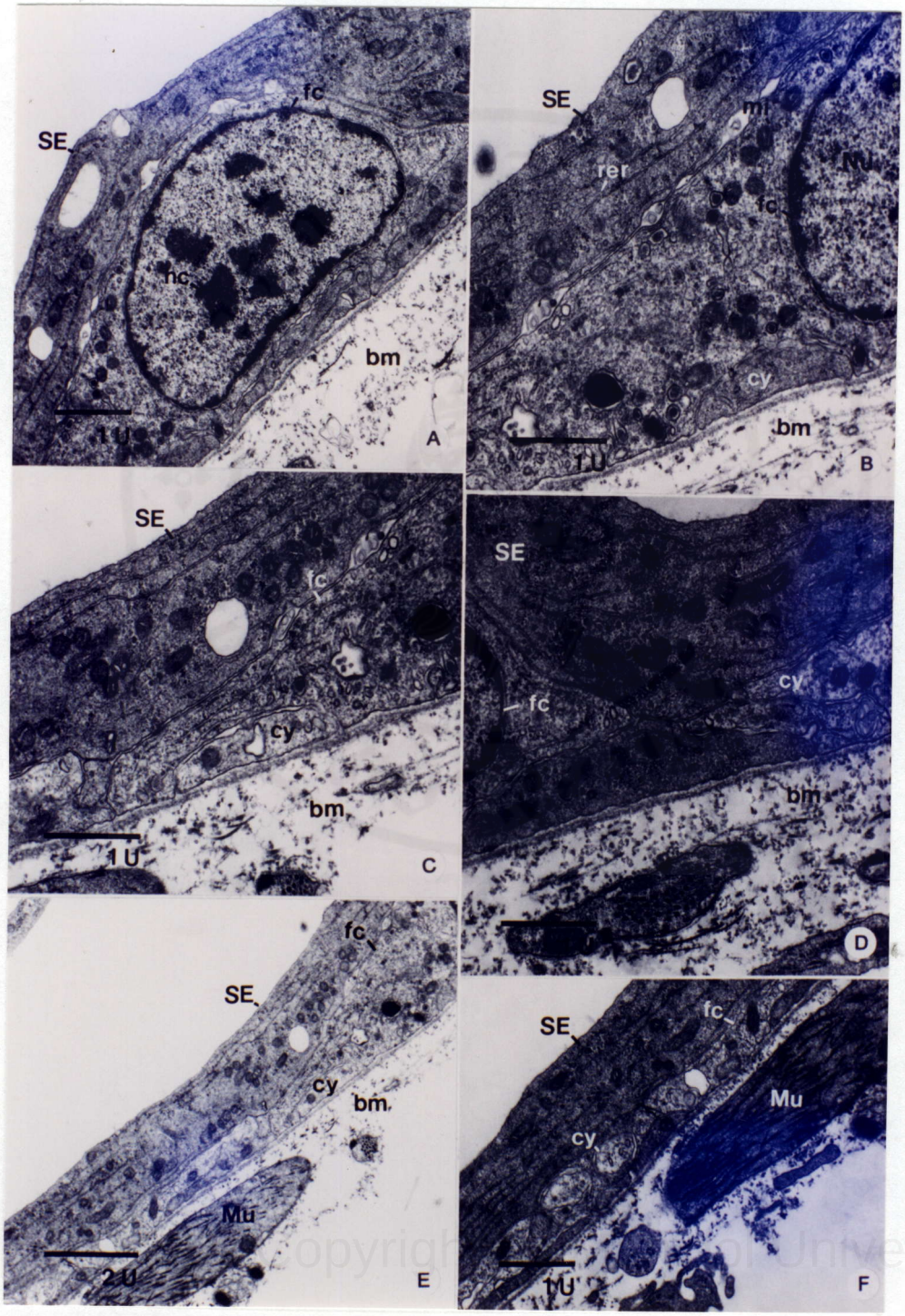

**Figure 34.** Diagrammatic illustration of classified stage of spermatids ($St_{1-10}$) and spermatozoa (Sz) during spermiogenesis based on the size, shape, and chromatin condensation pattern.

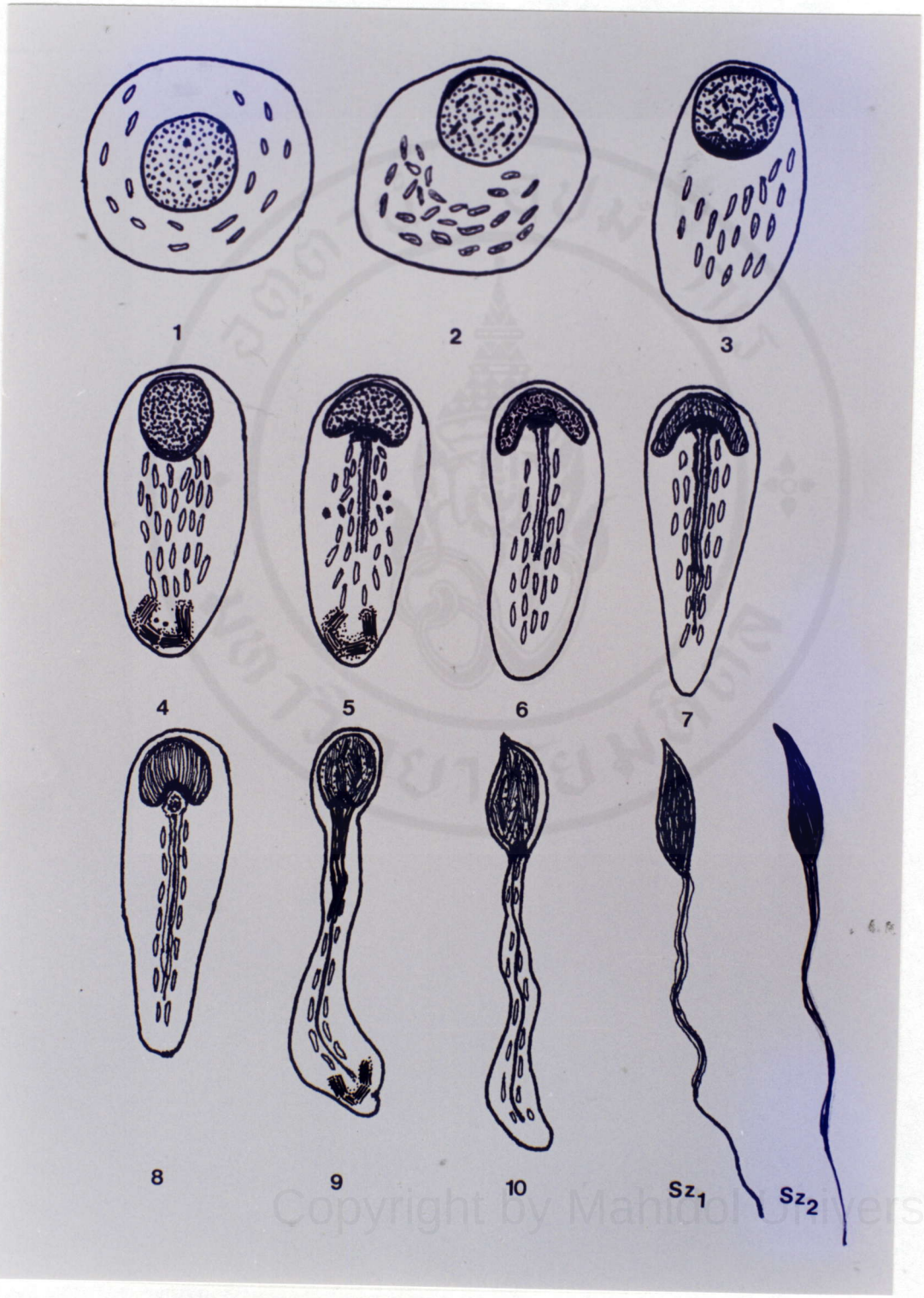

**Table 1:** The dimension of chromatin fibers in the nuclei of various stages male germ cells in the ovotestis of *A. fulica*. Straight fibers (level 4) usually form lamellae or bundles, each about 110-120 nm thick, and are coalesced together to become opaque mass in the mature spermatozoa. Finally, the level 5 fibers exist in the crystal-lattice-liked structure with regular spacing about 3-4 nm.

* The diameter of twenty chromatin fibers in EM negatives taken from at least five nuclei of each cell stage were measured by using a Nikon profile projector.

| Male germ cells in *A. fulica* ovotestis | Chromatin fibers (diameter ± SE) | | | | | |
|---|---|---|---|---|---|---|
| | N* | Level 1 (coiled fibers) | Level 2 (coiled fibers) | Level 3 (semi-coiled) | Level 4 (straight fibers) | Level 5 (Crystal lattices) |
| Spermatogonia | 20 | 10.06± 0.13 | 30.37 ± 0.19 | - | - | - |
| Leptotene spermatocyte | 20 | 10.49 ± 0.19 | 30.61 ± 0.21 | - | - | - |
| Zygotene spermatocyte | 20 | 10.69 ± 0.13 | 30.60 ± 0.14 | - | - | - |
| Pachytene spermatocyte | 20 | 10.64 ± 0.43 | 30.01 ± 0.17 | - | - | - |
| Diplotene spermatocyte | 20 | 10.47 ± 0.20 | 30.73 ± 0.19 | - | - | - |
| Diakinesis spermatocyte | 20 | 10.74 ± 0.17 | 29.80 ± 0.21 | - | - | - |
| Metaphase spermatocyte | 20 | - | 30.51 ± 0.21 | - | - | - |
| Secondary spermatocyte | 20 | 11.63 ± 0.20 | 30.42 ± 0.19 | - | - | - |
| Spermatid stage I | 20 | 10.44 ± 0.12 | 30.20 ± 0.12 | - | - | - |
| Spermatid stage II | 20 | 10.75 ± 0.09 | 30.19 ± 0.14 | - | - | - |
| Spermatid stage III | 20 | 10.30 ± 0.07 | 30.33 ± 0.09 | - | - | - |
| Spermatid stage IV | 20 | 10.18 ± 0.07 | 30.39 ± 0.07 | - | - | - |
| Spermatid stage V | 20 | 10.01 ± 0.13 | 30.31 ± 0.08 | - | - | - |
| Spermatid stage VI | 20 | - | - | 20.08 ± 0.20 | - | - |
| Spermatid stage VII | 20 | - | - | - | 16.05 ± 0.13 | - |
| Spermatid stage VIII | 20 | - | - | - | 16.00 ± 0.10 | - |
| Spermatid stage IX | 20 | - | - | - | 16.02 ± 0.07 | - |
| Spermatid stage X | 20 | - | - | - | - | - |
| Spermatozoa ($Sz_1$) | 20 | - | - | - | - | - |
| Spermatozoa ($Sz_2$) | 20 | - | - | - | - | 10.89± 0.14 |

# CHAPTER VI

# DISCUSSION

## Gonadal Histology

The gonad of *Achatina fulica,* unlike those of other gastropods and bivalves (50, 51, 52, 53, 54), do not have delimiting fibrous capsule. The gonadal tissue is mixed with the hepatopancreatic tissue within the same connective tissue bed. However, gametogenesis is carried out within the circumscribed tubules which are surrounded by the thick basement membrane. Perhaps, this barrier together with an, as yet, unidentified gonadal-hemolymph barrier could provide the sequestered environment for the specialized meiotic division as occurring in vertebrates (55, 56). Despite the presence of the germ cells of both sexes within the same tubule, the cellular association of male germ cells is generally similar to the germinal epithelium in the seminiferous tubules of vertebrates' testes (57, 58, 59, 60, 61, 62), *i.e.*, the early staged germ cells are disposed toward the periphery of the tubules, with spermatogonia and some early primary spermatocytes (LSc) attached to the surrounding basement membrane. Eventhough oogonia and oocytes appear lying next to the groups of developing spermatocytes, they are in fact completely partitioned from the latter by a thin wall formed by the flat sheets of follicular and Sertoli cells, which could help to create the special mileu for oogenetic and spermatogenic processes apart from the main tubular microenvironment. Eventhough both types of sex cells are present, the ovotestis of a single snail either has a male-dominated or

female-dominated phases. In the former, the proliferation of male germ cells is actively occurring, while the female germ cells remain dormant in oogonia and $Oc_1$ stage, and vice versa for the female-dominated gonad. Genetic and/or environmental factors that control the expression of sexual dimorphism of this hermaphroditic snail remain to be elucidated.

## Spermatogenesis

Generally, the stages of cells in spermatogenesis are similar to those of other mollusks and vertebrates. However, there is only one stage of spermatogonia, whose cytoplasmic characteristics are indicative of cells which are preparing themselves for the forthcoming synthetic activity. Sg has large and sometimes more than one nucleoli, and intensely basophilic cytoplasm. Under TEM, it was demonstrated that the cytoplasm of Sg is rich in polyribosomes but with only few mitochondria, rough endoplasmic reticulum, and slender Golgi complex. These characteristics imply that this cell is actively engaged in ribosomal synthesis, while there is no secretory activity. The presence of abundant heterochromatin blocks also suggests that there is still probably a low level of transcriptional activity in producing mRNA. Subsequent stages of primary spermatocytes exhibit the pattern of heterochromatinization similar to those in other gastropods (25, 26, 63) and vertebrates (61, 64). It seems, therefore, that these developmental steps of the first meiosis and the mechanism of heterochromatization in male germ cells of animals are evolutionarily conserved. In *A. fulica*, as in higher vertebrates, the varying forms of the heterochromatin from LSc to DSc and MSc is brought about by the increasingly tighter aggregation of 30-nm nucleosomal-type fibers (27; see Table 1), eventhough the molecular mechanism that

brings about this tight packing is not understood. It is interesting to note that the axis of chromatin condensation which appears as a single dense line is present in LSc; and their number is increasing in ZSc which also have the synaptonemal complexes, which are differentiated from the former by the tripartite structure. The two chromosomal accessory structures are similar to that of the vertebrates' LSc and ZSc (64, 65) axis of condensation may be involved in the initial condensation and packaging of 30 nm chromatin fibers into the chromosomes. Later, this structure may transform into proteinaceous scaffold forming the axis of each chromosome as reported previously (65, 66). On the other hand, the synaptonemal complex may play similar role as those found in vertebrates' spermatocytes, that is in pairing the homologous chromosomes together and initiating the process of crossing over.

In PSc, as a result of chromatin condensation around the axes, large blocks of heterochromatin are formed and they become evenly distributed throughout the nucleus. It is noticable that there is no heterochromatin lining on the nuclear membrane which is probably due to the complete retrieval of all chromatin fibers to be wound into dense blocks around the axes. After this stage the heterochromatin blocks transform into large and fewer pieces of chromosomes in DSc and DiSc. After MSc, the two halves of the chromosomes are segregated and the daughter SSc are formed. And like in mammals, SSc is extremely few in number which implies that this stage may pass through quickly; in contrast to spermatogenesis in bivalves (40, 41, 67) and in primitive gastropods (36, 50, 53), in which there are quite numerous SSc which imply the longer transit time for SSc stage.

## Spermiogenesis

The many diversified stages of male germ cells during spermiogenesis in *A. fulica* represent a complex variation of the same theme as those observed in higher vertebrates especially mammals. In order to achieve fairly drastic change in shape, complete chromatin condensation, acrosomal and tail formations, the developing spermatids have to pass through at least ten identifiable morphological stages in comparison to twelve stages in mouse and nineteen stages in rat (60, 61, 68), in contrast to only four stages in bivalves and primitive gastropods (25, 69, 70, 71). In 1991, Sretarugsa and coworkers (12) studied the spermiogenesis in *A. fulica* and classified spermatids into four stages based on their shape, chromatin appearance, and distribution of organelles. In the present study, we have further investigated the spermiogenesis in *A. fulica* and classify the spermatids into ten stages. The change in shape of the spermatid's nucleus during its differentiation to spermatozoon represents one of the most remarkable examples of spermiogenesis, where the nuclear configuration transforms from spherical or ovoid to flat disc, and later boomerang or arrow-liked shapes whose "wings" could be folded together to form the pear-liked shape that eventually transforms to the falciform shape. It is remarkable to note that when SSc stage transits to $St_1$ the originally dense chromosomes of SSc are "reorganized" again by being decondensed into evenly dispersed 10 and 30 nm fibers (see Table 1), while the Golgi complex is transformed to the "giant" multisectorial structure with clearly increased synthetic activities (Figs. 14B-F). It is possible that $St_1$ needs to form this very large secretory organelle not only for producing the proacrosomal granules but also for forming other granules of unknown function, such as multigranular bodies (Fig. 14E), and possibly the membrane of specialized

mitochondria that are wrapping around the proximal end of the sperm's tail (Figs. 23A-F). The "reorganization" of chromatin in $St_1$ may be correlated with these synthetic activities, which may need a large amount and varieties of mRNA that must be derived from the once again highly decondensed chromatin. This feature is similar to mammalian spermiogenesis when proacrosomal granules begin to be formed in the early spermatids, in contrast to lower gastropods and bivalves in which the granules are presynthesized early in primary spermatocytes, and the already dense chromatin of SSc tends to condense further and transform into dense mass in the early spermatids (26, 40, 41, 67, 72). Like in mammals after $St_1$ that 30-nm chromatin fibers start to condense again into increasing larger heterochromatin blocks in $St_2$ and $St_3$. The cephalic part of the nuclear membrane is thickened and it serves as the site where proacrosomal granules are later assembled. Interestingly, the caudal part of the nuclear membrane is also thickened in $St_3$, and this domain of nuclear membrane induce the preferential chromatin condensation along its inner surface. In $St_4$ the 30-nm fibers become homogeneously condensed throughout the nucleus except for the area close to the caudal part of the nuclear membrane where the chromatin remains denser. In comparison to 30 nm chromatin fibers, the 10-nm fibers are rapidly decreased in quantity until they disappear completely in $St_6$. The Golgi complexes, meanwhile, are still very prominent and maintain their multisectorial configuration and highly active synthetic activities until $St_6$ or $St_7$. Chromatin begins to change noticeably again in $St_6$ where the fibers is reduced in size to about 20 nm which is the only level of chromatin organization found in this stage (see Figs. 18C, D; Table 1). These fibers also are much denser than 30-nm fibers in earlier spermatids and appear less coiled. Eventually they transform in $St_7$ and $St_8$ into straight fibers running

parallel course from the thickened caudal part to the cephalic part of the nuclear membrane (see Figs.19 A-F; Table1). In $St_9$ and $St_{10}$ the straight fibers start to form bundles, each about 110 to 120 nm in width. Initially, these bundles are separated from each other by large pale-stained channels devoided of chromatin material. Eventually, they are fused together to form completely electron opaque mass in $Sz_2$, which is the fully mature spermatozoa. However, at high magnification and resolution the dense chromatin in $Sz_2$ still appear as crystal lattice structure with each dense line about 10 nm thick and the lattice space about 3-4 nm. Thus, the DNA packing in the male germ cells of *A. fulica* present a unique pattern where the 30 nm supposedly nucleosomal-type fibers are transformed to the more rigid and straight fibers of reduced size (20 nm), that become laterally associated into crystal-like tight packing. Since the profiles and changes of the basic nuclear proteins (histones and/or protamine-like proteins) have not yet been studied in this species, it is not possible to conclude whether these proteins play any role in the tight packing. However, it is clear that this fibrous to bundle type packing is quite different from the fibrous to granular type or fibrous to toroidal type packing as reported in higher mammals and human (73, 74). Whether the changes in chromatin fiber sizes and their aggregation have direct influence on the head transformation remained to be proven.

In contrast to mammals, the formation of acrosome, as visualized by light microscopy and TEM, is not prominent. Proacrosomal granules appear to be synthesized in $St_1$ when the Golgi complexes become highly enlarged to the multisectorial structure. The dense vesicles continue to be produced well into $St_5$ and begin to assemble at the mid-point of the cephalic part of the nuclear membrane in $St_6$ (see Figs. 18E, F). The acrosome is fully formed in $St_{10}$ where it appears as a dense

cup fitting over the dense cylindrical anterior tip of the sperm head (see Figs. 24A, B, C). It is covered externally by the plasma membrane which also covers the remaining part of the head. There appear to be little cytoplasm remaining around the head of the sperm, a row while row of microtubules exist around the nucleus even in the fully mature spermatozoa (see Figs. 27A-E).

In comparison to the acrosome, the formation of the tail could be easily followed. Beginning from stage 5, the tail rudiment could be detected in the concavity of the highly flattened nucleus where mitochondria gravitate to surround it. Earlier electron microscopic study by our group indicated that the tail of *Achatina fulica* is accorded with strong fibrous sheath akin to the tails of vertebrates' and higher mammals' sperm, which is the characteristic of the internally-fertilizing spermatozoa (29, 32, 75, 76). The present TEM studies of the tail formation reveal even more intricate details of the sperm' s tail in this mollusk. In $St_8$ and $St_9$, while the wings of the nucleus are pulled inward to form the pear-shape nucleus, the most proximal portion of one centriole projects deep into the caudal end of the nucleus (level 1). The centriolar core is surrounded by the thickened caudal membrane derived from $St_5$ and $St_6$, from which the straight chromatin fibers are attached (see Figs. 19E, F; 21E, 24F). Below this centriolar core the centriolar microtubules are surrounded by a rhomboid shape crystalline substance (level 2) that may help to anchor the "wings" of the nucleus together, as well as contributing to the sturdiness of the proximal part of the tail. This crystalline mass is a unique feature not seen in other mollusks and vertebrate species. Below the crystalline mass is the parts of the tail which is equivalent to the mid-piece of vertebrates' sperm (level 3, 4, 5), where the nine columns of dense fibrous sheaths surround the axonemal complex akin to

those found in mammalian sperm (47, 75, 76). Four to five rows of specialized mitochondria form concentric layers around the axoneme-fibrous sheath complex (Figs. 22A-E). This mid-piece slims down distally due to the decrease in number of rows of mitochondria which eventually disappear (level 6). The redundant Golgi complex is relegated to the distal end of the tail which appear bulbous and contains still a considerable amount of cytoplasm (see Figs. 20, 22F, G).

In $St_{10}$ and maturing spermatozoa the major modification is on the distal end of the tail where the cytoplasmic mass is lost, and the tail consists of the axonemal complex surrounded two or three layers of fence-liked cylindrical sheaths disposed at regular intervals (level 7). Finally, the end piece (level 8) consists of only the axonemal core surrounded by the plasma membrane. From level 3 downward to level 5 the axomemal-fibrous sheath complex exists side-by-side in helical formation with the column of clear cytoplasm that contains glycogen-like material. Both are surrounded in turn by the cylindrical sheaths. The presence of abundant glycogen deposit within this clear cytoplasmic column may provide reserve energy for the axonemal movement. In other words, spermatozoa of *A. fulica* may depend more on glycolysis to yield energy for its movement than in vertebrates and mammalian spermatozoa that receive ATP mostly from the Kreb's cycles in the mitochondria (47, 48, 76).

The close association of developing spermatids with Sertoli-liked cells was observed, especially at stage 10 and immature spermatozoa when their heads are embedded within the apical cytoplasm of the Sertoli cells. This implies that Sertoli cells may play a more complex role in supporting and controlling the spermatids' differentiation. In contrast, in more primitive gastropods and bivalves, the earliest

stages of spermatids are already detached from the germinal epithelium, and the subsequent differentiation and cellular morphogenesis appear to occur independently in each developing spermatid (36, 40, 53). Indeed, the Sertoli cells in *Achatina fulica* ovotestis are very large and appear to have very complex cytological features similar to that of Sertoli cell in the mammalian testes (77, 78). Apart from its role in nuturing spermatids and spermatozoa, Sertoli cells may be the major component of hemolymph-testis barrier since their basal cytoplasm also branch out into thin sheets that, together with the branches of flattened follicular cells, form the complex interdigitation that completely line the basal lamina (see Figs. 31E, 32A-F). Thus, through this rather tight barrier the internal environment of the ovotestis tubules may be kept isolated from the hemolymph.

From the aforementioned characteristics of developing male germ cells, the multi-stage spermatids and their close and prolonged association with the Sertoli cells, we believe that spermiogenesis of *A. fulica* represents an evolutionarily advance step from other mollusks which progresses more toward the mammalian patterns.

# CHAPTER VII

# CONCLUSIONS

The ovotestis histology and ultrastructure of the male germ cells in *Achatina fulica* were studied by light and electron microsopy. Classification of male germ cells and the organization of chromatin during spermatogenesis and spermiogenesis were also concluded:

## Ovotestis Histology

*Achatina fulica*'s gonad contains both male and female germ cells, hence it is called "ovotestis", which is located at the apex of a coiled shell. It consists of numerous small tubules, each of which contains various stages of male and female germ cells, Sertoli cells, and follicular cells which help to segregate oogenetic cells from spermatogenic cells. Each stages of spermatogenic cells is found aggregating in groups and make up the main mass of the germinal epithelium of each tubules, while clusters of spermatozoa existed close to the tubular lumen.

## Cells in Spermatogenesis & Chromatin Condensation



The male germ cells during the process of spermatogenesis and spermiogenesis can be classified into 20 stages according to the cell size, shape, ultrastructural features and the chromatin condensation. Spermatogenic cells consist of spermatogonium (Sg), six stages of primary spermatocytes (PrSc), i.e., leptotene

(LSc), zygotene (ZSc), pachytene (PSc), diplotene (DSc), diakinesis (DiSc) and metaphase (MSc) spermatocytes, secondary spermatocyte, ten stages of spermatids ($St_1$-$St_{10}$), and two stages of spermatozoon ($Sz_1$-$Sz_2$). Sg has the feature of a stem cell, i.e., the presence of mostly euchromatin and few small heterochromatin blocks in the nucleus and prominent nucleolus. LSc and ZSc contain increasingly large heterochromatin blocks that could be condensed by the axis of condensation which appear as a single dense line, and cross-linked by synaptonemal complexes, the tripartite structure. These heterchromatin blocks are transformed into larger and fewer pieces of chromosome in DSc and DiSc. Finally, in MSc the paired chromatids are arranged along the cells' equatorial region. Following MSc stage, the two halves of chromosomes are segregated and daughter SSc are formed. SSc shows large clumps of heterochromatin along the nuclear envelope and in the central area; and this cell stage is rarely observed.

## Spermiogenic Cells and Spermatozoa

Spermatids display ultrastructural characteristics as follows: spematid stages1-4 ($St_{1-4}$) have round nuclei which become progressively smaller. The chromatin of $St_1$ exhibits the reorganization of dense chromosome from SSc into evenly distributed euchromatin containing 30-nm and 10-nm fibers. Moreover, $St_1$ shows very large Giant "multisectorial" Golgi complex indicating increased synthetic activities. Chromatin start to condense in to short blocks in $St_2$ and $St_3$. $St_2$ shows the thicken nuclear membrane at the cephalic part that is the site where proacrosomal granules will adhere. In $St_3$ the caudal part of the nuclear membrane is also thickened and could be the site of induction of further condensation of chromatin in later stages. In

$St_4$, the 30-nm chromatin fibers become homogeneous condensed throughout the flattening nucleus. $St_5$ nucleus is highly flattened in cephalo-caudal direction and the chromatin remains dense with decreasing amount of 10-nm fibers. These fibers completely disappear in $St_6$ whose nucleus is curved into a disc shape. Furthermore, in $St_6$ the chromatin begins to be reduced in size to about 20 nm and begin to be straightened. The Golgi complexes still maintain their multisectorial configuration and have highly active synthetic activities. $St_7$ nucleus has an arrow or boomerang-shape, which is transformed to pear shape in $St_8$. The chromatin in $St_7$ is transformed to straight fibers as well as reduced in size to about 14-16 nm in diameter. These fibers appear much denser in $St_7$ and $St_8$, and extend in parallel from the thickened caudal part to the cephalic part of the nuclear membrane. In $St_9$ and $St_{10}$, the nuclei start to elongate with increasingly tapered anterior end, while the straight chromatin fibers are aggregated into become bundles 110-120 nm in width. The chromatin bundles are separated from each other by the irregular electronlucent area devoided of chromatin material, and they are fused in $Sz_1$. $Sz_2$ into completely the opaque chromatin mass which, at high resolution, that appear as parallel 10 nm dense lines quit similar in conformation with crystal lattice structure with the lattice interval of 3-4 nm.

## Acrosome Formation

Proacrosomal granules begin to be synthesized in $St_1$ when the Golgi complex becomes highly enlarged to the multisectorial structure, and they are produced from $St_1$ to $St_5$ when they begin to be coalesced on the mid-point of the cephalic part of the nucleus. In $St_{10}$, the acrosome appears as a dense cup fitting over the dense

cylindrical rod at the anterior tip of the sperm's head which is covered externally by the plasma membrane.

## Tail Formation

The tail of *A. fulica* sperm is a highly complex structure and can be divided into 8 levels ($L_1$-$L_8$) according to the ultrastructural characteristics of the cross sectional profiles. $L_1$ is formed by centriolar core that deeply projects into the nucleus and surrounded by the thickened and highly invaginated caudal nuclear membrane; this occurs in $St_5$. The axoneme of the flagellum is growing in $St_6$ and is surrounded by a large number of mitochondria. In $St_7$, the tail further elongates and completely formed in $Sz_2$. At $L_1$ of the tail is the part of the centriolar core surrounded by the thickened caudal membrane. At $L_2$ consists of the centriolar microtubules surrounded by a rhomboid shaped crystalline substance. At $L_3$ and $L_4$, the axonemal microtubules are surrounded by a longitudinal column of fibrous sheath that is in turn covered by concentric rows of mitochondrial derivatives. At $L_3$ to $L_5$ which correspond to the mid-piece, the tail slims down distally due to the decrease of numbers of layers of mitochondria which evenly disappear at level 6. From level 3 to level 5 the axonemal-fibrous sheath complex exists side-by-side in helical formation with column of clear cytoplasm containing glycogen-like material. At level 7, the longitudinal fibrous sheaths disappear, and the axonemal complex is surrounded by two or three layers of fence-liked cylindrical sheaths with regular intervals. Level 8, is the end piece, the axonemal core is surrounded only by the plasma membrane.

## Sertoli Cell and Follicular Cell

Sertoli cell is the largest cell located on the basement membrane of the ovotestis' tubule. It has a large round nucleus with deep indentation, and contains evenly scattered patches of heterochromatin. The cytoplasm contains abundant organelles such as Golgi complex, mitochondria and RER. The apical branch of Sertoli cells embrace developing spermatocytes, spermatids and spermatozoa, while their basal branch form thin sheets that interlace with branches of follicular cells, to form the complete lining over the basal lamina. This composite structure could serve as the haemolymph testis barrier.

The follcular cell has flattened nucleus containing mostly euchromatin, and only a few clumps of heterochromatin along the nuclear envelope. The cytoplasmic organelles are sparse. Their cytoplsmic processes also branch out into thin slender sheets that interdigitate with those of adjacent follicular cells and Sertoli cells. This basal follicular cell may form part of the haemolymph-testis barrier, while other may form covering of the oocytes that help to segregate female from male germ cells.

# REFERENCES

1. Duncan CJ. Reproduction. In: Fretter V, Peake J, editors. Pulmonates: Functional anatomy and physiology. Vol. 1. New York: New York Academic press; 1975. p.309-65.

2. Stanisic J, Smith BJ. Class Pulmonate. In: Beesley PL, Ross GJB, Wells A, editors; The Mollusca: The South Synthesis Part B. Fauna of Austraia. Vol 5. CSIRO Publishing, Melbourne; 1998. p.1037-1125.

3. Morton JE, editor. Molluscs. 4$^{th}$ed. London Hutchisin Lth; 1967.

4. Mead AR. The Giant African Snail. A Problem in Economic Malacology. Chicago: University of Chicago Press; 1961.

5. Berry AJ, Chan LC. Reproductive condition and tentacle extirpation in Malayan *Achatina fulica* (Pulmonate). Aust J Zool 1968;16:849-55.

6. Kruatrachue M, Upatham ES, Seehabutr V, Chavadej J, Sretarugsa P, Sobhon P. General anatomy and histology of the nervous system in *Achatina fulica*. J Sci Soc Thailand 1993;19:1-24.

7. Dudek FE. Bag cell peptide acts direcly on ovotestis of *Aplysia californica*: basis for an in vitro bioassay. Gen Comp Endrocrin 1978;36:618-27.

8. Buckland-Nicks JA, Chia FS. Spermatogenesis of a marine snail, *Littorina sitkana*. Cell Tissue Res 1976;170:455-75.

9. De Jong-Brink M, Boer HH, Hommes TG, Kodde A. Spermatogenesis and the role of Sertoli cells in the freshwater snail, *Biomphalaria glabrata*. Cell Tissue Res 1977;181:37-58.

10. Elsaadany MM. Ultrastructural changes in the male germ cells of *Bulinus truncatus* during spermatogenesis. Folia Morphol (Praha) 1989;37:302-7.

11. De Jong-Brink M, De Wit A, Kraal G, Bore HH. A light and electron microscopy study on oogenesis in the fresh water pulmonate snail *Biomphalaria glabrata*. Cell Tissue Res 1976;171:195-219.

12. Sretarugsa P, Ngowsiri U, Krutrachue M, Sobhon P, Chavadej J, Upatham ES. Spermiogenesis in *Achatina fulica* as revealed by electron microscopy. J Med & Appl Malacol 1991;3:7-18.

13. Kgowsiri U. Structure and development of reproductive system in *Achatina fulica*. MS Thesis in Anatomy. Faculty of Graduate Studies, Mahidol University; 1988.

14. Ngowsiri U, Sretarugsa P, Sobhon P, Kruatrachue M, Chavadej J, Upathum ES. Development and seasonal changes of the reproductive system of *Achatina fulica*. J Sci Soc Thailand 1989;15:237-49.

15. Pawson PA, Chase R. The life cycle and reproductive activity of *Achatina fulica* (Bowdich) in laboratory culture. J Moll Stud 1984;50:85-91.

16. Luis O. Postembryonic changes in the reproductive system of the slug, *Arion ater rufus* L. Proc Zool Soc Lond 1961;137:433-68.

17. Runham NW, Hogg N. The gonad its development in *Deroceras reticulatum* (pulmonate: limacidae). Malacologia 1979;18:391-99.

18. Goddard C. A study of the reproductive tract of *Helix aspera* after gonadectomy. Aust J Biol Sci 1960;13:378.

19. Griffon B, Gomot L. Ultrastructural study of the follicular cells in the freshwater gastropod, *Viviparus viviparus* L. Cell Tissue Res 1979;202:25-32.

20. Odiete W. Histological and histochemical observations on the ovotestis and reproductive tract of the African giant land snail, *Achatina (Achatina) achatina* L. and *Archachatina (Calachatina) margina*. Haliotis 1980;10:174.

21. Joosse J, Reitz D. Functional anatomical aspects of the ovotestis of *Lymnaea stagnalis* . Malacologia 1969;9:101-09.

22. Hill RS, Bowen ID. Studies on the ovotestis of the slug, *Agriolimax retuculatus* Muller. Cell Tissue Res 1976;173:465-82.

23. Baweb FM, el-Sherief SS, Abd-el-Kerim HM. The gonad of desert snail *Eremina ehrenbergi* Roth, 1839 (Stylommatophora- Gastropoda) and its role in the production of the male gametes. Funct Dev Morphol 1992;2:103-10.

24. Buckland-Nicks J.A. and Chia F.S., Spermatogenesis of a marine snail, *Littorina Sitkana*. Cell Tissue Res 1976;172:503-15.

25. Sobhon P, Apisawetakan S, Linthong V, Pankao V, Wanichanon C, Meepool A, *et al.* Ultrastructure and chromatin condensation in male germ cells of *Haliotis asinina* Linnaeus. Invert Reprod Dev (in press).

26. Amor MJ, Durfort M. Changes in nuclear structure during eupyrene spermatogenesis in *Murex brandris*. Mol Reprod Dev 1990;25:348-56.

27. Caceres C, Ribes E, Muller S, Cornudella L, Chiva M. Characterization of chromatin-condensing proteins during spermiogenesis in a neogastropoda mollusc (*Merex brandis*). Mol Reprod Dev 1994;38:440-52.

28. Hodgson AN. Invertebrate spermatozoa structure and spermatogenesis. Arch Androl 1986;17:105-14.

29. Franzen A. On spermiogenesis, morphology of spermatozoon and biology of fertilization among invertebrates. Zool Bidr Uppsala 1956;31:356-482.

30. Medina A, Moreno J, Lo'pez-Campos JL. Nuclear morphogenesis during spermiogenesis in the Nudibranch Mollusc *Hypselodoris tricolor* (Gastropoda, Opisthobranchia). Gamete Res 1986;13:159-71.

31. Patisson C, La Corre I. Fine structure of the germinating cells during the spermiogenesis of *Arion rufus* (Mollusca, Pulmonate Gastropoda). Mol Reprod Dev 1996;43:484-94.

32. Healy JM. Spermatozoa ultrastructure and its bearing on gastropod classification and evolution. Aust Zool 1987;24:108-13.

33. Apisawetakan S, Sobhon P, Wanichanon C, Linthong V, Kruatrachue M, Upatham ES. *et al.*, Ultrastructure of spermatozoa in the testis of *Haliotis asinina* Linnaeus. J Med & Appl Malacol 2000;10:101-09.

34. Henley C. Chromatin condensation involving lamellar strands in spermiogenesis of *Goniobasis proxima*. Chromosoma (Berl.) 1973;42:163-74.

35. Jaramillo R, Garrido O, Jorquera B. Ultrastructural analysis of spermiogenesis and sperm morphology in *Chorus giganteus* (Lesson, 1829) (Prosobranchia: Muricidae). The Veliger 1986;29:217-25.

36. Hodgson AN, Heller J, Bernard RTF. Ultrastructure of the sperm and spermatogenesis of five South African species of the *trochid* genus *oxystele* (Mollusca, Prosobranchia). Mol Reprod Dev 1990;25:263-71.

37. Healy JM. Sperm morphology and its systemic importance in the gastropoda. Malacol Rev 1988;4:251-66.

38. Healy JM. Ultrastructure of spermiogenesis in the gastropod *Calliotropis glyptus* Watson (Prosobranchia: Trochidae) with special reference to the embedded acrosome. Gamete Res 1989;24:9-19.

39. Dufresne-Dube L, Picheral B, Guerrier P. An ultrastructure analysis of *Dentalium vulgare* (Mollusca: Scaphopoda) gametes with special reference to early events at fertilization. J Ultra Res 1983;83:242-57.

40. Bozzo MG, Ribes E, Sagrista E, Poquet M, Dufort M. Fine structure of the spermatozoa of *Crassostrea gigas* (Mollusca, Bivalve). Mol Reprod Dev 1993;34:206-11.

41. Johnson MJ, Casse N, Le Pennec M. Spermatogenesis in the endosymbionet-bearing bivalve *Loripes lucinalis* (Veneroida: Lucinidae). Mol Reprod Dev 1996;45:476-84

42. Azevedo C, Corral L. The fine structure of the spermatozoa of *Siphonaria algisirae* (Gastropoda, Pulmonata). J Morphol 1985;186:107-17.

43. Atkinson JW. An ultrastructural analysis of the mature spermatozoa of *Anguispira alternata* (say) (Pulmonata Stylommatophora). J Morphol 1982;173:249-57.

44. Bayne CHJ. Organization of the spermatozoa of *Agriolimax reticulatus*, the grey field slug (Pulmonata: Stylommatophora). Z Zellforsch 1970;103:75-89.

45. Anderson WA, Personne P. The cytochemical localization of glycolytic an oxidative enzymes within mitochondria of spermaotzoa of some pulmonate gastropods. J Histochem Cytochem 1970;18:783-93.

46. Parivar K. Spermatogenesis and sperm dimorphism in the land slug *Arion ater* Z Mikrosk Anat Forsch 1981;95:81-92.

47. Anderson WA, Personne E. The localization of glycogen in the spermatozoa of various invertebrate and vertebrate species. J Cell Biol 1979;44:29-51.

48. Medina A, Moreno FJ, Garcia-Herdugo G. Sperm tail differentiation in the Nudibranch Mollusc *Hypselidoris tricolor* (Gastropoda, Opisthobranch). Gamete Res 1988;20:223-32.

49. Hodgeson AN. Spermatozoon structure and spermiogenesis in *Narsarius kraussianus* (Gastropoda: Prosobranchia, Nassariinae). Invert Reprod Dev 1993;23:115-21.

50. Apisawetakan S, Thongkukiatkul A, Wanichanon C, Linthong W, Kruatrachue M, Upatham ES, Poomthong T, Sobhon P. The gametogenetic processes in a tropical abalone, *Haliotis asinina* Linnaeus. J Sci Soc Thailand 1997;23:225-40.

51. Goggin CL. Gonal development of the hairy mussel, *Trichomyu hirsuta* (Mollusca:Bivalvia) from Lake Macquarie, New South Wales. Moll Res 1994;15:21-28.

52. Tomita, K., The testis maturation of the abalone, *Haliotis discus hannai* Ion, in Rebun Island, Hokkaido, Japan. Sci Rep Hokkaido Fish. Exp Sta.1968;9:56-61.

53. Brown DI. Testicular organization and spermatogenesis in *Tegula (chlorostoma) tridentata* (Potiez and Michaud, 1838) (Mollusca Achaeogastropoda: Trochidae). Microsc Electron Biol Cellular 1992;16:17-33.

54. Eble AF, Scro A. General anatomy. In: Newell RIE, Eble AF, editors; The Eastern Oyster *Crassostrea virginica*. Maryland: Maryland Sea Grant Colledge. 1996. p. 19-71.

55. Pelletier RM, Byer SW. The blood testis barrier and Sertoli cell junctions: structural considerations. Microsc Res Tech 1992;20:3-33.

56. Holash JA, Harik SI, Perry G, Stewart PA. Barrier properties of testis microvessels. Proc Natl Acad Sci USA 1993;90:11069-73.

57. Van Haaster LH, De Rooij DG. Cycle of the seminiferous epithelium in the Djungarian hamster (*Phodopus sungorus sungorus*). Biol Reprod 1993;48:515-21.

58. Meithing A. The establishment of spermatogenesis in the seminiferous epithelium of the pubertal golden hamster (Mesocricetus auratus). Adv Anat Embry Cell Biol 1998;140:1-92.

59. Pudney J. Spermatobenesis in nonmammalian vertebrates. Microsc Res Tech 1995;32:459-97.

60. Dym M. Spermatogonial renewal in the rat as shown by whole mounts of seminiferous tubules. Anat Rec 1968;160:342-43.

61. Leblond CP, Clermont Y. Definition of the stages of the cycle of the seminiferous epithelium of the rat. Ann N Y Acad Sci 1952;55:548-73.

62. Dym M, Fawcett DW. Further observations on the numbers of spermatogonia, spermatocytes, and spermatids connected by intercellular gridges in the mammalian testis. Biol Reprod 1971;4:195-215.

63. Sobhon, P., Apisawetakan, S., Chanpoo, M. & Wanichanon, C., Classification of germ cells, reproductive cycle and maturation of gonad in *Haliotis Asinina* Linnaeus. Science Asia 1999;25:3-21.

64. Clermont Y. The cycle of the seminiferous epithelium in man. Am J Anat 1963;35-51.

65. Karp G. Cellular reproduction. In: Harris D, editor; Cell and Molecular Biology: Concepts and experiment. 2nd ed. California: John Wiley&Son; 1996. p. 608-54.

66. Sadava DE. Cell cycle: The meiotic cell cycle. In: Cell Biology: Organelle structure and function. London: Jones and Bartlett; 1993. p. 484-91.

67. Hodgson AN, Bernard RTF. Ultrastructure of the sperm and spermatogenesis of three species of *Mytilidae* (Mollusca, Bivalvia). Gamete Res 1986;15:123-35.

68. Oakberg E F, A description of spermiogenesis in the mouse and its use in analysis of the cycle of seminiferous epithelium and germ cell renewal. Am J Anat 1956;99:391-414.

69. Cacas MT, Subirana JA. Chromatin condensation and acrosome development during spermiogenesis of *Ensis ensis* (Mollusca, Bivalvia). Mol Reprod Dev 1994;37:223-28.

70. Longo FJ, Dornfeld EJ. The fine structure of spermatid differentiation in the Mussel, *Mytilus edulis*. J Ultrastruct Res 1967;20:462-80.

71. Panasophonkul S, Thonkukiatkul A, Apisawetakan S, Pankao V, Wanichanon C, Linthong V, *et al*. Ganadal histology and gametogenesis in a marine oyster, *Saccostrea forskali* Gmelin. J Med Appl Malacol (submitted).

72. Lalli M, Clermont Y. Structural changes of the head components of the rat spermatid during late spermiogenesis. Am J Anat 1981;160:19-34.

73. Hud NV, Allen MJ, Dowing KH, Lee J, Balhorn R. Identification of the elemental packing unit of DNA in mammalian sperm cells by atomic force microscopy. Biochem Biophy Res Comm 1993;193(3):1347-54.

74. Brewer LR, Corzett M, Balhorn R. Protamine-induced condensation and decondensation of the same DNA molecule. Science 1999;286:120-3.

75. Fawcett DW. The mammalian spematozoon. Develop Biol 1975;44:394.

76. Fawcett DW. A comparative view of sperm ultrastructure. Biol Reprod 1970;2:90-127.

77. Bawa S. Fine structure of Sertoli cell of human testis. J Ultrastruc Res 1963;9:459-74.

78. Dym M. The fine structure of monkey (Macaca) Sertoli cell and its role in maintaining the blood-testis barrier. Anat Rec 1973;175:639-56.

# APPENDIX

## 1. Solutions for Paraffin Technique

**Fixatives: Bouin 's solution**

| | | |
|---|---|---|
| picric acid (saturated aqueous) | 75 | ml |
| 40% formaldehyde | 25 | ml |
| glacial acetic acid | 5 | ml |

add 0.14 M sodium chloride (MW 58.44)

**Staining Solutions**

1. Harris' s Hematoxylin Solution

| | | |
|---|---|---|
| hematoxylin crystals | 5 | g |
| ethyl alcohol, 95% | 50 | ml |
| potassium or ammonium alum | 100 | ml |
| single distilled water | 950 | ml |
| mercuric oxide | 2.5 | g |
| glacial acetic acid | 40 | ml |

2. Alcoholic Eosin Solution

| | | |
|---|---|---|
| eosin-y | 2 | g |
| single distilled rater | 160 | ml |
| ethyl alcohol, 95% | 640 | ml |

## 2. Solutions and Embedding Media for Semithin Technique

**Fixatives:** 1. 4% glutaraldehyde plus 2% paraformaldehyde in o.1 M sodium cacodylate buffer

2. 1% osmium tetroxide in 0.1 M sodium cacodylate buffer

**Buffer Solutions**

0.2 M sodium cacodylate buffer pH 7.4

| | | |
|---|---|---|
| sodium cacodylate | 4.28 | g |
| single distilled water | 100 | ml |

0.2 M calcium acetate

| | | |
|---|---|---|
| calcium acetate | 0.32 | g |
| single distilled water | 10 | ml |

0.1 M sodium cacodylate buffer pH 7.4

| | | |
|---|---|---|
| 0.2 M sodium cacodylate buffer | 96 | ml |
| 0.2 M calcium acetate | 4 | ml |
| single distilled water | 100 | ml |

**Staining Solutions**

1% Methylene blue in 1% Borax

| | | |
|---|---|---|
| methylene blue | 0.5 | g |
| borax | 0.95 | g |
| single distilled water | 50 | ml |

**Embedding Media**

| | | |
|---|---|---|
| Araldite 502 resin | 27 | ml |
| DDSA | 20 | ml |
| DMP-30 | 1 | ml |

## 3. Solutions and Embedding Media for TEM

**Fixatives:**

1. 2.5% Glutaraldehyde in 0.1 M cacodylate buffer, pH 7.4

| | | |
|---|---|---|
| 5% glutaraldehyde | 5 | ml |
| 0.2 M sodium cacodylate | 4 | ml |
| 0.2 M calcium acetete | 1 | ml |

2. 1% Osmium tetroxide in 0.1 M cacodylate buffer, pH 7.4

| | | |
|---|---|---|
| 2% Osmium tetroxide | 5 | ml |
| 0.2 M cacodylate buffer | 5 | ml |

**Buffer Solution**

1. 0.2 M sodium cacodylate buffer, pH 7.4

| | | |
|---|---|---|
| sodium cacodylate | 4.28 | g |
| single distill water | 100 | ml |

2. 0.2 M calcium acetate

| | | |
|---|---|---|
| calcium acetate | 3.16 | g |
| single distill water | 100 | ml |

3. 0.1 M cacodylate buffer, pH 7.4

| | | |
|---|---|---|
| 0.2 M sodium cacodylate buffer | 24 | ml |
| 0.2 M calcium acetate | 1 | ml |

| | | |
|---|---|---|
| single distill water | 25 | ml |

**Staining Solutions**

1. 5% Uranyl acetate

| | | |
|---|---|---|
| uranyl acetate | 2 | g |
| distill water | 40 | ml |

2. Lead citrate

| | | |
|---|---|---|
| NaOH | 2 | g |
| lead citrate | 0.25 | g |
| distill water | 50 | ml |

**Embedding Media**

| | | |
|---|---|---|
| Araldite 502 | 27 | ml |
| DDSA | 23 | ml |
| Accelerator DMP-30 | 1 | ml |

# BIOGRAPHY

| | |
|---|---|
| **NAME** | Miss Viriya Pankao |
| **DATE OF BIRTH** | 15 September 1975 |
| **PLACE OF BIRTH** | Bangkok, Thailand |
| **INSTITUTIONS ATTENDED** | Mahidol University, 1993-1997<br>Bachelor of Science (Physical therapy)<br>Mahidol University, 1997-2000<br>Master of Science (Anatomy) |
| **RESEARCH GRANT** | Thailand Research Fund (TRF)<br>(Senior Research Scholar Fellowship to Prof. Prasert Sobhon) |